GRM1, A POTENTIAL TARGET FOR HUMAN MELANOMA

By

BRIAN A. WALL

A Dissertation submitted to the

Graduate School-New Brunswick

Rutgers, The State University of New Jersey

and

The Graduate School of Biomedical Sciences

University of Medicine and Dentistry of New Jersey

in partial fulfillment of the requirements

for the degree of

Doctor of Philosophy

Graduate Program in Toxicology

written under the direction of

Dr. Suzie Chen

and approved by

_____

_____

_____

_____

_____

New Brunswick, New Jersey

January, 2013

ABSTRACT OF THE DISSERTATION

GRM1, a potential target for human melanoma

By Brian A. Wall

Dissertation Director:
Suzie Chen

The survival rate for patients with advanced metastasis ranges from 2 to 8 months with prolonged survival rates of 5% after 5 years. Targeted therapies have emerged as a paradigm for cancer treatments with the inhibition of multiple signaling pathways required to achieve greater successes in pre-clinical and clinical settings. Recent studies have demonstrated that disrupting the glutamatergic system yields promising therapeutic benefits in several cancers [1, 2, 3, 4]. The impediment of glutamate signaling in several of these cancer cell types activated apoptosis leading to decreased tumor cell proliferation and survival *in vitro* and *in vivo*. The amino acid, glutamate, is produced rapidly in tumor cells by the conversion of glutamine for use in protein and nucleotide synthesis, ATP production, and expulsion of excess carbon resulting from increased glucose metabolism (Warburg effect) in cancer cells. More recently, aberrant glutamate signaling has been shown to play a role in the transformation and maintenance of various cancer types, including melanoma. Glutamate secretion from these cells has been found to stimulate regulatory pathways that control tumor growth, proliferation and survival *in vitro* and *in*

vivo. Our group showed that treatment of human melanoma with the glutamate release inhibitor, riluzole, caused a decrease in extracellular concentrations of glutamate in correlation with arrest at the G_2/M phase of the cell cycle, followed by apoptotic cell death. Despite these observations, the precise mechanisms through which riluzole hampers melanoma cell survival remain to be elucidated. The present study begins to unravel the modes of action of riluzole in *in vitro* cultured melanoma cells. We identified a previously unknown consequence in cells treated with riluzole, DNA damage. Furthermore this observation was detected exclusively in melanoma cells expressing metabotropic glutamate receptor 1 (GRM1). Based on these two observations, we hypothesize that suppression of glutamate export from within the cells causes a disruption of intracellular homeostasis of glutamate/cystine exchange by the intracellular accumulation of unreleased glutamate. The limited amount of cystine results in a decrease of available glutathione (GSH) potentially increasing the levels of intracellular reactive oxygen species (ROS) followed by a rise in DNA damage.

Acknowledgement

I would like to express my dearest, humble gratitude to my advisor and mentor, Dr. Suzie Chen. It is because of her that I was able to complete the tasks that led me to and through the path of becoming a scientist. Dr. Chen gave me the opportunity, showed me the discipline and taught me the art of scientific thought and creative idea. Thank you, Suzie, for turning this "pair of hands" into an independent thinker.

I would like to show my gratitude to Dr. Lori A. White for her initial mentorship throughout my collegiate career. Dr. White provided me with the techniques and knowledge that became the foundation of my graduate studies. Thank you, Lori, for seeing me through the beginning and being there with me at the end.

I would like to express my special thanks to Dr. Nan Joo Suh for her mentorship throughout my graduate studies. Dr. Suh has supported me by sharing her knowledge of the field and showing me encouraging words. Thank you, Nan Joo, for your invaluable support throughout.

I would like to thank my other committee members, Dr. Helmut Zarbl and Dr. Bruce Haffty for not only their expertise and serving on my committee, also for their performance in their fields. They have contributed immensely to the understanding of cancer biology and have given me invaluable advice allowing my advancement through my studies.

Dedication

I would like to dedicate this dissertation to my family and friends. Without them, I would not be who I am today**.**

Table of Contents

ABSTRACT OF THE DISSERTATION ii

Acknowledgement iv

Dedication v

Table of Contents vi

List of Tables ix

List of Figures x

Introduction 1

Part I: Classification of skin cancers 5

A. Squamous cell carcinoma 6

B. Basal cell carcinoma 7

C. Melanoma 9

Part II: Melanocytic Transformation 11

A. Normal melanocytes 11

B. Nevus 12

C. Primary melanoma 13

Part III: Contribution of genetic alterations in melanocytic neoplasia 17

A. Proto-oncogenes / tumor suppressor genes 17

B. Current therapies 26

Part IV. Glutamate and cancer 31

A. The role of glutamate in normal and cancer cells 32

B. Aerobic glycolysis 34

Part V: G-protein coupled receptors 36

A. GPCR signaling 39

B. G-protein coupled receptors and cellular transformation 41

C. Ectopic expression of GRM1 42

D. Inhibition of GRM1 expression 47

Section I: GRM1 Expression is Necessary in Riluzole-Induced G_2/M Arrest 58
Aim 1: Rationale 58
Materials and Methods 59
A. Antibodies and reagents 59
B. Cell culture 59
C. Cell Cycle Analysis 59
D. Clonogenic cell survival assays 60
E. DNA transfections 60
F. Glutamate release assay 61
G. Antibodies and Western immunoblots 61
H. Immunofluorescent staining 62
I. Immunohistochemistry (IHC) 63
J. Murine xenograft model 63
Results 64
1.1 Human melanoma cells excrete elevated levels of glutamate 64
1.2 Cell cycle arrest of GRM1-expressing human melanoma cells after riluzole treatment 64
1.3 Riluzole causes hyper sensitivity to ionizing irradiation in GRM1 expressing human melanoma cells 65
1.4 Effects of ionizing radiation and Riluzole in a murine xenograft model: 66
1.5 Riluzole induces DNA damage in human melanoma cells that express GRM1 67
1.6 ATM is activated in GRM1-expressing cells after treatment with riluzole 68
1.7 Riluzole-induced DNA damage is dependent on GRM1 expression 69
1.8 Formation of γ-H2AX foci after riluzole treatment is independent of apoptosis 70
1.9 DNA damage increase in riluzole treated biopsies from responding patients 71

Section II. The molecular mechanisms of riluzole-induced G_2/M arrest in GRM1 expressing human melanoma cells 83
Aim 2: Rationale 84
Materials and Methods 84
K. Cell culture 84
L. DNA transfection 85
M. Ponasterone inducible system 85
N. Immunofluorescent staining 86
O. Western immunoblots 87
P. Detection of reactive oxygen species (ROS) 87
Q. Measurement of intracellular levels of glutathione (GSH) 88

R. Measurement of intracellular levels of glutamate 88

Results 90

2.1 Riluzole-induced DNA damage only occurs in human melanoma cells that express functional GRM1 90

2.2 Riluzole promotes accumulation of intracellular glutamate in GRM1 positive human melanoma cells 91

2.3 Riluzole treatment in GRM1-expressing human melanoma cells increases oxidative stress 92

2.4 Decrease in GSH in human melanoma cells that express GRM1 95

Section III: Riluzole is a Radio-Sensitizing Agent in an *in vivo* Model of Brain Metastasis Derived from GRM1 Expressing Human Melanoma Cells 110

Aim 3: Rationale 110

Materials and Methods 111

S. Cell culture and DNA transfections 111

T. Lucigenin chemiluminescence assay 111

U. Xenograft animal model 111

V. Orthotopic human melanoma cell injections in immunodeficient nude mice 112

W. Visualization of orthotopic mouse model of brain metastasis 113

Results 114

4.1 Isolation of stable luciferase-expressing C8161 cells 114

4.2 Tumor volumes of subcutaneously injected cells measured by IVIS optical imagining system 114

4.3 Combination of riluzole and IR reduces human melanoma cell growth in orthotopic model of brain metastasis 115

Section IV. Discussion 121

Conclusion 137

References 142

List of Tables

Table 1. Expression of GRMs in select non-neuronal cells 52

Table 2. Implications of GRMs in human Cancer 53

List of Figures

Figure 1. Conversion of Tyrosine to eumelanin 54

Figure 2. Metabolic pathways including glycolysis and glutaminolysis. 55

Figure 3. Glutamate metabolism in the mitochondria 56

Figure 4. Signal transduction pathways activated by GRM1 stimulation. 57

Figure 5. GRM1-expressing human melanoma cell excrete excess glutamate 73

Figure 6. Cell cycle analysis of GRM1 expressing human melanoma cells 74

Figure 7. Clonogenic assays 75

Figure 8. Murine Xenograft Model 76

Figure 9. Western blot showing histone 2A phosphorylation 77

Figure 10. ATM is activated in GRM1 expressing cells treated with riluzole 78

Figure 11. Riluzole induces DNA DSBs in GRM1 expressing human melanoma cells. 80

Figure 12. D3-Grm1 clones express functional Grm1 81

Figure 13. Amount of DSB in riluzole treated human melanoma cells is independent of apoptosis. 82

Figure 14. Markers of DNA damage detected in post-treatment human melanoma tumor samples from responding patients in Phase 2 trial of riluzole. 83

Figure 15. GRM1 expression in hTERT/CDK4^{R24C}/p53^{DD} human melanocytes transformed with human *GRM1* 97

Figure 16. Riluzole induces DNA DSBs in human only in melanocytic cells that express GRM1 99

Figure 17. PonA inducible shGRM1 clones 100

Figure 18. Knock down of GRM1 expression reduces amount of DSB in riluzole treated human melanoma cells independent of apoptosis. 102

Figure 19. Riluzole treatment of GRM1-positive human melanoma cells induces an increase in intracellular levels of glutamate 104

Figure 20. Riluzole treatment results in an increase in ROS in human melanoma cells and is rescued by inclusion of NAC or reduced GSH-Et. 106

Figure 21. GRM1 expression is necessary for riluzole-elicited increases in ROS 107

Figure 22. Riluzole treatment of GRM1-positive human melanoma cells induces a reduction in glutathione levels 109

Figure 23. Stable C8161 luciferase containing clones 117

Figure 24. Comparison of actual tumor volume vs. luminescence intensity 119

Figure 25. Intracranial orthotopic transplants of human melanoma..... 120

Introduction

The management of malignant disease remains a challenge for contemporary medicine. To date, the development of anticancer therapeutics with the ability to target tumor-specific proteins or pathways faces significant challenges owing to the acquired drug resistance resulting from the abnormal physiology of cancer cells. Cancer cells are able to respond with epigenetic as well as genetic alterations to escape therapeutic treatment. However, the multitude of abnormalities and deregulated behaviors that occur while transitioning from a normal to a neoplastic transformed cell type makes it difficult to effectively target all of the critical changes that occur in the cellular biochemistry and molecular biology within a given mass [5]. Although each cancer harbors unique genetic variations, they all share the ability to successfully bypass regulation checkpoints that would otherwise detect errors that arise in critical events such as DNA replication and chromosome segregation which would normally prevent heritable transmission of the genetic lesion to future cellular generations. These mutations, in part, desensitize the cell to antigrowth signals that would normally block proliferation as well as cause the cell to become resistant to programmed cell death resulting in deregulated cell proliferation and aberrant growth. For this reason, compounds that are capable of delaying the mitotic entry of cells, inhibiting their progression through the cell cycle, could offer a therapeutic advantage when used in conjunction with chemotherapies that target specific signaling pathways, there-by increasing their efficacy.

To move from a quiescent state to an active proliferative state, cells require mitogenic growth signals [6]. These signals are transmitted into the cell by

transmembrane receptors that bind distinctive classes of signaling molecules simulating proliferation. Cancer cells either overexpress the receptors that transduce these growth stimulatory signals or acquire the ability to synthesize the growth factors to which they are responsive, creating a positive signaling loop [7].

Like most other cancers, melanoma is a genetically heterogeneous disease in which single agent therapies are likely to fail due to multiple variations in the genomic signatures identified in these tumor types. To this end, the availability of a model system that exhibits a single type of neoplasm that recapitulates on both pathological and molecular levels of that tumor type is a powerful tool to characterize the molecular events leading to initiation, promotion and progression of a given neoplasia. Toward this goal, our group has been using transgenic mouse lines that spontaneously develop melanoma with 100% penetrance [8, 9, 10]. Molecular approaches identified that the ectopic, aberrant expression of metabotropic glutamate receptor 1 (GRM1) in melanocytes in these animals is the apparent cause for melanoma development [10]. To extend to the human system, we have established that about 65% of human melanoma biopsies and cell lines also displayed ectopic expression of the human version of the receptor, suggesting its involvement in some human melanomas [11].

GRM1 is a member of the metabotropic glutamate receptor (mGluR) family. There are eight subtypes identified to date, GRM1 belong to the G-protein coupled receptor (GPCR) superfamily, which is widely expressed in both neuronal and non-neuronal tissues [12]. The natural ligand for GRM1, glutamate, has trophic functions in early central nervous system (CNS) development where it is involved in the regulation, the proliferation, migration, and survival of neuronal progenitor stem cells and immature

neuron [13, 14]. Many GPCRs have been found to be either overexpressed or aberrantly expressed in various cancer types, contributing to tumor cell growth once activated by circulating or locally produced ligand. It has been well established that the oncogenic transformation of various cell types by the ectopic expression of GPCRs is characterized by the development of autocrine and paracrine loops that enhance cellular proliferation [15].

Earlier studies by our group have shown that mGluR-1-expressing human melanoma cells have elevated concentration of glutamate in their surroundings suggesting the existence of autocrine loops in these cells. These findings prompted us to examine the consequences of inhibiting glutamatergic signaling in these melanoma cells. We found that an inhibitor of glutamate release, riluzole, was able to disrupt the glutamatergic signaling cascade and led to a reduction in cell proliferation. Further studies showed that inclusion of riluzole in the growth media of cultured human melanoma cells led to an initial cell arrest in the G_2/M phase of the cell cycle followed by accumulation in the pro-apoptotic/ sub G_1 phase while having much less effect on normal human melanocytes under same conditions [11].

It is known that cells arrested in the G_2 phase tend to be more sensitive to the effects of agents that cause DNA damage, such as ionizing radiation (IR) [16, 17, 18, 19, 20, 21, 22]. Ionizing radiation remains one of the most effective tools in the therapy of cancer. It is an efficient DNA-damaging agent with and able to be spatially specific. The class of lesion that is most closely correlated with cell death is the DNA double strand break (DSB), which can be the result of direct ionization of DNA or by the generation of free radicals. As a result, mammalian cells exposed to IR show a delay of progression in

the cell cycle from G_1 to S phase, inhibition of DNA synthesis and a delay in the progression from G_2 phase into mitosis (G_2/M) [23]. Therefore, to take advantage of riluzole-elicited G_2/M arrest, we performed a series of pre-clinical studies to test whether riluzole could sensitize melanoma cells and augment the effects of sub-lethal doses of IR. We were able to demonstrate that riluzole in combination with IR elicits a further increase in apoptotic cell death and a decrease in tumor cell proliferation than each one alone in *in vitro* cultured melanoma cells and in *in vivo* tumorigenicity assays[4]. We assessed a well-known marker of DNA DSB, the phosphorylated form of histone variant H2A (γH2AX) which has been shown to localize around sites of DSB and is frequently used to assess damage induced by IR. Surprisingly, we found that not only did IR treatment result in DNA DSB, but riluzole treatment alone also yielded substantial levels of positive γH2AX staining. Combining IR with riluzole led to further increase in γH2AX levels detected. These results suggested that riluzole exposure of human melanoma cells that express GRM1 contributes to G_2/M arrest and further sensitizes the cells to the effects of IR.

Riluzole is an FDA approved drug for the treatment of Amyotrophic Lateral Sclerosis (ALS). In the CNS, inhibition of glutamate release from nerve terminals in the CNS results in a decrease in the concentration of the excitatory amino acid, glutamate, in the synaptic cleft, causes a reduction in post-synaptic activation of glutamate receptors. Recent reports also indicate that, in addition to the ability of riluzole to inhibit glutamate release from melanoma cells, similar observations have been made in other cancer cells [11, 24, 25, 26, 27]. This thesis describes studies in a previously unknown mode of

action of riluzole: induction of DNA damage in cells, furthermore, this unexpected property was dependent on mGluR-1 expression. To understand the underlying mechanisms of riluzole-mediated DNA damage in melanoma may provide a better means to achieve increased therapeutic activity and selectivity for this deadly disease.

Part I: Classification of skin cancers

Cancer is characterized by the uncontrolled growth of an abnormal cell to produce a population of cells that have acquired the ability to multiply and invade surrounding and distant tissues (metastasis). The invasive characteristic of cancers is what deems them lethal to the organisms in which they arise. The majority of cancers are derived from a single cell (monoclonal) and the sequential accumulation of somatic mutations, each providing the cell a proliferative/survival advantage that drives expansion in cell number and tumor development. The mutations acquired result in gain-of-function of oncogenes and loss-of-function of tumor suppressor genes. Mutations arise from imperfect DNA replication and repair, oxidative DNA damage, DNA damage caused by environmental carcinogens and epigenetic changes. These alterations allow the cancer cell the ability to produce their own growth signals making them independent of growth factors for proliferation indefinitely as well as the ability to evade apoptosis, invade surrounding tissue, and induce the formation of new blood vessels (angiogenesis) and tumorigenesis [6, 28, 29].

Skin cancer is the most common of all cancer types with more than 3.5 million new cases diagnosed each year in the United States [30]. There are three major types of

skin cancer: squamous cell carcinoma, basal cell carcinoma and melanoma. Solar ultraviolet (UV) light has been the major carcinogenic agent for non-melanoma skin cancer (NMSC). The induction of NMSCs is mainly caused by the absorption of UV by DNA forming UV-specific dipyrimidine photoproducts. The two main photo products believed to be responsible for most of the carcinogenic effects of UV radiation are cyclobutane pyrimidine dimer (CPD) and 6-4 pyrimidine –pyrimidone [31, 32]. These photoproducts interfere with DNA replication leading to mutations with more specific mutations induced by UV-B in DNA sequences most often including single-base substitutions of cytosine (C) for thymine (T). Lesions involving double-base changes from CC to TT also occur, however, but less frequently [32]. This damage can be efficiently repaired by nucleotide excision repair or replicated by low fidelity class Y polymerases. Insufficient repair of these lesions followed by errors in replication produce characteristic mutations in dipryimidine sequences resulting in initiation events that lead to carcinogenesis.

A. Squamous cell carcinoma

Skin squamous cell carcinomas (SCC) are derived from epidermal keratinocytes and commonly manifest at the ages of 60-70 [33]. SCCs can be confined to cells in the epidermis or can radiate down into the dermal layer (Bowen disease or SCC *in-situ*). Clinically, lesions present themselves as an erythematous, indurated papule, plaque or nodule with adherent scale. In the United States, an estimated 700,000 cases of SCC are diagnosed each year resulting in approximately 2,500 deaths [30]. SCC is mainly caused by cumulative UV exposure and for this reason occurs most often in areas on the body

frequently exposed to the sun. Ultraviolet B radiation (wavelength, 290 to 320 nm) from the sun causes the majority of the damage with ultraviolet A radiation exposure (320 to 400 nm) causing an increased risk of incidence [34]. Ultraviolet radiation exposure produces mutations in DNA, frequently via the formation of thymidine dimers in the p53 tumor-suppressor gene [35].

In addition to UV radiation, other agents are known to cause SCC's, however, whether the molecular progression for these lesions are the same as those caused by UV is not well established. Arsenic exposure has been shown to cause skin cancer through causation of gene amplifications [36]. Arsenical SCC develops as hyperkeratotic lesions on the skin called arsenical keratoses often on the palms of the hands and soles of the feet. In addition chemicals such as 7,12-dimethylbenz[α]anthracene (DMBA) and 12-O-Tetradecanoylphorbol 13-acetate (TPA) have been shown to induce SCC in mice [37].

B. Basal cell carcinoma

Basal cell carcinoma (BCC) is a malignant neoplasm that arises from the basal cells of the skin and the follicular infundibulum [38]. BCC constitutes approximately 80 percent of all non-melanoma skin cancers occurring predominantly in fair-skinned individuals and is more common in males than females [39]. Clinically, BCC presents itself as a slow-growing pearly papule with overlying spidery red skin lesions caused by dilated blood vessels known as telangiectases or poorly demarcated erythematous. Depending on the configuration of cells in the tumor, BCC's are classified as superficial, nodular, infiltrative or morpheaform. Superficial BCCs occur commonly on the torso and

presents as a scaly erythematous patch or plaque on the surface of the skin. Superficial BCCs are attached to the epidermis with little penetration into the dermal layer of the skin [40]. Superficial BCC is very responsive the topical chemotherapies, imiquimod and Fluorouracil [41, 42]. Nodular BCC is the classic form of the disease which presents itself as a pearly papule or nodule with overlying telangiectases and a rolled border that may exhibit central crusting or ulceration. Nodular BCC is found usually embedded in a fibroblastic stroma located in the dermis with the tumor mass itself mainly located in the dermal layer and not at the dermal-epidermal junction [43]. Both nodular and superficial types may contain melanin and appear brown, blue, or black in color. Infiltrative BCC, also known as sclerosing, fibrosing, or morpheaform, typically appears as an indurated, whitish, scar-like plaque with indistinct margins. This form of BCC is considered the most aggressive type and is characterized by the tumor penetrating deeply into the dermis. Infiltrative BCC can invade deep into the dermis and invade bone, cartilage along the outside of nerves (perineural invasion).

In addition to sporadically occurring BCC, heritable disorders exist that cause BCC to develop at an earlier age and a higher rate than the general population. These include nevoid basal-cell carcinoma (or Gorlin's) syndrome, albinism, xeroderma pigmentosum, the Rombo syndrome and the Bazex syndrome [44, 45]. Inappropriate activation of the hedgehog (HH) signaling pathway is found in both sporadic and familial cases of BCC. Secreted sonic HH (SHH) protein binds the tumor-suppressor patched homologue 1 (PTCH1), abrogating PTCH1-mediated suppression of intracellular signaling by a transmembrane protein, the G-protein-coupled receptor smoothened

(SMO). Constitutive activation of SMO results in the activation of members of the GLI family of zinc finger transcription factors leading to upregulation of target genes [46]. In addition, mutations in the p53 tumor-suppressor gene are found in approximately 50% of cases of sporadic BCC with many being C→T and CC→TT transitions at dipyrimidine sequences, indicative of exposure to UVB radiation [47].

C. Melanoma

Human cutaneous malignant melanoma is potentially a highly aggressive, metastatic form of skin cancer. Although melanoma accounts for only 5% of the three major forms of skin cancer, it has the highest mortality rates of all skin cancers and is the leading cause of cancer death in people under the age of 30. Patients who are diagnosed of advanced malignant melanoma have a median survival of approximately 8 month and a 5-year survival rate of about 5% [48]. While the incidence of many other cancers is falling, the incidence of malignant melanoma is increasing rapidly worldwide at a rate faster than that of any other cancers [49, 50]. In the United States, melanoma is the 3rd most common cancer in men, the 4th most common cancer in women and the most common fatal malignancy among young adults [51, 52, 53, 54]. An estimated 76,250 new cases of melanoma will be diagnosed in the United States in 2012 alone and estimates indicate that more than 1 in 50 Americans will be diagnosed with melanoma during their lifetime [54, 55, 56]. Worldwide, the incidence of melanoma is increasing 3-7% per year in people of European descent [57]. At the present time, prevention and early detection are the only effective measures of successfully treating this disease.

Once diagnosed, melanoma is commonly treated by surgical removal of the tumor area. However, if melanoma cells become metastatic, these cancer cells can rapidly spread throughout the body, resulting in poor prognosis and reduced survival. Despite screening and early detection programs, the rising incidence of melanoma has been correlated with stable or increasing melanoma-related mortality in the US [58].

Cancer staging systems are specific for each cancer type. Melanoma is classified into different stages based on the size, growth and spreading of the tumor. It can range from stage 0, where melanoma cells are only located in the epidermis, to stage IV, where the tumor has metastasized and spread to other parts of the body. Histological features such as the tumor thickness, mitotic rate and ulceration of the primary melanoma become important hallmarks of melanoma prognosis and staging [59]. During diagnosis, physicians will determine the stage of the melanoma through several procedures including biopsies, x-ray imaging (particularly in the chest area for lung metastasis), computed tomography (CT) scan, magnetic resonance imaging (MRI) and positron emission tomography (PET) scan. Once diagnosed, stage 0 and I melanomas and/or nearby lymph nodes are surgically excised [60, 61]. In these early stages, melanoma is confined to the skin, where the disease is curable in a high percentage of cases through surgical removal of the tumor [62]. Once melanomas undergo metastasis and surgical removal is not sufficient to remove the tumor, patients undergo adjuvant cancer therapies such as chemotherapy, radiotherapy and immunotherapy.

Part II: Melanocytic Transformation

A. Normal melanocytes

In mammals, pigment is produced exclusively by pigment-producing cells called melanocytes. The majority of melanocytes reside in the skin, particularly within the epidermis and hair follicles. Melanocytes can also be found in the dermal and the basal cell layer of the epidermis (cutaneous melanocytes) as well as the orbital cavity including the retina, iris, and choroid; the inner ear, leptomeninges and the mucous membranes (extracutaneous melanocytes) [63]. Melanocytes in mammals traditionally synthesize three prototypes of melanin: eumelanin which is brown-black and insoluble; pheomelanins which are reddish yellow and alkali soluble; and trichromes which, like pheomelanins, occur in certain types of yellow or red and insoluble at neutral pH. Epidermal melanocytes contribute to photoprotection and thermoregulation by packaging melanin-containing melanosomes and delivering them to neighboring keratinocytes, a relationship that has been termed the *epidermal melanin unit* [64, 65]. Melanocytes found in hair follicles actively synthesize and transfer melanin into hair matrix cells during the anagen phase of the hair cycle [66].

Eumelanin consists of a mixture large molecular weight polymers consisting of 5, 6-dihydroxyindole units. Pheomelanin is a polymer formed by cysteinyl-dopas through reactions of dopaquinone with cysteine or glutathione and is more photoliable than eumelanin. The metabolic biosynthesis of eumlenins, pheomelanins and trichomes involve the oxidation of L-tyrosine by the enzyme tyrosinase to 3, 4-

dihydroxyphenylalanine (L-DOPA). L-DOPA is then oxidized to dopaquinone by the same enzyme (Figure 1). During development, melanocytes are derived from pluripotent, trunk neural crest cells that differentiate into numerous cell lineages that include neurons, glial cells, medullary secretory cells, smooth muscle cells, and bone and cartilage cells [67].

Melanogenesis is stimulated by melanocortins, including melanin-stimulating hormone (MSH) and andrenocorticotropic hormone (ACTH), as well as androgens, estrogens, and inflammatory mediators [68].

B. Nevus

The term "nevus" is a general term used to designate a benign tumor composed of melanocytic cells [69]. In the skin, there are two main groups of nevi: the superficial and the deep or blue nevi [70, 71]. Pathologically, there are three groups of nevi classified by their distinct features in the skin (1) Common acquired nevi which include atypical melanocytic nevi; (2) congenital melanocytic nevi; and (3) spitz nevus. Superficial nevi are further subdivided into dermo-epidermal (junctional), dermal, compound (junctional plus dermal) and spindle/epithelioid cell nevi [72, 73]. Epidemiological studies have suggested that persons with high numbers of acquired and dysplastic nevi are at an increased risk of developing melanoma [74]. Persons who have at least 12 nevi with a diameter of 6.35 mm or larger have a 41-fold increased risk of developing melanoma while those having atypical, relatively large (dysplastic) nevi have a 5-10% life-time risk of developing the disease [75, 76]. Approximately 40% of

melanomas develop in a dysplastic nevus and symptoms of neoplastic transformation include a change in color, development of a depigmented halo or total loss of pigment, and superficial spreading of the borders. Surface elevation, itching, bleeding, and oozing tend to occur at more advanced stages of initiation/progression [77].

C. Primary melanoma

Primary melanomas evolve from melanocytes or precursor lesions, nevi. The steps of primary melanocytic neoplasia have been divided into six evident steps of tumor progression from the neoplastic system that affects the human epidermal melanocyte: (1) the common acquired melanocytic nevus; (2) a melanocytic nevus with lentiginous melanocytic hyperplasia; (3) a melanocytic nevus with aberrant differentiation and melanocytic nuclear atypia; (4) the radial growth phase of primary melanoma; (5) the vertical growth phase of primary melanoma; and (6) metastatic melanoma. An acquired nevus, or mole, is considered to be a focal proliferation of melanocytes that is to follow a distinct pathway of differentiation resulting in the disappearance of the nevus; however, if this pathway is not followed, aberrant differentiation occurs forming a characteristic lesion termed melanocytic dysplasia which is regarded as the formal histogenetic precursor of melanoma.

There are several criteria for classifying a new melanoma as an independent primary. The presence of a melanocytic nevus (*in situ* melanoma) is the strongest evidence in favor of a primary tumor. Additional criteria separating metastatic and

primary lesions include location, grouping, invasion of lymphatic capillaries, and the presence of inflammatory cell infiltrate [78, 79].

Primary malignant melanomas progress through two growth phases: radial and vertical. Radial growth is characterized by the net enlargement of the tumor at its periphery along the radii forming an imperfect circle spreading laterally into the surrounding epidermis. Over time, the lesion may progress to the vertical growth phase at which time the malignant cells become invasive and spread to the dermal layer of the skin. Tumors at this stage can be further transformed and gain the ability to metastasize to distal organs in of the body.

Radial Growth Phase (RGP)

This class of primary melanoma is classified by the enlargement of the tumor slowly along the periphery of the lesion. The neoplastic lesion is considered a malignant melanoma that is confined to the epidermis above an intact basement membrane (*in situ*) or invasive, non-tumorigenic in the dermis [80]. These lesions are indolent and tend to expand in a horizontal, plaque-like manner and do not invade into the dermal mesenchyme. RGP melanomas found in the dermis are usually surround by an intact basement membrane zone and are interpreted as invasive histologically, however, since they are contained, metastases does not occur [81]. Primary melanomas found in the RGP are easily removed by surgical excision with a cure rate that approaches 100% [82]. In culture, several cell lines derived from RGP melanomas lose their pigmentation markers such as tyrosinase and tyrosinase related protein 1 (TRP-1) however, the

expression of melanoma-associated antigens such as MART-1 are sustained [83]. Additional cellular features observed in RGP melanomas include lack of autocrine stimulation for growth and independence of growth factors [84].

Vertical Growth Phase (VGP)

The vertical growth phase (VGP) of the primary melanoma is characterized by focal, dermal growth that forms an expansile nodule [60, 85]. This stage of primary melanoma grows rapidly and penetrates the basement membrane that separates the epidermis from the dermal mesenchyme. These lesions contain a greater proportion of metastatically competent melanoma cells [86]. Certain attributes of VGP melanomas that predict whether or not they will become metastatic or not are: (1) the mitotic rate of the lesion mm^{-2}; (2) presence of tumor infiltrating lymphocytes; (3) the tumor thickness; (4) the anatomic site of the primary; (5) the sex of the patient; and (6) the histologic foci of complete regression of the primary lesion [87]. Thick vertical growth phase tumors have chromosomal abnormalities, usually at chromosomes 1, 6, and 7 and these genetic alterations appear in parallel with increasing biological aggressiveness. All VGP melanomas are tumorigenic and independent of the phorbol ester, 12-O-tetradecanoylphorbol-13-acetate (TPA). Additionally, the expression of proliferation markers such as the antigen Ki-67, is increased in VGP melanomas compared to RGP. The protein Ki-67 is a cellular marker strictly associated with cellular proliferation due to its presence during all active phases of the cell cycle and its absence in resting cells [88]. The dermal Ki-67 staining index (SI) in RGP melanomas is 3.5% whereas the Ki-67 SI in VGP was shown to be 13% [89]. Additionally, VGP melanoma cells display extensive,

non-random chromosomal abnormalities as opposed to those of RGP cells which are minor in comparison [85].

Part III: Contribution of genetic alterations in melanocytic neoplasia

All cancers are fundamentally genetic. The transformation of normal cells is caused by a series of genetic alterations including deletions, amplifications, chromosomal translocations and inversions [90]. Approximately 10% of melanoma cases result from the familial transmission of susceptibility loci in the germline [91]. Acquisition of the melanoma phenotype occurs as a stepwise process resulting from the accumulation of mutations at critical genetic loci that confers a growth advantage of the nascent "cancer" cells [92]. Normal cellular genes termed proto-oncogenes are converted through gain-of-function mutation to oncogenes which permit enhanced cellular proliferation. Tumor-suppressor genes act in a recessive fashion since the genetic alterations associated with these genes in carcinogenesis are loss-of-function mutations in which both alleles at the genetic locus must sustain inactivating genetic lesions in order for the transformation to occur [93, 94]. Most genes that are targeted for activation or inactivation during the development of melanoma are involved in the control of cellular proliferation or cellular survival.

A. Proto-oncogenes / tumor suppressor genes

The uncontrolled proliferation that represents the hallmark of neoplastic disease involves deregulated cell proliferation through the quantitative or qualitative activation of proto-oncogenes that lead to the aberrant expression or activation of their protein products, or high frequency deletion of tumor suppressor genes [95]. Activation of an oncogene is dominant in action over a proto-oncogene since only a single copy of an activated oncogene is required to have an impact on the transformation of the cell [96].

Many oncogenes encode growth factors and their receptors that participate in regulating cellular proliferation. Inherited mutations leading to the gain-of-function of proto-oncogenes or the loss-of-function of tumor suppressor genes increase individual cancer susceptibility [97]. Cancer predisposition resulting from a mutation in a tumor suppressor gene is inherited in a dominant fashion in that it is only necessary to inherit one copy of the gene to be predisposed for cancer development.

Receptor Tyrosine Kinases

Signal transduction pathways are used by cells to receive and process information to produce a cellular response. These molecular circuits detect, amplify, and integrate information from the outside to the inside of the cell generating responses such as changes in enzyme activity and gene expression in order to carry out the cellular responses. The protein products of oncogenes are involved in signal transduction and are represented by growth factors, growth factor receptors, small-molecular-weight GTPase, receptor tyrosine kinases, nonreceptor tyrosine kinases, serine/threonine kinases, and transcription factors [97, 98, 99, 100, 101].

Receptor tyrosine kinases are receptors that use intrinsic tyrosine kinases (RTK) activity to mediate their proliferative effects. RTKs consist of three domains: an extracellular N-terminal domain that binds to its specific ligands, a transmembrane domain that spans the plasma membrane and an intracellular C-terminal domain that contains intrinsic tyrosine kinase activity [102, 103]. Some RTKs are proto-oncogenes that are involved in alteration of reactive oxygen species (ROS), activation of

downstream signal transduction molecules, cellular proliferation, migration, and survival. Examples of such RTK proto-oncogenes include c-Kit, Eph, PDGF, Flt3, and c-Met.

KIT

The *KIT* receptor tyrosine kinase gene (*c-kit*) was first identified in 1987 [104]. KIT is a type III receptor tyrosine kinase characterized by a glycosylated extracellular ligand transmembrane binding domain and an intracellular segment containing a juxtamembrane inhibitory domain and two tyrosine kinase domains [105]. The ligand for KIT, stem cell factor (SCF, also known as kit ligand, steel factor, or mast cell growth factor) is expressed as a heavily glycosylated transmembrane protein whose biologically active form is a noncovalently associated dimer. Binding of SCF to KIT results in receptor dimerization, autophosphorylation, and activation of the intracellular tyrosine kinase domain. Once activated, KIT has been shown to initiate multiple downstream signaling pathways such as MAPK/MEK, PI3K/AKT and JAK/STAT [105, 106]. KIT and SCF are important for proper melanogenesis, proliferation, migration, and survival with loss of function of KIT resulting in the ability of melanocytes to migrate to distant sites from the neural crest during development [107]. Although KIT is expressed in some melanomas, loss of expression is observed with progression of the disease from superficial to invasive to metastatic stages suggesting that expression of the receptor in melanomas had tumor suppressive activities [108, 109]. Overexpression of KIT in melanoma cells resulted in reduced tumor growth and cell death [108]. However, it has been shown that specific subtypes of melanomas, particularly those of the acral lentiginous, mucosal, and chronic sun-damaged sites frequently harbor activating

mutations or increased copy number in the *KIT* tyrosine kinase gene. More specifically, patients with melanoma harbor activating mutation K642E (KIT^{K642E}) as well as a 7-codon duplication of exon 11 [110]. Melanoma patients with mutated KIT have been reported to respond to treatment using imatinib mesylate, an orally available ATP-competitive inhibitor of several tyrosine kinases including KIT [110, 111, 112].

c-MET

The receptor tyrosine kinase c-Met encodes the hepatocyte growth factor receptor (HGFR), a membrane receptor that is primarily expressed in epithelial and mesenchymal cells [113, 114]. Its normal function is associated with wound healing, liver regeneration, and embryonic development. Dysregulation of c-Met through overexpression, gene amplification, mutation, or a ligand-dependent autocrine/paracrine loop is known to play a significant role in the pathogenesis of many types of solid tumor types via mediating increased invasion and metastasis [103, 115].

The natural ligand for c-Met is hepatocyte factor/scatter factor (HGF/SF), a disulfide-linked α-β heterodimeric RTK that has been previously identified as a proto-oncogene and is produced predominantly by mesenchymal cells that acts primarily on Met-expressing epithelial cells in an endrocrine/paracrine fashion [116, 117]. HGF is known to be a paracrine factor that is produced by stromal and mesenchymal cells and act on Met-expressing cells [118]. Activation of c-Met by HGF leads to autophosphorylation of tyrosine residues located within the intracellular region that result in the intrinsic activation of key oncogenic pathways such as RAS, PI3K, STAT3, and β-catenin [119].

The HGF/c-Met signaling pathway leads to an array of cellular responses including proliferation, survival, angiogenesis, wound healing, tissue regeneration, scattering, motility, invasion, and branching morphogenesis [120].

PI3K/AKT/PTEN

The serine-threonine protein kinase, AKT (also known as protein kinase B or PKB) and phosphoinositide-dependent kinase 1 (PDK1) are important downstream targets of PI3K. The main biological consequences of AKT activation are cell survival and increased cell growth. AKT activation is known to involve in both mitogenic signaling and cell survival in a number of human cancer types. Human AKT exists in three isoforms: AKT1, AKT2 and AKT3. PI3K mediates cleavage of PIP_2, which produce PIP_3 at the inner surface of the plasma membrane. PIP which acts as a second messenger to recruit AKT through interaction of its pleckstrin homology (PH) domain, a domain conserved in signaling proteins that accumulate at sites of PI3K activation. Phosphorylation of AKT is dependent on phosphorylation, in part, by PDK1 [121, 122]. Activated AKT in turn mediates signaling through the phosphorylating inactivation of a multitude of downstream targets involved in apoptosis, including the phosphorylation of cyclic AMP response element--binding protein (CREB) as well as IκB kinase (IKK), which further activates central regulators of cell death: nuclear factor –κB (NF-κB) and p53. AKT-mediated induction of NF-κB occurs via activation of IκB which induces degradation of the NF-κB inhibitor IκB leading to release of NF-κB from the cytoplasm and translocation to the nucleus leading to the expression of survival genes such as IAP that promotes survival by inhibiting downstream activation of caspase-9 and -3 [123, 124,

125, 126, 127]. AKT influences p53 activity through phosphorylation of the p53-binding protein, MDM2. MDM2 regulates p53 function by targeting p53 for degradation by its E3 ubiquitin ligase. AKT phosphorylation of MDM2 allows increased translocation of the proteasome to the nucleus where it binds p53 resulting in its degradation [127, 128]. In addition, the oncological significance of amplified AKT expression has been well documented in gastric carcinoma, ovarian, pancreatic and breast tumors [129, 130, 131]. AKT phosphorylation of the apoptosis-inducing protein, Bad, prevents binding of Bad to the antiapoptotic Bcl-2-type proteins, Bcl-2 and Bcl- x_L. Bad promotes cell death by forming a non-functional hetero-dimer with the survival factor Bcl-x_L [132]. Upregulation of Bcl-x_L promotes survival by regulating coupled respiration through supporting ATP/ADP exchange across the outer mitochondrial membrane [133]. Phosphorylation of Bad by AKT prevents heterodimerization with Bcl- x_L restoring its anti-apoptotic function [134, 135]. In addition, it has also been implicated that PI3K-AKT modulates tumor-induced angiogenesis in part through hypoxia-induced factor-1α and NF-κB, which induces expression of the pro-angiogenic growth factor, vascular endothelial growth factor (VEGF) and suppression the endogenous anti-angiogenic molecule, thrombospondin-1 (TSP-1) [136, 137]. VEGF and its receptor, VEGFR are major angiogenesis inducers associated with tumor angiogenesis in numerous malignancies [138].

The PTEN tumor suppressor is a dual-specificity phosphatase, which has protein phosphatase activity and lipid phosphatase activity that antagonizes the PI3K-AKT pathway and is found to contain inactivating mutations in many human cancers including

melanoma. PTEN negatively regulates PIP_3-mediated signaling cascades by hydrolyzing the 3-phosphate to generate PIP_2 making PTEN critical in phosphatidylinositol homeostasis and regulating the proliferation and invasion of many cancer cells [139].

NRAS/BRAF

The mitogen-activated protein kinase (MAPK) pathway which encompasses the Ras/Raf/MEK-extracellular signal-regulated kinase 1 and 2 (ERK1/2) signaling cascade is one of the most frequently dysregulated pathways in melanoma as well as other human cancers [140, 141]. Mutations in codon 12, 13, or 61 of the three *RAS* genes convert the three major isoforms, H-RAS, K-RAS and N-RAS respectively, into oncogenes [142, 143]. The RAS family of small G proteins transduces signals triggered by extracellular growth factors, a wide variety of hormones, and differentiation factors. Activation of RAS proteins leads to an exchange of GDP with GTP dependent on the recruitment of guanine nucleotide exchange factors (GEFs) to the cell membrane where RAS resides. In response to receptor activation, the RAS GEF, SOS1 (son of sevenless) is recruited to the membrane by the adaptor protein GRB2 (growth-factor-receptor-bound protein 2) which recognizes tyrosine phosphate docking sites located on the receptors themselves or on the receptor substrate proteins [144]. The binding of SOS1 to GBR2 causes its localization to the plasma membrane where it activates membrane bound RAS [145]. Phosphorylation of the SOS complex mediated by activated ERK signaling induces disassembly and termination of RAS activation. Activated RAS has a high affinity for, and binds to downstream RAF kinases, causing their translocation to the cell membrane where RAF activation occurs [146]. In melanoma, activating mutations in the N-RAS

isoform are the second most commonly activated oncogene leading to constitutive activation of MAPK signaling followed by activating mutations in BRAF [147]. Activating mutation Q61R has been found to be common in familial melanoma cases suggesting its significance as a genetic marker for familial melanomas [148, 149].

RAF genes encode serine/threonine-specific protein kinases. In mammals, three isoforms of Raf proteins, Raf-1 (or C-Raf), A-Raf, and B-Raf are expressed with C-Raf being ubiquitously expressed in all tissues and isoforms A and B having more specialized functions. Deficiencies in A-RAF expression have been shown to result in intestinal and/or neuronal defects while defects in B-RAF expression show defects in neuroepithelial differentiation and the maturation and maintenance of endothelial cells [150]. Although the three Raf proteins share high amino acid homology, they are differentially regulated and exert different functions. B-Raf has higher affinity and stronger stimulation toward MEK than either A-Raf or C-Raf due to its high binding affinity for GTP- bound Ras proteins [151]. Activation of Ras causes B-Raf to translocate to the plasma membrane from the cytosol and bind to the activated, GTP-bound Ras. Inappropriate and/or persistent activation of B-Raf results in abnormal differentiation and proliferation and cancer development through activation of the MAPK pathway [152]. Among the different B-Raf mutations, a single-base missense substitution resulting in a T to A transition at nucleotide 1799 causes the substitution of a valine for a glutamic acid at codon 600 (V600E) of the kinase domain. The mutant $BRAF^{V600E}$ causes the hyper-activation of the MAPK pathway as a result of a conformational change in the protein structure caused by a phosphomimetic glutamic

acid located between the Thr 598 and Ser 601 phosphorylation site [153]. This disrupts the interaction between the P-loop and the activation segment of the B-RAF protein [154, 155]. Activating mutation $BRAF^{V600E}$ is the most prevalent activating mutation found in human malignant melanomas, being detected in 66% of cases [156]. In addition, approximately 70% of benign nevi and 10% of RGP melanomas carry the activating mutation implying that B-RAF may be involved in the initiation rather than progression of the disease [157, 158].

Cyclin-dependent kinase N_2A ($CDKN_2A$)

For decades, familial occurrences of melanoma and dysplastic nevi were recognized in families having common deleterious germline mutations found on chromosome 9p21 [159, 160]. This locus generates at least two alternatively spliced variants: the cyclin-dependent kinase inhibitor $_2$A ($CDKN_2A/p16^{nk4A}$) and $p14^{ARF}$, translated in alternate reading frame (ARF). Both proteins are potent tumor suppressors that function in cell cycle regulation. $p16^{nk4A}$ binds to and inhibits activity of cyclin dependent kinases 4 and 6 (CDK4 and CDK6) preventing them it from phosphorylating the retinoblastoma (RB) protein [161]. G_1-S phase transition is usually dependent on hyperphosphorylation of RB by the cyclin D_1/CDK_4 complex [162, 163]. Phosphorylation of RB causes the release of transcription factor E2F1, an inducer of S-phase genes. Loss of $p16^{nk4A}$ promotes G_1-S transition and re-entry into the cell cycle. $p14^{ARF}$ binds to human double minute-2 (HDM2) protein at its *N*-terminus and promotes its rapid degradation. Loss of $p14^{ARF}$ results in a decrease in HDM2 degradation and an increase in HDM2-mediated ubiquitination and degradation of p53 [164]. In both the

germline and somatic levels, lesions in the $CDKN_2A$ region eliminate both the RB and p53 pathway through loss $p16^{nk4A}$ of and $p14^{ARF}$, respectively.

B. Current therapies

Staging and Surgical Removal

Once diagnosed, early stage melanoma is commonly treated by surgical removal of the tumor. However, if melanoma becomes metastatic, the cancer can rapidly spread throughout the body, resulting in poor prognosis and reduced survival. Despite screening and early detection programs, the rising incidence of melanoma has been correlated with stable or increasing melanoma-related mortality in the US [58].

Melanoma is classified into different stages based on the size, growth, and spreading of the tumor. The tumor-node-metastasis (TNM) classification system is used for all solid tumors based on the size and extension of the primary tumor, its involvement of lymphatics and presence of metastases [165, 166]. T denotes the description of the primary tumor in regard to size and whether it has invaded surrounding tissue. N denotes the degree of nodal involvement. M denotes the degree of metastasis to distant sites. Further classification by use of letters and/or numbers after each category provides further description as to the degree of the T, N or M staging with each cancer type having its own version of this classification system. All TNM cancer staging is determined by either a clinical stage or a pathological stage [167]. The clinical stage is an estimate of how much cancer there is based on an overall physical exam including imaging tests, and tumor biopsies. This stage is a key determinant for deciding the type of treatment and

provides a baseline for the overall response of the cancer to therapies. Pathological staging (also called surgical staging) allows direct examination of the tumor following removal of tissue during surgery or a biopsy allowing microscopic examination of the tumor. Clinical stage and pathological stage are denoted by a small "c" or "p", respectively preceding T, N or M. Once the values for T, N and M have been determined they are combined and the overall stage is assigned [167, 168]. The overall numerical staging (also known as Roman numeral staging) describes the degree that the cancer has advanced from the primary stage using numerals I, II, III and IV (including 0) [169, 170]. Stage 0 indicates that the malignant melanoma is localized to the part of the body where it initially developed (carcinoma *in situ*). Stage IV is the most advanced and indicates that more cancer is present than in the lower stages. Stage IV is usually associated with metastasis to distant organs throughout the body. Histological features such as the tumor thickness, mitotic rate and ulceration of the primary melanoma become important hallmarks of melanoma prognosis and staging [59]. During diagnosis, doctors will determine the stage of the melanoma through several procedures including biopsies, x-ray imaging (particularly in the chest area for lung metastasis), computed tomography (CT) scan, magnetic resonance imaging (MRI) and positron emission tomography (PET) scan [171, 172]. Once diagnosed, stage 0 and I melanomas and/or nearby lymph nodes are surgically excised [60, 61]. In its earlier stages, melanoma is confined to the skin, where the disease is curable in a high percentage of cases through surgical removal of the tumor [62]. Once melanomas undergo metastasis and surgical removal is not sufficient to remove the tumor, patients undergo adjuvant cancer therapies such as chemotherapy, radiotherapy and immunotherapy.

Chemotherapy

As is the case for numerous types of cancer, chemotherapy remains the most common form of treatment for melanoma. Chemotherapy is generally initiated along with surgical removal of the tumor in the case of melanoma. Currently, dacarbazine (DTIC) is the only FDA-approved chemotherapeutic agent for the treatment of metastatic stage IV melanoma [173]. Although the exact mechanisms of action are not known, DTIC acts as an alkylating agent resulting in methylation of nucleic acids and inhibition of DNA, RNA and protein synthesis. Resistance develops from increased activity of DNA repair enzymes such as O6-alkylguanine-DNA alkyltransferase (AGAT). DTIC is a prodrug and is metabolized by microsomal cytochrome P450s to the active metabolites MTIC (monomethyl triazeno imidazole carboxamide) and AIC (5-aminoimidazole-4-carboxamide). Studies conducted in the 1970s showed treatment response rates ranging from 10 to 20% following intravenous administration of the compound [174]. Patients treated with DTIC intra-arterially showed a reduction of lesions after 20 months of treatment, although distant metastasis was not significantly affected [175].

Derivatives of DTIC, such as the prodrug temozolomide (TMZ), are also under investigation as potential therapies for melanoma. TMZ acts in a similar manner to DTIC having the ability to alkylate/methylate DNA, preventing cell proliferation and triggering tumor cell death, but appears to undergo faster chemical conversion to the therapeutically active compound MTIC than DTIC due to its rapid chemical conversion in systemic circulation at physiologic pH to MTIC [176]. In addition to being orally administered,

TMZ had an improvement on the response rate, overall survival and progression-free survival of patients with advanced melanoma [177].

Unfortunately, melanoma is highly chemo-resistant after prolong treatment with DTIC or TMZ and thus ongoing studies exploring combinatorial therapies and new compounds to increase the efficacy of currently available drugs [178].

Radiotherapy

The goal of radiotherapy is to cause reproductive cell death of all malignant cells in a tumor [179]. Radiotherapy for cancer treatment involves the use of ionizing radiation caused by highly energized subatomic particles or electromagnetic waves to cause cell death or genetic change either directly or indirectly. The class of lesion which correlates with cell death is the DNA double strand break (DSB) that can be induced directly by ionization of the DNA or indirectly by the formation of free radicals [180]. The majority of lesions are repaired rapidly either by conserved enzymatic pathways such as homologous recombination (HR) repair which occurs mainly in the S and G_2 phases of the cell cycle or by non-homologous end joining (NHEJ) which can occur throughout the cell cycle [181]. Lesions that are misrepaired result in a loss of fidelity of the genetic message and give rise to mutations. Lesions that remain unrepaired may generate chromosomal aberrations leading to cell death following several rounds of the cell cycle. This mode of death is referred to as mitotic or clonogenic cell death and is the major mechanism by which the majority of solid tumors respond to clinical radiotherapy [182]. Alternatively, apoptotic cell death also occurs following irradiation. Radiation-induced

apoptosis involves DNA damage repair (DDR) response and subsequent initiation in the activities of the phosphatidyl-inositol-3-OH kinase-like kinases (PIKKs), ataxia telangiecstasia mutated (ATM) and aminomethyltrimethylpsoralen (AMT)-and Rad3-related (ATR) signal transduction pathways that inhibit cell-cycle progression. The ATM kinase is activated following DNA damage whereas ATR is critical following the arrest of replication forks during cellular replication [183]. ATM/ATR activation inhibits the mitosis-promoting activity of cyclin B/CDK1 kinase causing cell cycle arrest at the G_2/M check point preventing cells from initiating mitosis [184] to permit repair of DNA damage, if the damage is not repaired within a given time (about 24 hours) the cells undergo apoptosis. Numerous studies have cast doubt on the effectiveness of radiotherapy for the treatment of melanoma, categorizing this cancer as radio-resistant [185, 186]. However, Olivier et al. found a positive correlation between radiotherapy dose and survival in patients with melanoma [187]. Indeed, numerous other studies have recorded various rates of melanoma palliation after radiotherapy treatment, offering a new perspective on the use of this therapy as a treatment tool for melanoma [188, 189, 190].

Immunotherapy

Immunotherapy encompasses a series of methods used to target tumor cells for eradication by stimulation of the immune system. The most common method used, monoclonal antibody therapy, takes advantage of the unusual antigens found in the surface of tumor cells. However, the immunosuppressive effect of melanoma limits the effectiveness of this treatment [191]. Numerous biological components that are present at

the tumor site, such as transforming growth factor β, nitric oxide, metalloproteinases and interleukin 10, all contribute to the immunosuppressive cell network.

The first immunotherapy approved by the Federal Drug Administration (FDA) for the treatment of unresectable melanoma was the cytokine interlekukin-2 (IL-2). The administration of IL-2 by intra-venous injection causes the activation of killer T-cells that can then attack tumor cells. Different doses of IL-2 are used when treating metastatic melanoma; however, high-dose IL-2 has proven to be the most effective treatment in which response rates generally range from 10% to 20% [192, 193, 194].

Cytotoxic T lymphocyte-associated antigen-4 (CTLA-4) is a protein receptor that is recruited to the plasma membrane on T-cell activation where it binds to members of the B7 family of accessory molecules expressed by dendritic cells and other antigen-presenting cells [195] CTLA-4 ligation effectively inhibits further activation lessening the chances of autoimmune response. Ipilimumab (Yervoy®) is the most recent human monoclonal antibody approved by FDA for the treatment of melanoma. Ipilimumab is a monoclonal antibody to CTLA-4 blocking its inhibitory signal therefore allowing cytotoxic T lymphocytes to recognize and destroy cancer cells [196]. Several studies have shown that the drug effectiveness against malignant melanoma varies widely upon patients and also causes a variety of immune related adverse events [197, 198].

Part IV. Glutamate and cancer

The amino acid L-glutamine is a precursor for peptide and protein synthesis, amino sugar synthesis, and nucleotide synthesis [199]. This amide of L-glutamate is the most abundant free amino acid in the human body with a concentration ranging from 500-900 μmol/L depending on tissue type [200, 201]. In the majority of cell types, the glutamine is rapidly converted to L-glutamate (glutamate), which is the most abundant intracellular amino acid. Glutamate is a key component in cellular metabolism contributing as a metabolic fuel for intermediates in energy producing pathways as well as an important component in the body's disposal of excess, or waste, nitrogen [202, 203]. Glutamate is a principal excitatory neurotransmitter in the mammalian central nervous system where it is involved in cognitive functions such as learning and memory. In an attempt to appease the insatiable needs that transformed cell types require to sustain their energy expenditure and biosynthetic requirements, tumor cells become major consumers of glutamine.

A. The role of glutamate in normal and cancer cells

Normal eukaryotic cells process the conversion of glucose to pyruvate via the metabolic pathway glycolysis in the cytosol, then to carbon dioxide in the mitochondria under aerobic conditions through the process of cellular respiration [204, 205]. In oxygen deprived environments, or hypoxic conditions, glycolysis is the preferred energy-generating pathway resulting in a decrease in the amount of pyruvate available to the oxygen-consuming mitochondria. It has been observed that even in the presence of physiological relevant levels of oxygen cancer cells have the ability to reprogram their glucose metabolism allowing them to preferentially produce energy via the glycolysis

while maintaining the same level of respiration. This "anaerobic respiration" is a process known as the Warburg Effect [206, 207, 208]. Although aerobic metabolism including oxidative phosphorylation is up to 15 times more efficient then anaerobic metabolism. However, the metabolism of cancer cells occurs at an increased glycolytic rate up to 200 times than those of their normal surrounding tissues [209, 210]. Cellular ATP production during such high rates of glycolytic flux can easily exceed the ATP produced via oxidative phosphorylation. This high consumption of glucose requires much more nicotinamide adenine (NAD+), which is consecutively regenerated from the conversion of pyruvate to lactate by increased expression of lactate dehydrogenase making glycolysis self-sufficient [211].

Glutamine serves as a major respiratory fuel of tumor cells and has been shown to be the absolute requirement over glucose for many malignant cell types [212]. The importance of glutamine in tumor cell metabolism is derived from its ability to satisfy the bioenergetic needs of tumor cells as well as providing intermediates for macromolecular synthesis [213]. During periods of rapid growth, the cellular demand for glutamine surpasses its supply. At this time glutamine becomes essential and it is this reason that glutamine has been designated a 'conditionally' essential amino acid. Traditionally, the role of glutamine has been viewed to function as storage for excess nitrogen and to traffic the nitrogen within, and between, various organs. Metabolically, glutamine is used directly for reactions that require its γ-nitrogen, such as nucleotide and hexosamine synthesis, or indirectly in reactions that utilize the α-nitrogen (amino nitrogen) or its carbon skeleton for energy production and biosynthesis [214]. These indirect reactions

are necessary to generate the metabolic intermediates required for cell growth, which begin with the conversion of glutamine into glutamate. Being an abundant extracellular nutrient, glutamine is regularly converted into glutamate by phosphate-dependent glutaminase (GLS), an enzyme found within the inner mitochondrial membrane that has been shown to be overexpressed in both solid tumors and many tumor cell lines [215, 216]. In fact, the majority of glutamine consumption in cancer cells is owed to mitochondrial GLS activity. Consequentially, tumor cells have large intracellular pools of glutamate; through increased GLS activity, the abundantly available amino acid glutamine is converted to less abundant glutamate, there-by maintaining the cells' increasing demand for glutamate metabolism. This is the initial step in glutaminolysis, a series of biochemical reactions by which glutamine is degraded to glutamate, aspartate, pyruvate, alanine, citrate and carbon dioxide thereby providing metabolic intermediates to feed and maintain cells in which aerobic respiration is the biosynthetic hub [211].

B. Aerobic glycolysis

Glycolysis and glutaminolysis both share the capacity to generate NADPH and the secretion of lactate (Figure 2). As mentioned previously, the initial step of glutaminolysis is the conversion of glutamine to glutamate, which is used, intracellularly, as a primary source of energy for proliferating cells [204]. This rate-limiting step of glutamine metabolism is the deamidation reaction catalyzed by GLS. The products formed from this reaction, glutamate and ammonia, are released into the cytosolic compartment of the inner mitochondrial membrane. Glutamate is then further metabolized by conversion to α-ketoglutarate via either oxidative deamination by

glutamate dehydrogenase (GIDH) or alanine transaminase (ALT) (Figure 3). The deamination reaction is localized to the mitochondrial matrix compartment and yields both α-ketoglutarate and ammonium. The transamination can occur in either the cytosolic and mitochondrial compartments and produces α-ketoglutarate and alanine [217, 218, 219]. Alpha-ketoglutarate is a key intermediate in the citric acid cycle where it is metabolized to regenerate oxaloacetate (OAA) through the production of malate. Mitochondrial metabolism of α-ketoglutarate into malate also generates NADPH via oxidation into pyruvate in the cytosol [220]. The NADPH produced is used by the rapidly metabolizing cell as a required electron donor in lipid synthesis and nucleotide metabolism as well as in antioxidant defense by maintaining glutathione (GSH) in its reduced state. GSH is the major thiol-containing endogenous antioxidant used by the cell to protect against various sources of oxidative stress. Maintaining a supply of GSH is critical for tumor cell survival since the elevated metabolic demand of the rapidly growing cell generates DNA-damaging byproducts that lead to oxidative stress [221].

Proliferating cancer cells consume vast amounts of glucose but only a small portion of which undergoes oxidative phosphorylation, even in the presence of sufficient oxygen [206]. It has been established that these rapidly dividing cells prefer to utilize glycolysis, which yields less net ATP molecules per glucose molecule. However, glycolysis can occur in hypoxic conditions that are usually associated with the highly necrotic regions of rapidly proliferating tumor masses [222]. The end-product of glycolysis, pyruvate, can then enter the TCA cycle or is reduced into lactate by lactate dehydrogenase A, which is then excreted in the interstitial fluid. Within a tumor mass is

a composition of genetically heterogeneous subpopulations of cancer cells that differ in their energy production pathways [223, 224]. It is possible that these subpopulations have the ability to function symbiotically within the tumor mass; one subpopulation of cells, consisting of hypoxic, glucose-dependent cells, secretes lactate as waste while the other subpopulation, located in a region that is more oxygenated, preferentially imports and utilizes the lactate produced by the first subpopulation to be used in the citric acid cycle [225, 226]. The idea of "metabolic symbiosis" that exists between hypoxic and aerobic cells in which lactate produced by hypoxic cells and taken up by aerobic cells to be used in oxidative support the bioenergetic needs of rapidly proliferating cancer cells within a solid tumor mass.

Cancer cells utilize TCA cycle intermediates to provide proliferating tumor cells with biosynthetic precursors (cataplerosis) as well as the production of ATP. The influx of metabolic intermediates in an attempt to maintain the mitochondrial TCA cycle (anaplerosis) is due to, in large part, glutaminolysis in which the first step is the conversion of glutamine to glutamate [211]. Beyond its role in intermediary metabolism and biomass production, glutamate is also involved in influencing signal transduction pathways involved in promoting cellular proliferation, survival, and tumorigenesis.

Part V: G-protein coupled receptors

Guanine nucleotide binding-protein coupled receptors (GPCRs; G-protein coupled receptors) comprise a large and diverse family of seven-pass membrane helix proteins found in most eukaryotic organisms. The principal function of GPCRs is to

transmit information about the extracellular environment via recognition of a variety of ligands including peptide and non-peptide hormones and neurotransmitters, chemokines, prostanoids and proteinases, biogenic amines, nucleosides, lipids, growth factors, odorant molecules and light to the interior of the cell by interacting with G-proteins [227, 228, 229, 230]. G-proteins are heterotrimeric subunits, G_{α}, G_{β} and G_{γ}, associated with the inner surface of the plasma membrane where they function as dimers. These G-proteins regulate the activity of small molecules that act as second messengers. Most of the human GPCRs can be divided into five families based on phylogenetic criteria: *Glutamate, Rhodopsin, Adhesion, Frizzled/Taste2 and Secretin* (GRAFS classification system) [231]. The total number of verified human GPCRs is over 800 members. The Glutamate family consists of 22 human proteins categorized into ionotropic receptors (iGluRs) and metabotropic receptors (GRMs). The iGluR family consists of *N*-methyl-D-aspartate receptors (NMDAR, α-amino-3-hydroxy-5-methyl-4-isoazolepropionic acid receptors (AMPAR), and kainite receptors (KAR). The GRM family consists of eight different subtypes (GRM1-8) [232]. The GRMs are coupled to G-proteins, which distinguishes them from iGluRs, which contain ligand-gated ion-channels. The GRMs are key receptors in the modulation of excitatory synaptic transmission in the central nervous system (CNS). The eight subtypes of GRMs are further classified into three groups (I, II, III) based on sequence homology, signal transduction pathways, and agonist selectivity. GRM1 and 5 belonging to subgroup I; GRM2 and 3 belonging to subgroup II; and GRMs 6, 7, and 8 belonging to subgroup III [233]. The structures of GRMs are composed of a heterotrimeric extracellular region, a seven-α helical transmembrane region and a cytoplasmic region. The extracellular region is further divided into the ligand-binding

region (LBR) and the cysteine–rich region. The LBR has a sequence homologous with the extracellular regions of both iGluR and the γ-amino butyric acid (GABA) receptor [234, 235]. In recent years, expression of GRMs also has been detected in non-neuronal cells (Table 1), suggesting GRMs may also function in non-neuronal cells.

Ionotropic glutamate receptors (iGluRs) are ion-gated channels where cations such as Ca^{2+}, K^{+}, and Na^{+} are transferred into the intracellular cytoplasm upon binding of glutamate to the receptor. These iGluRs are classified into three different classes based on the homology and agonist/ antagonist response: N-methyl-D-aspartate (NMDA), α-amino -3-hydroxy -5-methyl-4- isoxazole propionic acid (AMPA), and Kinate Receptor (KAR) [236, 237]. The NMDA (N-methyl-D-aspartate) receptor is highly permeable to calcium ions and plays a critical role in glutamatergic signaling in the synapse. Abnormal activation has been suggested to lead to apoptosis of neuronal cells, which is observed in many neuronal disorders including Alzheimer's disease and Huntington's disease [238, 239]. The AMPA (α-amino -3-hydroxy -5-methyl-4- isoxazole propionic acid) receptor is also an ion channel transferring Na^{+} and K^{+} ions preferably with low affinity to calcium ions. AMPA receptor has four isoforms: AMPAR1 (GluR1)--4 (GluR1-GluR4). Most AMPARs are composed of symmetrical heterotetramers, mainly dimmer of GluR2 with dimmer of GluR1, GluR3 or GluR4 [240]. GluR2 subunit determines the permeability of calcium of AMPA receptor. When GluR2 is absent, calcium ion is permeable together with K+ or Na+ ions [241]. There are five types of KAR subunits, GluR5-GluR7, KA1 and KA2. They are less well understood than NMDA and AMPA and are involved in excitatory neurotransmission [242].

A. GPCR signaling

The two principal signal transduction pathways involving GPCRs are the cAMP signaling pathway and the phosphatidylinositol signaling pathway. Glutamate-stimulated activation causes a conformational change in the extracellular domains, which catalyze the exchange of a GTP for a GDP on the Gα subunit of the intracellularly coupled G-protein [229, 243]. This exchange decreases the affinity of the Gα subunit for the Gβγ monomer at which time they either dissociate or rearrange [244, 245]. The dissociated Gα and Gβγ subunits interact with and modulate downstream signaling targets including adenylyl cyclases, phosphodiesterases, phosphlipases, tyrosine kinases, and ion channels [246, 247]. Group I GRMs are coupled to $G_{\alpha q}/G_{\alpha/11}$ G-proteins that, upon glutamate-mediated activation, result in stimulation of phospholipase C beta (PLC_{β}) [248]. Activation of PLC_{β} causes hydrolytic cleavage of phosphatidylinositol-4, 5-diphosphate (PIP_2) resulting in the formation of diacyl glycerol (DAG) and inositol 1, 4, 5-triphosphate (IP_3) [227]. DAG remains bound to the membrane while IP3 is released as a soluble structure into the cytosol. Release of these secondary messengers results in increased calcium release from the endoplasmic reticulum and activation of protein kinase C (PKC) which phosphorylates other molecules, leading to altered cellular activity (Figure 4). Group II and III GRMs are coupled to $G_{\alpha i/o}$ G-proteins that, upon activation prevent the formation of cyclic adenosine monophosphate (cAMP). Upon activation, group II GRMs couple to $G_{\alpha i/o}$ subunit. $G_{\alpha i/o}$ G-proteins can inhibit adenylyl cyclase activity. Activation of the $G_{\alpha i/o}$ results in $G_{\alpha i/o}$ -mediated inhibition of adenylyl cyclase causing a reduced production of cyclic adenosine monophosphate (cAMP) [229, 249].

GPCRs comprise the largest known family of cell surface receptors that mediate cellular responses to a diverse array of signaling molecules including hormones, neurotransmitters, and chemokines. In addition, potent mitogens such as thrombin, bombesin, lysophosphatidic acid (LPA), gastrin-releasing peptide (GRP), endothelin and prostaglandins can stimulate cell proliferation by interacting with their cognate GPCR in various homologous cell types [250, 251, 252, 253, 254].

A fundamental trait of cancer cells involves their ability to sustain chronic proliferation [95]. In normal cells, the production and release of growth-promoting signals that allow entry and progression through the cell cycle are tightly regulated [255]. This regulation maintains cellular homeostasis promoting normal tissue structure and function and is controlled, in part, by growth factors that bind cell-surface receptors, which usually transmit signals through branched signaling pathways. By deregulating these signals, cancer cells are able to bypass regulatory control allowing them to proliferate and grow unconditionally. Cancer cells can acquire the ability to sustain proliferative signaling by producing these growth factors themselves in which the cells respond through the expression of cognate receptors which results in autocrine proliferative stimulation [256, 257]. Alternatively, cancer cells may send signals to the surrounding tissue in a paracrine-like manner causing them to release various growth factors that promote growth of the cancer cells [256]. Activation of the surface receptors may also cause the constitutive activation of downstream signaling pathways.

Overexpression of GPCRs is detected in various cancer types, contributing to tumor cell growth once activated by circulating or locally produced ligands. The oncogenic potential of G protein-coupled receptors was revealed with the discovery of the *MAS* receptor in 1986, which provided a direct link between misregulated cell growth and GPCRs [15]. In contrast to most oncogenes identified at that time, *MAS* did not harbor genetic mutations resulting in its constitutive activation. Subsequent to its discovery, studies demonstrated that wild-type GPCRs have the ability to become tumorigenic when exposed to an excess of locally produced or circulating ligands and agonists while other GPCRs harboring mutations in key conserved residues can have transforming activity even in the absence of their ligands [244, 246, 247, 258, 259, 260, 261]. It has also been found that the level of expression of GPCRs is not as imperative to oncogenesis as is the receptor simply being expressed [261]. Since then, abnormal functioning of GPCR pathways have been shown to be the cause of several human diseases, and a large body of evidence links aberrant G-protein signaling to the development and progression of certain cancers [247].

B. G-protein coupled receptors and cellular transformation

The oncogenic transformation of cell types by way of GPCRs occurs, in part, by the establishment of autocrine or paracrine feedback in which the cell releases the ligand which binds and activates the receptor, maintaining its activation, as well as that of downstream effector proteins leading to enhanced cell proliferation [262, 263]. GRMs are members of GPCR with glutamate as the natural ligand [264, 265]. Glutamate is the predominant excitatory neurotransmitter in the central nervous system and stimulates

both ionotropic (ligand-gated ion channels) and metabotropic (G-protein-coupled) glutamate receptors [266]. Previously, glutamate signaling was believed to be exclusive to the central nervous system (CNS). It has since become apparent that various peripheral, non-neuronal cells express different types of glutamate receptors and these receptors are required for normal physiological function [267]. Studies have demonstrated that not only are GRMs involved in the normal maintenance and regulation of physiological homeostasis, but they can also be involved in the progression of a variety of human malignancies. Initially, because of prior implications of GPCR expression being exclusive to the CNS, the first speculations of GRMs in human cancers were in neuronal tumors such as neuroblastoma, medulloblastoma and glioma [268, 269, 270]. It was found that among these neuronal tumors that released excess amount of glutamate into the surrounding microenvironment were growing at a much-increased rate compared to neuronal tumors that were not secreting glutamate into their surroundings [271]. Subsequent studies revealed that inhibition of glutamate release correlated with a decrease in the proliferation of not only neuroblastoma, rhabdomyosarcoma, brain astrocytoma, but also thyroid carcinoma, lung carcinoma, colon adenocarcinoma and breast carcinoma while having no effect on the growth rates of normal human fibroblast or bone marrow stromal cells [270].

C. Ectopic expression of GRM1

Our group has previously described an unknown mechanism of melanoma pathogenesis in which the expression of an otherwise normal receptor, metabotropic glutamate receptor 1 (GRM1) in an unnatural cellular environment (melanocytes) is able

to upregulate cell proliferation and tumor development *in vitro* and *in vivo*. Chen and colleagues have established a transgenic mouse line (TG-3) that spontaneously develops melanoma with 100% penetrance that was constructed using a 2-kb genomic fragment, termed clone B, which was previously shown to commit fibroblasts to undergo adipocyte differentiation [8, 9]. In an attempt to establish an animal model of obesity, five founder animals were established using clone B DNA: TG-1 through -5. Instead of the expected obese phenotype, one of the five founders, TG-3, developed heavily pigmented lesions on the ears, around the eyes, and the perianal region at approximately eight months of age [9]. Upon histological analyses these pigmented lesions were identified as melanoma. Further examination shown these lesions were metastatic as evident by detecting these pigmented lesions in distant organs including the lymph nodes, brain, bone, lung and muscle. Using physical mapping we identified a single insertion of clone B in mouse chromosome 10, region A2, which is orthologous to human chromosome 6q23-24. Further molecular mapping found a concurrent insertion of clone B in a head-to-head, head-to-tail, tail-to-tail configuration and a deletion of approximately 70-kb of the host sequences located in intron 3 of the gene encoding GRM1 [158]. Assessment of GRM1 at both the protein and mRNA levels revealed the expression of the murine form of metabotropic glutamate receptor 1 only in the pigmented lesion but not normal counterpart. These results suggested that ectopic expression of GRM1 in melanocytes might be the driving basis for melanoma development [10]. To verify this hypothesis, we engineered a new transgenic mouse line [TG(Grm1)EPv] directing GRM1 expression in melanocytes under the control of a melanocyte-specific promoter, dopachrome tautomerase (DCT). This new transgenic line displays a melanoma susceptibility

phenotype and progression very similar to the TG-3 line [158]. It was concluded that *in vivo*, aberrant GRM1 expression in melanocytes is sufficient to induce spontaneous melanoma development with 100% penetrance. Progeny that are heterozygous at the transgenic integration site develop melanotic lesions as soon as 4 months post-natal while those homozygous at the integration site develop lesions within 30 days after birth. Ohtani and co-workers confirmed our observation with an inducible GRM1 transgenic mouse model, when the expression of GRM1 is conditionally activated in adult mice melanoma develops in these animals 100% of the time [272]. The results that GRM1 has a role in melanocytic neoplasia in the murine system prompted our group to examine human melanoma for ectopic expression of the human form of metabotropic glutamate receptor 1. Examination of numerous melanoma biopsies and cell lines demonstrated aberrant expression of the receptor in approximately 60% of the samples suggesting that GRM1 may be involved in the oncogenesis of a subset of human melanomas [10, 11]. These findings as well as those by others prompted our group to explore the underlying mechanisms of GRM1- mediated melanocytic transformation. In a set of studies we confirmed that GRM1 expression in melanocytes confers oncogenic activities *in vitro* and is sufficient to cause malignant phenotype *in vivo* [273].

In both the murine and human melanoma cell lines, stimulation of GRM1 by glutamate results in similar if not identical formation of second messengers as described above for the CNS. One of the second messengers, DAG, stimulates PKC. PKC plays a key role in a multitude of cellular processes including apoptosis, malignant transformation, and metastasis [274] and once it is activated it in turn can activate the

MAPK and PI3K/AKT pathways [275, 276, 277, 278, 279]. It is well known that the RAS-RAF-MEK-ERK module of the MAPK signaling cascade regulates cell proliferation and inhibits apoptosis. PI3K/AKT pathway activation is important for tumor cell survival, epithelial-mesenchymal transition (EMT), and angiogenesis [280]. In addition, gain-of-function mutations causing constitutive activation in G-proteins also result in the activation of downstream effector pathways leading to uncontrolled cell proliferation and cell survival. This is often a consequence of specific amino acid substitutions in the GTP binding region of the Gα subunit resulting in defective GTPase activity. The inability for GTP to be cleaved to GDP allows constitutive activation of downstream effector molecules. Such hypermorphic mutant G proteins in melanocytes were initially found to cause increased dermal pigmentation in transgenic mice. It was later found that the two functionally related G protein subunits, GNAQ and GNA11 encoding the stimulatory $G\alpha_q$ and $G\alpha_{11}$ subunits of heterotrimeric G-proteins respectively, are genetic hotspots for somatic mutations found in early uveal melanoma pathogenesis [281]. These mutations were also detected in benign intradermal melanocytic tumors as well as primary and metastatic ocular melanocytic tumors. Therefore, activation of ectopically expressed metabotropic glutamate receptors in human cells upregulate signaling pathways known to be important in the pathogenesis of human cancers associated with increased growth and angiogenesis while interruption of such pathways would result in a decrease in cell proliferation and survival.

The acquisition of tumor phenotypes is dependent not on one, but on successive alterations in the genomes of neoplastic cells. Specific genotypes confer selective advantages on subclones of cells enabling them to outgrow, and eventually dominate, the

local tissue environment. This idea of multistage tumor progression can be viewed as a succession of clonal expansion each triggered by chance acquisition of mutant genotypes transitioning a cell from normal through pre-malignant and eventually cancer. One stage involved in malignant transformation of cell types is the ability of a cell to maintain its capacity to spread and divide in the absence of a stable or inter surface to attach. In a study performed by Prickett et al, exon capture sequencing of GPCRs in malignant melanoma specimens identified activating mutations within a region encoding for a member of the group II metabotropic glutamate receptors, GRM3. The mutations were found throughout the coding region and affected the extracellular domains as well as the seven-transmembrane domain with two mini-hotspots located proximal to the transmembrane domains. Four somatic mutations ($GRM3^{E767K}$, $GRM3^{S610L}$, $GRM3^{G561E}$, and $GRM3^{E870K}$) were found to selectively regulate the phosphorylation of MEK1/2 kinase *in vivo* and induce micro metastasis *in vivo*. This activation resulted in the increased migration and anchorage independence growth of melanoma cells. These studies suggest the existence of a melanoma tumor type in which activating mutations in GRM3 can lead to hypersensitivity to agonist stimulation of the MEK-MAPK pathway that bypasses the RAF/RAS genotypes.

In addition to melanoma, inappropriate glutamatergic signaling has been shown to be sufficient in the dysregulating growth leading to the transformation of other cell types. The ectopic expression of GRM1 alone was able to induce the neoplastic transformation of immortalized baby mouse epithelial cells (iBMK) *in vitro* and promote tumor cell proliferation *in vivo* [282, 283]. The iBMK cell model was engineered to be immortal

but not tumorigenic while also retaining normal epithelial characteristics. It was shown that full-length wild-type GRM1 is tumorigenic when ectopically expressed in epithelial cells via stimulated MAPK and AKT signaling pathways. Additionally, studies performed by Speyer and colleagues described GRM1 expression in several triple-negative breast cancer cell lines (TNBC) in which shRNA-mediated knockdown of GRM1 expression as well as antagonists to the receptor inhibited cell proliferation in TNBC lines [284]. Malignancies involving other GRMs include GRM4 first reported by Chang and colleagues that GRM4 is overexpressed in more than 40% of colorectal adenocarcinomas, malignant melanomas, laryngeal squamous cell carcinomas, and breast carcinomas tested [285]. Among these cancers, there was a correlation with GRM4 overexpression and increased mortality rate in patients with colorectal carcinoma. GRM5 overexpression was found to induce melanoma in transgenic mice [286]. The increased expression in GRM5 in the mouse melanocytes was correlated with enhanced levels of MAPK activation. These studies suggested that glutamatergic signaling plays a significant role in the initiation, progression and maintenance in human malignancies.

D. Inhibition of GRM1 expression

Targeting strategies for cancer therapy differ from chemotherapy and radiotherapy in their potential to provide tumor specificity. Preclinical studies have demonstrated that inhibition of glutamatergic signaling results in decreased tumor cell growth and increased cell death. Identifying key upstream molecular targets that lead to the activation of proliferation and survival pathways is important in cancer drug

discovery. Gene-targeting techniques that selectively inactivate gene expression assist in the validation of novel proteins involved in disease pathogenesis.

Suppression of GRM1 by siRNA

Gene silencing by short-interfering RNAs (siRNAs) has been used to investigate their roles in different cell types and in various organisms. However, constitutive suppression the expression of a gene could have deleterious consequences therefore, inducible silencing RNA approaches could be useful by relying on small molecules that act as inducers to modify synthetic transcription factors thereby regulating the expression of a target gene [287, 288]. The tetracycline operon based tetracycline inducible system and the non-mammalian steroid based ecdysone inducible system are two complementary approaches we have used. Previous attempts to inhibit GRM1 expression in human melanoma cells using constitutively expressed Grm1 specific siRNAs resulted in the cells exhibiting a dormancy-like state prior to dying. Employing the inducible knock-down of GRM1 was shown to result in suppression of MAPK as evident by a decrease in the phosphorylated form of ERK as well as inhibition of the PI3/AKT cell survival pathway seen by the reduced form of activated AKT [1]. Our previous studies on mouse melanoma cells as well as mouse melanocytic clones that stably expressed GRM1 showed elevated levels of glutamate were released into their surroundings compared to normal mouse melanocytes or vector controls [289]. From these results, Chen and co-workers hypothesized that instead of inhibiting GRM1 directly, if they were able to interrupt the autocrine/paracrine activity by limiting the amount of free ligand this may result in a similar decrease in cell proliferation/survival.

Suppression of GRM1 using an inhibitor of glutamate release

Glutamate is a major excitatory neurotransmitter in the CNS. The over activation of neurons by excessive glutamate stimulation is excitotoxic, resulting in neuronal death [290]. Interestingly, the brain is one of the most common sites of metastatic melanoma. It has been proposed that the excessive glutamate found in the brain inducing excitotoxicity to the surrounding neuronal tissue to create space for the growing tumor. Chen and co-workers took advantage of using an inhibitor of glutamate release, riluzole, a Food and Drug Administration (FDA)-approved drug for the treatment of amyotrophic lateral sclerosis (ALS or Lou Gehrig's disease). ALS is a degenerative motor neuron disease of the upper and lower motor neurons that progressively causes weakness, muscle atrophy and fasciculation. Riluzole is known to inhibit the release of glutamate from the presynapse led to a reduction in glutamate levels in the synaptic cleft resulting in a decrease in excitotoxicity mediated by the neurotransmitter and lessen progression of ALS [291]. Riluzole treated melanoma cells showed a reduction in the levels of glutamate in the surroundings *in vitro,* which correlated with a decrease in cell growth *in vivo* when compared to normal cells exposed to the drug. Additionally, melanoma cells treated with relatively low concentrations of riluzole were shown to undergo apoptosis by an increase in the levels of a well-known marker of apoptosis, the cleaved form of PARP [11]. The therapeutic potential of riluzole was validated *in vivo* using a human melanoma cell xenograft model where animals were treated with a human equivalent of the maximally allowed daily amount of riluzole per body weight per day via p.o. gavage and

a reduction in tumor volume in treated animals vs. control was detected. These results were translated to the clinic.

Translational study in patients

Clinical trials involving new compounds are classified into four phases: Phase 0, I, II and III. Phase 0 is the designation for exploratory, first-in-human trials conducted with the U.S. FDA's guidelines on Exploratory Investigational New Drug Studies (IND) [292]. Phase 0 trials are designed to speed-up the development of promising drugs or imaging agents by establishing very early on whether the drug or agent behaves in human subjects as was anticipated from preclinical studies. Based on results from previous findings in preclinical studies using riluzole, a phase 0 trial using the compound in patients with stage III and IV melanoma was performed to assess if its presence the target, glutamatergic signaling, is modulated. The trial resulted in a significant short-term response rate of 34% of patients. Tumors from patients that displayed shrinkage of tumors showed an inhibition of signaling through both the MAPK and PI3K/AKT pathways, reflecting results that were previously observed in preclinical studies [11, 293]. Positron Emission tomography (PET) documented complete resolve of multiple nodal and cutaneous metastases in several patients. One patient having six different tumors measured by PET/CT demonstrated shrinkage of the lesions by 10% to 20%. Out of eleven patients that completed the study, only two had shown progression of the disease after treatment [293]. The tumor samples were a composed of patients harboring both V600E BRAF as well as Q61K NRAS mutations. In addition all the patients admitted into the trial expressed GRM1, although GRM1 expression status was not a requirement

for entry. It is possible that, from this observation, that more advanced tumors, those found in stage III and IV metastases have a higher frequency of GRM1 expression and that ectopic GRM1 occurs and is more frequent in more progressed stages of the disease.

Cell Type	***GPCR***	***Reference***
Melanocytes	GRM5	*Frati et al.,2000*
Kerotinocytes	GRM1, 2	*Genever et al.,1999*
Osteoclasts	GRM8	*Morimoto et al.,2006*
Pancreatic Islets/β cells	GRM5,8	*Storto et al.,2006* *Tong et al.,2002*
Hepatocytes	GRM5	*Storto et al.,2000b*
Myocytes	GRM1,2,3,5	*Gill et al.,1999*
Thymocytes	GRM1,2,3,5	*Storto et al.,2000a*
Embryonic Stem Cells	GRM4,5	*Melchiorri et al.,2007*

Table 1. Expression of GRMs in select non-neuronal cells

	Subclass	Malignancy	Reference
Group I	***GRM1***	Melanoma Prostate	*Chen et al 1996* *Pollock et al.,2003* *Ohtani et al 2008* *Koochekpour et al 2012*
		Glioma Breast	*Aronica et al.,2003* *Albasanz et al.,1997* *Shinno et al.,1994* *Speyer et al 2011*
	GRM5	Osteosarcoma Oral squamous cell carcinoma Melanoma	*Kalariti et al.,2007* *Park et al.,2007* *Choi et al 2011*
Group II	***GRM2***	Glioma	*D'Onofrio et al.,2003*
	GRM3	Glioma	*D'Onofrio et al.,2003,* *Aronica et al , 2003* *Arcella et al 2005*
		Melaonma	*Prickett et al 2011*
Group III	***GRM4***	Colorectal adenocarcinoma	*Chang et al.,2005*
		Malignant Melanoma	
		Squamous cell carcinoma	
		Breast carcinoma	
		Medulloblastoma	*Lacovelli et al.,2006*
	GRM6	-	
	GRM7	-	
	GRM8	Melanoma	*Prickett et al 2011*

Table 2. Implications of GRMs in human Cancer

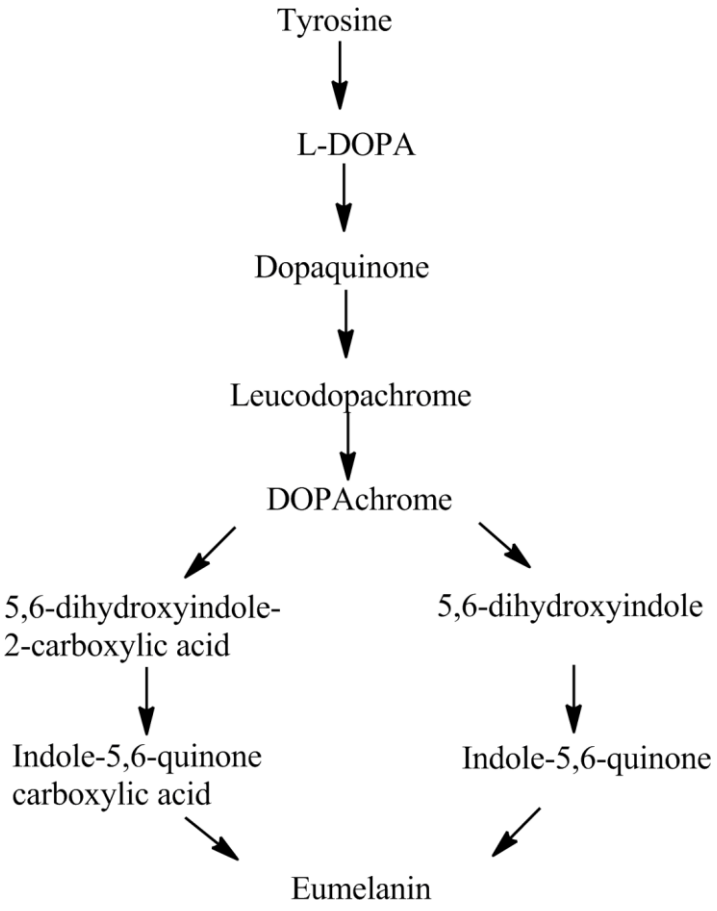

Figure 1. Conversion of Tyrosine to eumelanin

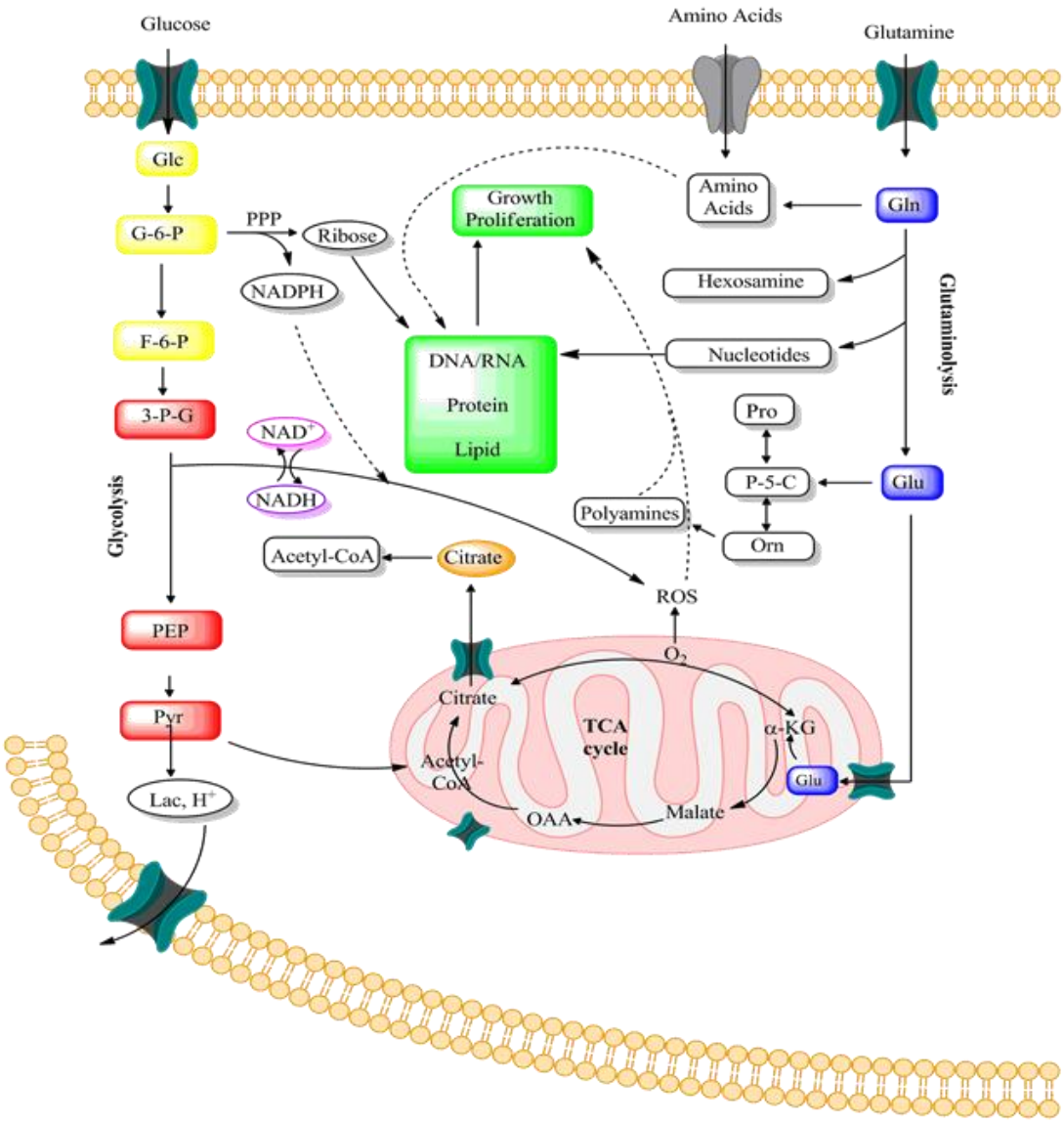

Figure 2. Metabolic pathways including glycolysis and glutaminolysis.

Glycolysis produces NADPH and 5-carbon ribose via the pentose phosphate pathway (PPP) at glucose-6-phosphate (G-6-P) and detours toward lactate production (aerobic glycolysis) at pyruvate. The carbons of glucose are further diverted into various synthetic pathways to generate the precursors of hexosamines, amino acids and lipids. Mitochondria are fueled by the anapleurotic substrate, α-ketoglutarate (α-KG), generated from glutamate. Depending on the oxygen supply, α-ketoglutarate metabolizes through the tricarboxylic acid (TCA) cycle to malate and oxaloacetate (OAA) providing energy and a carbon resource for lipids.

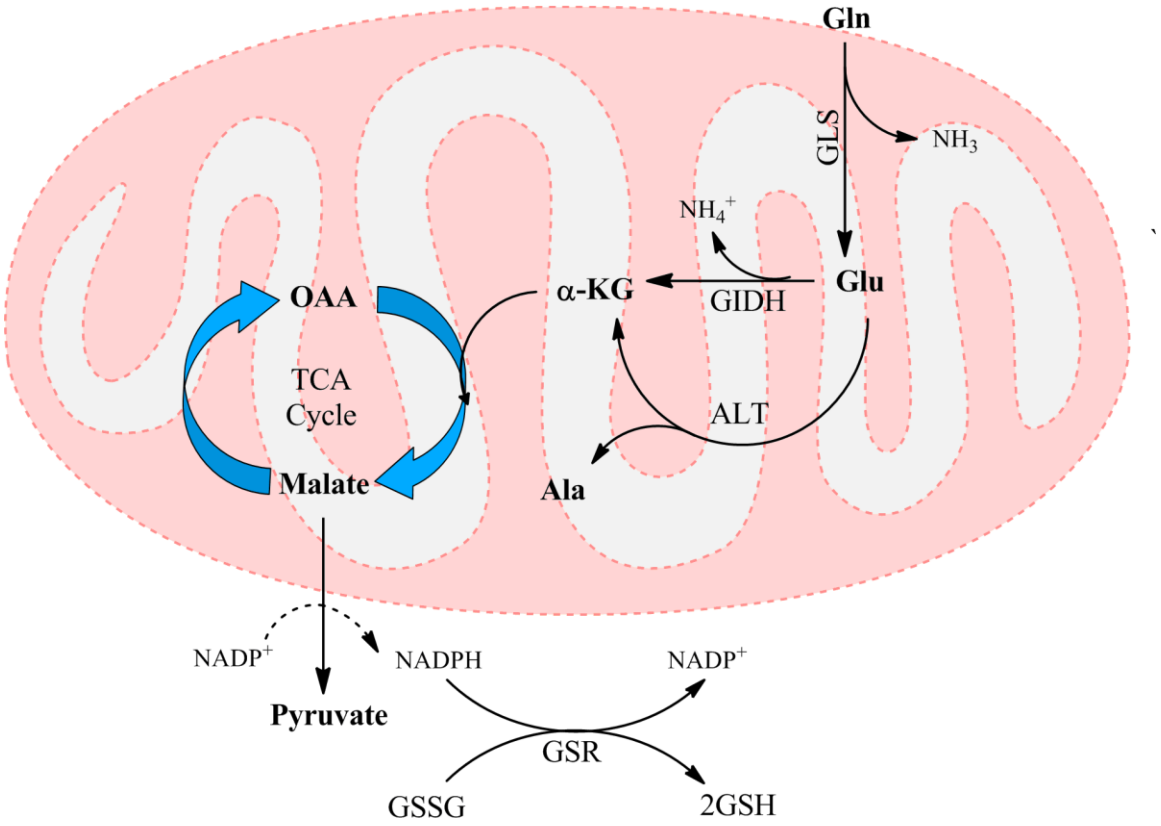

Figure 3. Glutamate metabolism in the mitochondria

Glutamine (Gln) is converted to glutamate (Glu) by the enzyme glutaminase (GLS) releasing both Glu and ammonia into the cytosolic compartment of the inner mitochondrial membrane. Glu is then metabolized to α-ketoglutarate (α-KG) either by oxidative deamination by glutamate dehydrogenase (GIDH) or alanine transaminase (ALT). α-KG is metabolized in the tricarboxylic acid cycle to oxaloacetate through the production of malate. Malate oxidation to pyruvate in the cytosol generates NADPH which is used to maintain glutathione in its reduced state.

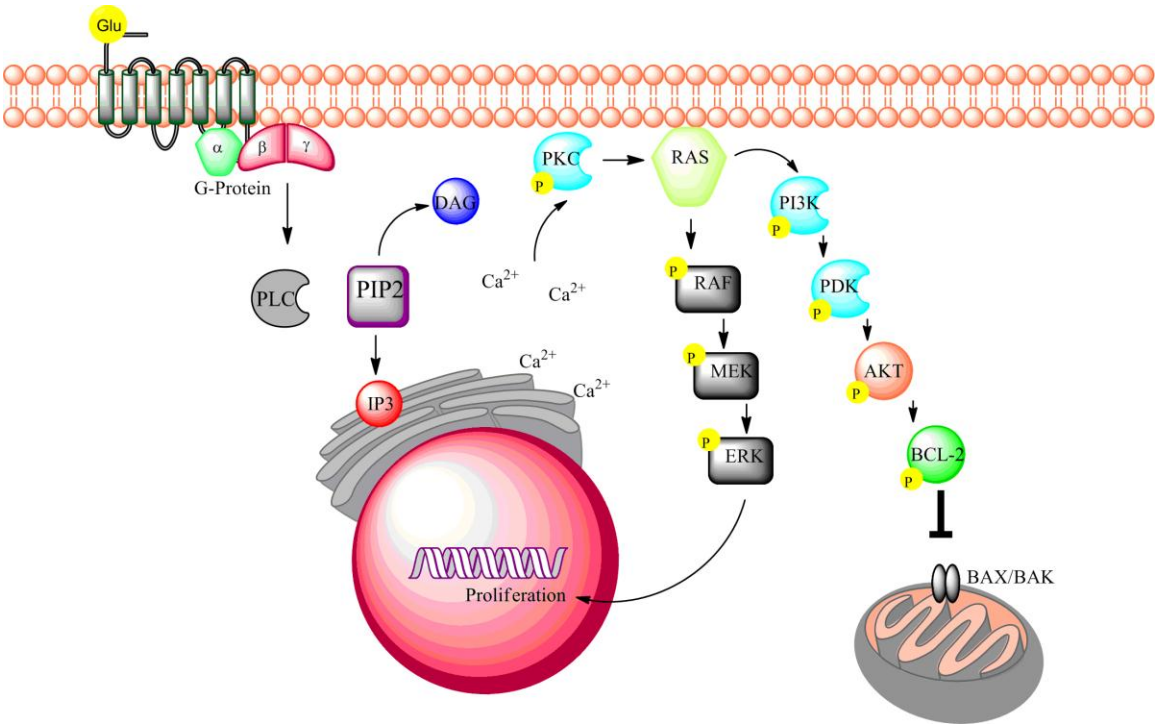

Figure 4. Signal transduction pathways activated by GRM1 stimulation.

Activation of GRM1 by its ligand, glutamate, results in the activation of signaling pathways that upregulate cell proliferation (MAPK) and promotes cell survival (PI3K/AKT).

Section I: GRM1 Expression is Necessary in Riluzole-Induced G_2/M Arrest.

Aim 1: Rationale

We demonstrated that human melanoma cells that do not express GRM1 are less sensitive to the effects of riluzole than cell lines expressing the receptor [11]. When GRM1 is aberrantly expressed in melanocytes, one of the consequences includes a metabolic switch that drives the cells to become addicted to glutamate, the natural ligand of GRM1, resulting in a disturbance to the redox balance within the cells and causes enhanced genome instability and, eventually, transformation. The occurrence of autocrine loops in these melanoma cells bring about a constitutively activated GPCR receptor, GRM1 [294]. Treatment of these cells with riluzole, an inhibitor of glutamate release, results in the disruption of the established autocrine loop and elevated intracellular glutamate levels. This leads to DNA damage and accumulation of the damaged cells in the G_2/M phase of the cell cycle, causing the cells to be more sensitive to the effects of ionizing radiation.

Materials and Methods

A. Antibodies and reagents

Anti-53BP1 antibody was purchased from Bethyl Laboratories Inc. (Montgomery, TX); phospho H2AX and H4 antibodies were purchased from EMD Millipore Corporation (Temecula, CA); monoclonal α-tubulin antibody, etoposide, glutathione reduced ethyl ester, N-acetyl cysteine, riluzole and dihydrorhodamine 123 were obtained from Sigma (St. Louis, MO). DMSO was purchased from Fisher Scientific (Pittsburgh, PA). Alexa fluor 488 goat anti-mouse IgG, alexa fluor 546 goat anti-rabbit IgG were purchased from Life Technologies (Carlsbad, CA).

B. Cell culture

Immortalized non-tumorigenic human melanocytes, hTERT/CDK^{R24C}/p53^{DD} were provided by Dr. David Fisher (Harvard Medical School, Boston, MA) and maintained in Medium 254 with added human melanocyte growth supplements (Invitrogen, Carlsbad, CA) [295]. UACC930 and UACC903 were provided by Dr. Jeffery M. Trent (Translational Genomics Research Center, Phoenix, AZ). C8161 and C81-61 were from Dr. Mary J.C. Hendrix (Children's Memorial Research Center, Chicago, IL). D3 iBMK cells were provided by Dr. Eileen White (Cancer Institute of New Jersey, New Brunswick, NJ) and derived as described previously [296]. Melanoma cell lines were grown in RPMI 1640 plus 10% fetal bovine serum (FBS).

C. Cell Cycle Analysis

For cell cycle analysis, cells were plated at 10^6 per 100-mm culture plate and treated as indicated. After 24 and 48 h, cells were collected and washed twice with ice-cold PBS. Cell pellets were fixed by drop-wise addition of ice-cold 70% ethanol and incubated for 20 min at 4° C. Fixed cells were then washed twice with ice-cold PBS and resuspended in 500 μL PBS. Cells were treated with RNase A solution (20 μg/mL; Sigma) and labeled with propidium iodide (50 μg/mL; Sigma) for 30 min. Cell cycle analysis was done by the Flow Cytometry Facility Core at Rutgers University (Piscataway, NJ) using a Beckman Coulter system (Epics XL-MCL model).

D. Clonogenic cell survival assays

Human melanoma cells were treated with the vehicle control or riluzole (25 μmol/L) for 20 hours and irradiated with escalating doses (0, 2, 4Gy) at room temperature. Drug concentration (25 μmol/L) was chosen on the basis of a 96-well plate ATP luminescence cell viability assay with increasing concentrations of drug in irradiated cells (data not shown). Following treatment, cells were trypsinized and counted. Known numbers were then replated in 100-mm tissue culture dishes and returned to the incubator to allow macroscopic colony development. Cells were irradiated by a Gamma Cell 40 Exactor (MDS Nordion) irradiator and then incubated overnight (20 hours). Plates were then monitored for 10 to 21 days and stained with crystal violet for visual counting. Colonies which contained more than 50 cells were scored as clonogenic survivors.

E. DNA transfections

The derivation of D3 baby mouse kidney epithelial cell line has been described [297]. D3 cells were cultured in DMEM supplemented with 5% FBS. All DNA transfections were performed with Lipofectamine 2000 according to the manufacturer (Invitrogen, Carlsbad, CA). Coding sequence for the full-length mouse form of the receptor was subcloned from mouse-brain Grm1 cDNA [270, 298] into mammalian expression vector pCI-neo (Promega, Madison, WI). Stable Grm1- or empty vector- transfected clones were selected in 2 mg/ml (D3) Geneticin (Invitrogen, Carlsbad, CA).

F. Glutamate release assay

10^3 cells of HEK, UACC930, UACC903 and C8161 and HEK293A cells were plated in each well of a 96 well plate and maintained in glutamine and glutamate free RPMI media supplemented with 10% dialyzed FBS and 2 mM Glutamax. 50 ul of conditioned medium was collected from the wells on day 0 and day 4 and the Amplex Red Glutamic Acid/Glutamate Oxidase assay kit used to measure levels of glutamate.

G. Antibodies and Western immunoblots

Anti- total-ERK1/2, phospho-ERK1/2, total-AKT, phospho-AKT, were obtained from Cell Signaling Technology (Danvers, MA); anti-GRM1 from BD Biosciences (San Jose, CA); anti-GRM1 from Upstate/Millipore (Billerica, MA); Anti-53BP1 was purchased from Bethyl Laboratories Inc. (Montgomery, TX); phospho H2AX and H4 antibodies were purchased from EMD Millipore Corporation (Temecula, CA); monoclonal α-tubulin antibody, etoposide and riluzole were obtained from Sigma (St. Louis, MO). DMSO was purchased from Fisher Scientific (Pittsburgh, PA). Alexa fluor 488 goat anti-

mouse IgG, alexa fluor 546 goat anti-rabbit IgG were purchased from Life Technologies (Carlsbad, CA). Cells and tissue extracts were prepared in NP40-containing buffer with protease and phosphatase inhibitors as described previously [299], and protein concentrations were determined with Detergent Compatible Protein Assay (Bio-Rad Laboratories, Hercules, CA). Proteins were resolved by Tris-Glycine polyacrylamide gel electrophoresis and transferred to nitrocellulose membrane by wet tank electroblotting. After overnight incubation with primary antibodies, blots were visualized with Amersham ECL-HRP Linked Secondary Antibodies and ECL Plus Western Blotting Detection Reagents (GE Healthcare Life Sciences, Piscataway, NJ). Densitometry of gel intensities were quantified by OptiQuant software (PerkinElmer, Shelton, CT).

H. Immunofluorescent staining

Cells were grown on glass coverslips to the appropriate density and synchronized by serum starvation for 48 h. Following synchronization cells were treated as indicated. At each time point, cells were fixed with 4% paraformaldehyde in PBS and permeabilized for 10 minutes in 0.5% Triton X-100 in PBS at room temperature. Cells were then washed with PBS and blocked in 5% goat serum/PBS. Primary antibodies (53BP1 anti rabbit IgG and phospho H2A anti mouse IgG) were incubated at room temperature in blocking solution. Cells were washed with PBS for 5 min and incubated with Fluorophore-conjugated secondary antibody (Alexa Fluor 488 goat anti-mouse IgG and Alex Fluor 546 goat anti rabbit IgG, Invitrogen, Carlsbad, CA) for 1 h in blocking solution. Cells were washed with PBS for 5 min and mounted using Vectashield (Vector Laboratories, Burlingame, CA). Images were captured using a Nikon Eclipse microscope

coupled with a Coolsnap EZ camera powered by NIS-Elements BR 3.1 software. All quantifications were performed using ImageJ software.

I. Immunohistochemistry (IHC)

Phase II human melanoma biopsy tissue IHC for γ-H2AX was performed by the Tissue Analytic Services at the Cancer Institute of New Jersey, and unbiased quantitative assessment of IHC staining was completed using a digital Aperio ScanScope GL system and Aperio ImageScope software (v 10.1.3.2028) (Aperio Technologies Inc., Vista, CA) according to the manufacture's protocol.

J. Murine xenograft model

GRM-positive C8161 cells (1×10^6) were injected into the flanks of 6-week-old nude mice (Taconic, Hudson NY). When the tumors reached approximately 6 to 10 mm^3 the mice were randomly divided into groups of 10 mice each: group 1 was left untreated (no treatment or NT), group 2 was treated with the dimethyl sulfoxide (DMSO) vehicle only (vehicle), group 3 was treated twice with 4 Gy of irradiation only (IR), group 4 was treated with 10 mg/kg of riluzole by oral gavage only (riluzole), and group 5 was administered 10 mg/kg of riluzole each day and radiation was delivered to these animals in 3 weekly fractions of 4 Gy each. The experiment was terminated after 25 days of treatment due to tumor burden in the NT and vehicle-treated animals.

Results

1.1 Human melanoma cells excrete elevated levels of glutamate

The oncogenic transformation of cell types by ectopic expression of GPCRs is characterized by the development of autocrine and paracrine activity that enhances cellular proliferation [262, 263]. To investigate if an autocrine loop was present in our system, we assessed the levels of glutamate release from human melanoma cell lines that were shown to express functional GRM1 (Figure 5). We were able to demonstrate that 10 out of 10 cell lines did in fact prove to elevate the level of free glutamate in their surroundings compared with *GRM1*-negative melanoma cells and normal melanocytes, suggesting that a pro-proliferative autocrine loop could contribute to increased proliferation in GRM1-expressing melanoma cells [11].

1.2 Cell cycle arrest of GRM1-expressing human melanoma cells after riluzole treatment

Riluzole has been shown to block the release of glutamate the natural ligand for GRM1 [11, 25, 300]. Depletion of extracellular glutamate interferes with downstream, intracellular events that would follow stimulation of the receptor such as activation of cell proliferation and survival pathways [11, 301]. Cell cycle profiles of GRM1-expressing and GRM1-negative human melanoma cell lines treated with riluzole were performed. In GRM1-positive cells, after 24 hours, half of the initial cell population is shown to arrest in G_2/M phase of the cell cycle. 48 hours following treatment, a substantial fraction of these cells are found to shift from G_2/M to sub G_1 which is indicative of apoptotic cell death. 72 hours post treatment 50% of the total cell population is found to accumulate in

sub G_1 of the cycle (Figure 6A). Apoptotic cell death was further confirmed on the protein level by increased levels of cleaved caspase 3, a known marker indicative of apoptosis (Figure 6C) [11, 263]. Human melanoma cells that do not express functional GRM1 were not very responsive to the treatment (Figure 6B).

1.3 Riluzole causes hyper sensitivity to ionizing irradiation in GRM1 expressing human melanoma cells

Cells that have the ability to successfully repair sublethal DNA damage can more successfully survive small to medium doses of radiation and display broad initial shoulders graphically when their survival fraction is plotted against increasing doses of irradiation. Cells that have little or no ability to repair sublethal damage are more sensitive to these doses of radiation and as a result graphically display shallower, steeper shoulders. These differences in single-fraction survival become more apparent over long, multifractional courses of radiotherapy. Our previous observations show that riluzole caused cells to accumulate in the G_2/M phase of the cell cycle 24 hours following treatments. Cells in this phase of the cell cycle have been shown to be hypersensitive to the sublethal doses of ionizing radiation [302]. To assess whether riluzole enhances the effects of ionizing irradiation in GRM1-expressing human melanoma cells, clonogenic assays were performed. It is important to note that in addition to expressing functional GRM1, C8161 cells are wild type for both NRAS and BRAF and contain a functioning p53 tumor repressor. Using the same experimental conditions, we performed the assay using the *GRM1*-negative melanoma cell line, UACC930, as a negative control. UACC930 cells express a truncated, non-functioning form of GRM1 and harbor

constitutively active $BRAF^{V600E}$ mutation. In *in vitro* experiments, cultured cells were treated with riluzole (25 μM) over a period of 24 hours and followed with increasing doses (0-8 Gy) of ionizing radiation. Clonogenic assays show that riluzole enhances the lethal effects of ionizing radiation at the 2 and 4 Gy dose levels with abrogation of the initial shoulder in the survival curve of GRM1-positive C8161 melanoma cells. The results shown in Figure 7A may appear subtle but are statistically significant ($p=0.048$) and were consistent across three independent experiments. Very similar results were observed in another GRM1-positive human melanoma cell line (data not shown). In contrast, there was no difference in the survival curves between riluzole-treated and untreated UACC930 cells that do not express GRM1. For GRM1-negative UACC930 melanoma cells, we increased riluzole concentration to 100 μM (Figure 7B) and the results were the same as those attained using riluzole at a concentration of 25 μM. Based on these observations, we propose that riluzole mediates its radiation sensitizing effects on melanoma cells most likely through GRM1 signaling. Subsequently, the existence of apoptotic C8161 cell populations was confirmed on the protein level showing elevated levels of activated caspase-3 in Western immunoblots (Figure 7C). This suggests that GRM1 expressing human melanoma cells treated with riluzole appear to be more sensitive to irradiation as evident by the appearance of enhanced levels of cleaved caspase-3 in comparison to irradiated cells alone.

1.4 Effects of ionizing radiation and Riluzole in a murine xenograft model:

To determine if riluzole-enhanced sensitivity to ionizing irradiation (IR) could cause arrest or delay in tumor cell growth progression over time, we performed a

xenograft experiment, spreading out the treatments of IR with daily riluzole treatment throughout the duration of the experiment. Animals that were irradiated were treated once a week with a dose of 4 Gy of irradiation. Animals that were receiving riluzole treatment received the maximum FDA approved dose (2.5 mg/kg/day) and was administered by oral gavage. Our results demonstrated that either riluzole or irradiation alone had a substantial effect on tumor progression when compared to untreated or vehicle-treated control xenografts. However, the combination of riluzole and irradiation resulted in significantly smaller tumors as compared to control groups or to tumors treated with riluzole or irradiation alone (Figure 8A). Since irradiation is known to elicit its effects through the formation of double stranded DNA lesions to the genome, we performed immunohistochemistry in order to detect the levels of the phosphorylated form of histone variant 2AX (γH2AX). Phosphorylation of histone protein H2AX on serine 139 occurs at sites flanking DNA double-stranded breaks (DSBs) and can provide a measure of the number of DSBs within a cell. Further analyses on excised xenografts from this experiment revealed a marked enhancement of DNA damage as measured by the formation of γH2AX foci by immunohistochemistry (Figure 8B). However, in addition to the expected foci formation being found in tumors that were treated with irradiation, there was also a substantial level of DNA DSBs found in tumors from animals treated with riluzole alone. This led us to hypothesize that riluzole enhances the effects of ionizing radiation by inducing DNA damage to GRM1-expressing melanoma causing them to accumulate in G_2/M phase of the cell cycle.

1.5 Riluzole induces DNA damage in human melanoma cells that express GRM1

Phosphorylation of histone H2AX (γ-H2AX) is among the earliest responses to DNA DSBs. To examine DNA damage elicited by riluzole, *in vitro* assays were performed in which cell lines were treated with either DMSO (Veh), etoposide (Etop), riluzole (Ril), or left untreated for 24 hours after which nuclear proteins were extracted [303]. Etoposide, a widely prescribed chemotherapeutic agent used in the treatment of various human cancers, was administered to cultured cells as a positive control for DNA double strand breaks (DSB). Briefly, etoposide increases topoisomerase II-mediated DNA breakage via inhibiting its ability to re-ligate nucleic acids [304]. *GRM1*-positive C8161 and GRM1-negative UACC930 melanoma cells were plated and subjected to the same experimental conditions. Protein lysates from both cell lines were isolated and analyzed by Western immunoblots using an antibody against γ-H2AX to assess DSBs. We show that, in both cell lines, etoposide treatment caused an increase in intensity in bands indicative of γ-H2AX when compared to untreated or vehicle treated samples (Figure 9). However, only GRM1 positive C8161 and not GRM1-negative UACC930 cells showed an increase in the levels of H2AX phosphorylation when treated with riluzole compared to the untreated or vehicle treated cells. These results confirmed our previously reported immunohistological findings that riluzole has the ability to induce DSBs in human melanoma cells that express GRM1 [4].

1.6 ATM is activated in GRM1-expressing cells after treatment with riluzole

Members of the PI 3-kinase family ATM (ataxia telangiectasia, mutated) and ATR (ATM and Rad3-related) are known responders of DSBs in mammalian cells and function as key regulators of the checkpoint pathways via activation of cell cycle

checkpoint kinase [305]. ATM is the primary mediator in the response to DNA double strand breaks by exposure to ionizing radiation. We wanted to know if the DNA damage we observed in our previous results elicited the activation of ATM kinase. GRM1-positive cell lines C8161 and UACC903 were treated with 10 μM of Ril and harvested at various time points to assess for induction of the activated form of ATM. The GRM1-negative cell lines UACC930 and C81-61 were used as a negative control (Figure 10). Our results show that only GRM1-expressing cell lines demonstrated a time dependent increase in levels of pATM compared to GRM1-negative UACC930 and C81-61 cells. These results showed that riluzole treatment induced the activation of ATM in our system, further suggested that the DNA damage that being caused by riluzole treatment was double strand breaks.

1.7 Riluzole-induced DNA damage is dependent on GRM1 expression

The tumor suppressor 53BP1 is a checkpoint regulator that binds to the central DNA-binding domain of p53. It relocates to the sites of DNA strand breaks in response to DNA damage and is a putative substrate for ATM. Both γ-H2AX and 53BP1 are known to form punctated foci in immunofluorescence microscopy which show co-localization at sites of DSBs [306, 307, 308, 309]. In an attempt to further assess the ability of riluzole to induce DSBs in human melanoma cells, we performed immunofluorescence staining against γ-H2AX and 53BP-1. GRM1-expressing C8161 human melanoma cells were seeded on coverslips in 35 mm culture dishes and synchronized by serum starvation for 48 h after which they were exposed to riluzole for 3, 5, 8, 12 or 24 hours. As a positive control, we treated cells with etoposide for 30 minutes. Coverslips containing adherent

cells were fixed, stained and visualized. GRM1 expressing, C8161 cells treated with riluzole showed an increase in the amounts of both γ-H2AX and 53BP1 sequestered to sites of DNA damage via foci formation in the nucleus compared to untreated cells as early as 3 hours and peaks at around 8-12 hours, an example is shown (Figure 11A). In parallel we also included a human melanoma cell line known to harbor a nonfunctioning form of the receptor, UACC930. Cells were treated in identical conditions as mentioned above. GRM1-negative UACC930 melanoma cells showed no significant change in the levels of γ-H2AX and 53BP1 between riluzole and untreated cells (Figures 11B). Fluorescence intensities were quantitated for statistical analyses and are shown in figures 11C and 11D. From these results, we further demonstrate that riluzole elicits DNA DSBs as scene by the co-localization of both 53BP1 ($p<0.005$) and γ-H2AX ($p<0.05$) in human melanoma cells that express GRM1.

1.8 Formation of γ-H2AX foci after riluzole treatment is independent of apoptosis

It has been proposed that the formation of γ-H2AX foci not only reflect the presence of local DNA double-strand breaks after exposure to DNA damaging agents, but can also be seen in cells that undergo apoptosis [310]. In order to be certain that the enhanced levels of γ-H2AX induced by riluzole was reflecting focal DNA breaks and was not simply an indicator of apoptotic cell death, we used immortalized baby mouse kidney epithelial cells (iBMK) that are deficient in apoptosis through the deletion of BAX and BAK (D3 cell line) derived previously by Dr. Eileen White and colleagues [282]. Introduction of the murine form of the receptor (Grm-1) into D3 cells caused them to be tumorigenic *in vivo* in comparison to those that were transfected with an empty vector

(Figure 12) [283]. We treated D3 vector-containing cells (D3-Vec) and D3-Grm1cells with etoposide as a positive control for DNA DSBs or riluzole for various time points up to 24 hours. We showed that etoposide treatment induced both D3-vec and D3-Grm1cells to display co-localization of 53BP1 and γ-H2AX foci, consistent with induction of DNA double-strand breaks (data not shown). Riluzole treated D3-vec cells showed barely visible 53BP1 staining while γ-H2AX stain yielded an overall diffused pattern (Figure 13A). In contrast, riluzole-treated D3-Grm1 cells displayed clear co-localization of nuclear 53BP1 and γ-H2AX foci, again consistent with the induction of DNA breaks in this setting (Figure 13B). Further quantification of these data show a significant difference exists in the amount of fluorescence detected in D3-Grm1 cells treated with riluzole compared to control in contrast to D3-vec cells (Figure 13C and 13D). These results support the idea that even in apoptosis deficient cells such as D3, riluzole still is able to induce DNA damage but this depends in upon the cells expressing functional Grm1, suggesting their necessity for glutamate signaling.

1.9 DNA damage increase in riluzole treated biopsies from responding patients

Previously, our group had reported on a completed Phase 0 and Phase II trials using single agent riluzole in stage III or IV resectable melanoma patients [293, 311]. Based on our *in vitro* results described in this report, we were interested to see if detectable changes in DNA damage markers would present themselves *in vivo.* We performed IHC staining using γ-H2AX antibody on pre- and post-riluzole treated tumor samples from the Phase II trial, these samples were positive for GRM1 expression [293, 311]. We detected a significant number of γ-H2AX-positive cells in the post-treatment

samples of 2 responding patients compared to samples from the same patients taken before treatment (Figures 14A and 14B). The intensity of the entire slide was quantitated using Aperio Imagescope imaging software (Fig 14C). These results further strengthen our working hypothesis that in human melanoma, GRM1- expressing melanoma cells are sensitive to the levels of intracellular glutamate and that intracellular accumulation of this ligand causes an increase in DNA damage response.

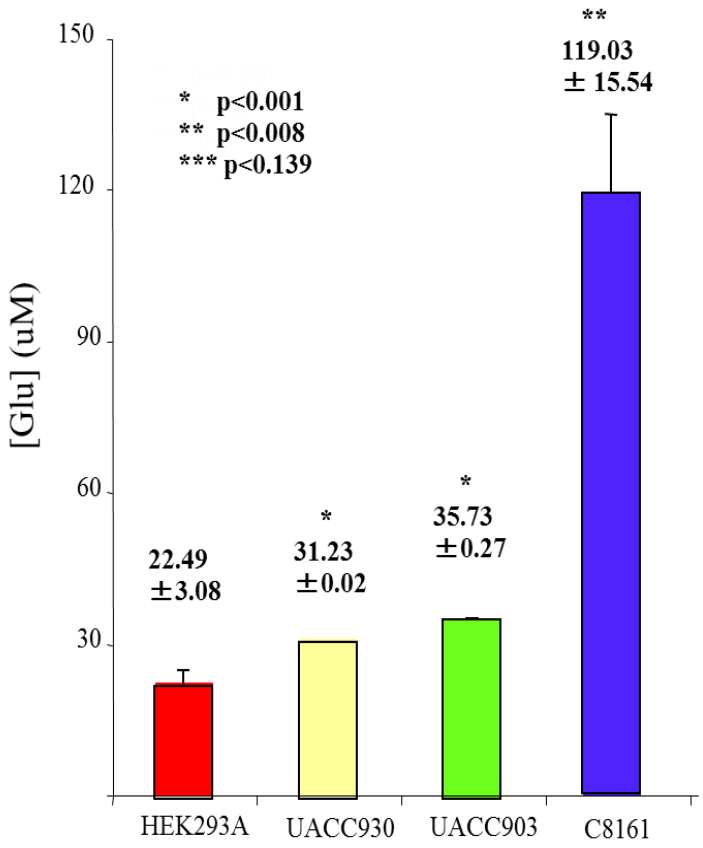

Figure 5. GRM1-expressing human melanoma cell excrete excess glutamate

Human melanoma cells that ectopically express GRM1 (UACC903 and C8161) have elevated concentrations of glutamate in their surroundings compared to cells that do not express the receptor (UACC930, HEK293A).

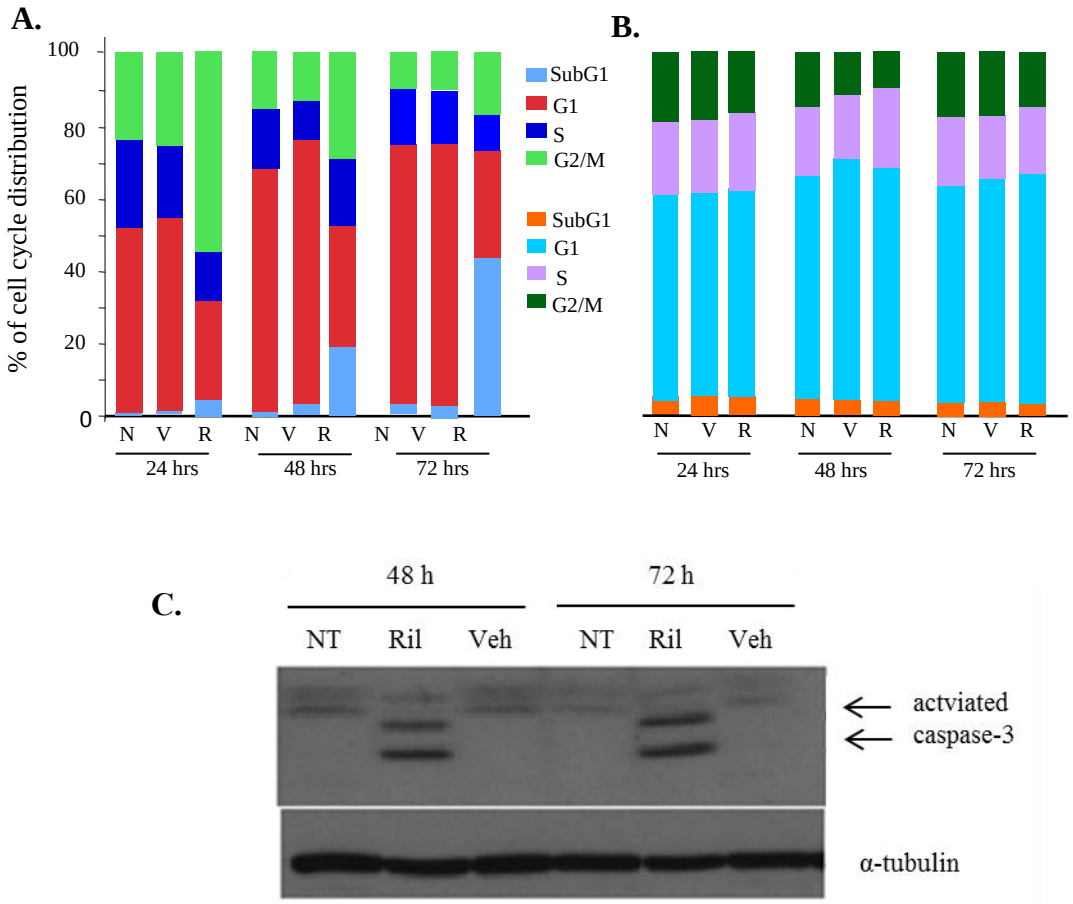

Figure 6. Cell cycle analysis of GRM1 expressing human melanoma cells

(A.) Cell cycle analyses were performed with three different GRM1 expressing human melanoma cell lines, all three gave very similar results and an example is shown. N (not treated), V (vehicle, DMSO) and R (Riluzole, 10 μM). Percentages of cells in subG$_1$, G$_1$, S and G$_2$/M phases were calculated from the resulting histograms, and mean values are shown in the diagrams. (B.) Cell cycle profiles were obtained using the same experimental conditions as in (A.) from two GRM1-negative human melanoma cell lines and both cell lines yielded very similar results, an example is shown. (C.) Activated caspase 3 was detected 48 and 72 hours after treatment with Riluzole in GRM1 expressing melanoma cells.

A.

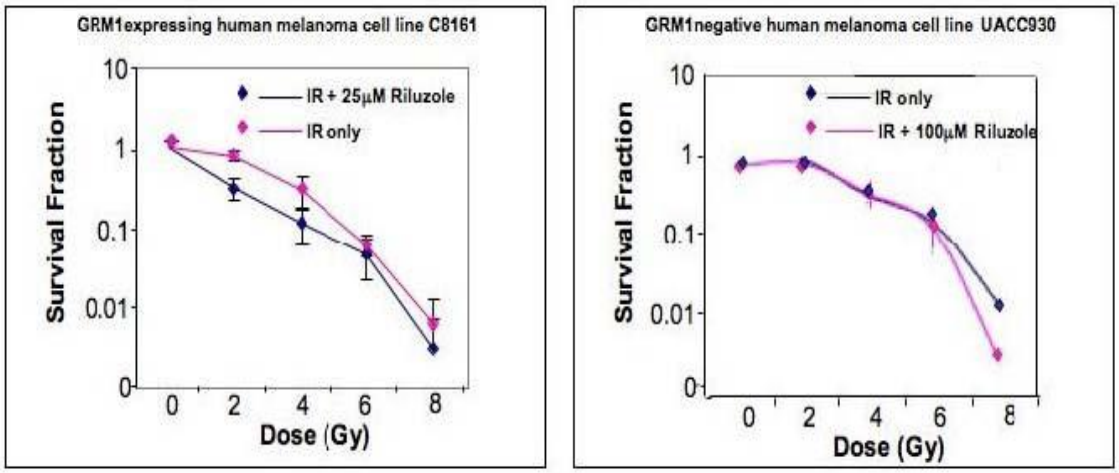

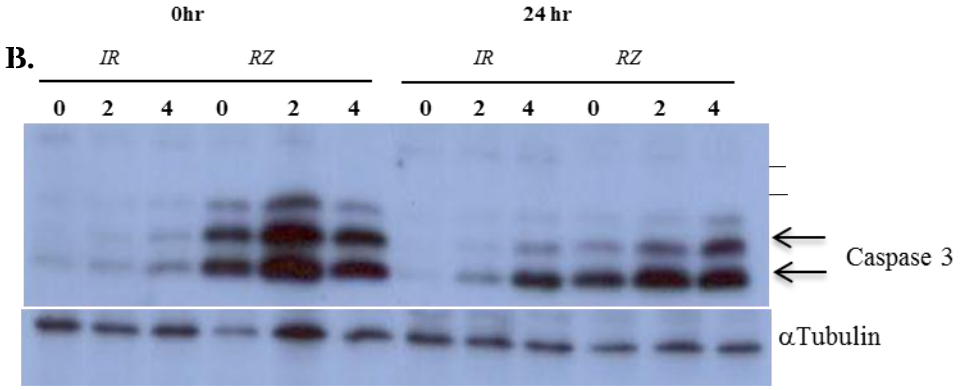

Figure 7. Clonogenic assays *Adapted from Khan and Wall et. al. Clin. Can. Res. 2011*

(A.) Left: GRM1-positive C8161 human melanoma cells treated with Riluzole at 25μM for 24 h followed by escalating doses of ionizing radiation. At 2Gy, there was a 48% reduction (0.78 ± 0.100 vs. 0.30± 0.089, p= .010) in cell survival in Riluzole treated cells versus non-treated cells. At 4 Gy, there was a 19% reduction (0.30 ± 0.121 vs. 0.11 ± 0.055, p< 0.05) in cell survival in riluzole-treated cells vs. non-treated cells. No differences were seen at 6 and 8 Gy. Right: There was no difference between treated and untreated control UACC930 cells that do not express GRM1 when treated with 25 μM riluzole concentrations (not shown) or at 100 mM concentration (shown). (B.) Western immunoblots of C8161 GRM1-positive human melanoma cells either treated with Riluzole for 24 h or no treatment. Both sets of cells were then either not irradiated or irradiated at 2 or 4 Gy. Lysates were made at 0 or 24 hours after irradiation and probed with activated-caspase-3 antibody to assess apoptotic cells.

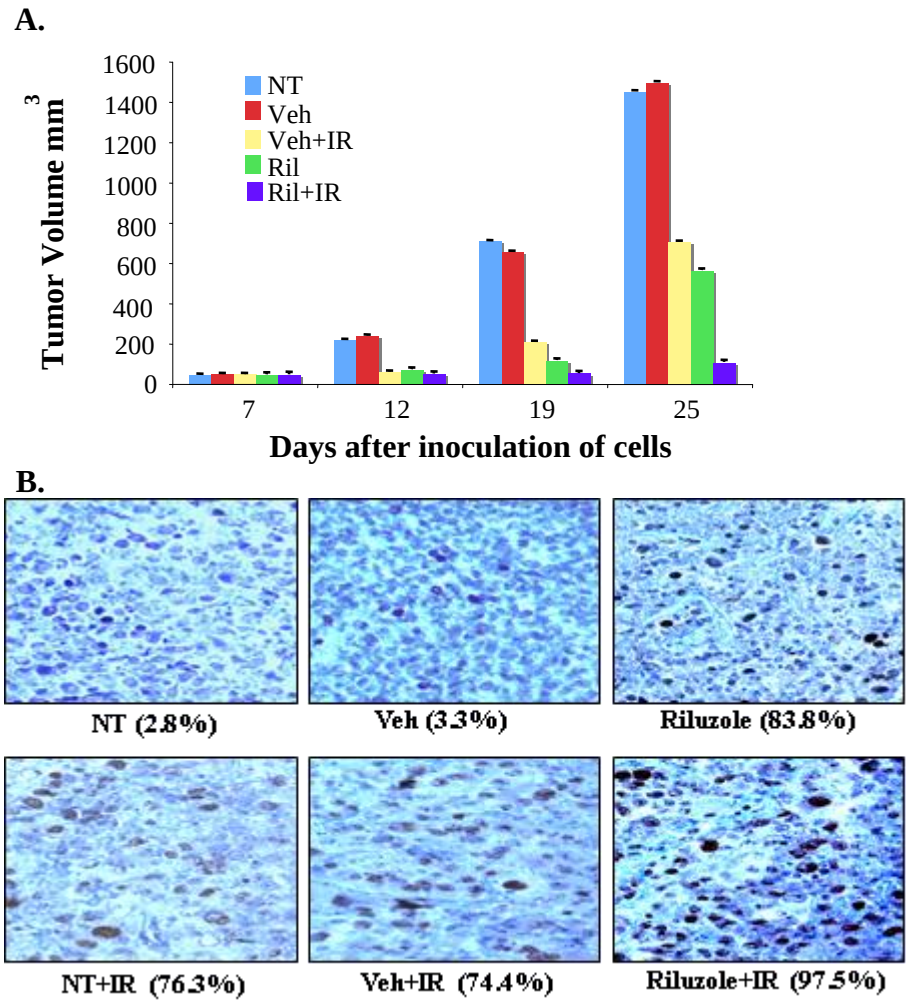

Figure 8. Murine Xenograft Model

(A.) C8161 cells were injected into flanks bilaterally at 10^6 cells per site. Tumor size was measured twice a week with a vernier caliper. When tumor volumes reach 6-10 mm3 the mice were randomly grouped into various treatments. Each treatment group consists of 10 mice. The groups were no treatment (NT), DMSO vehicle (Veh), Veh + irradiation (V+IR), Riluzole (10mg/kg) (Ril), and Riluzole (10mg/kg) plus irradiation (Ril+IR). Riluzole was given each day by oral gavage. Irradiation was delivered in three weekly fractions of 4 Gy. The experiment was terminated after 25 days due to tumor burden in the NT and vehicle treated animals. (B.) Staining of γ-H2AX in excised tumor xenografts. Tumor xenografts from the xenograft experiments (Figure 4) were stained with γ-H2AX, a commonly use marker for DNA damage. Ten random fields of 500 cells were scored and the percent of positive γ-H2AX cells is shown below each representative image.

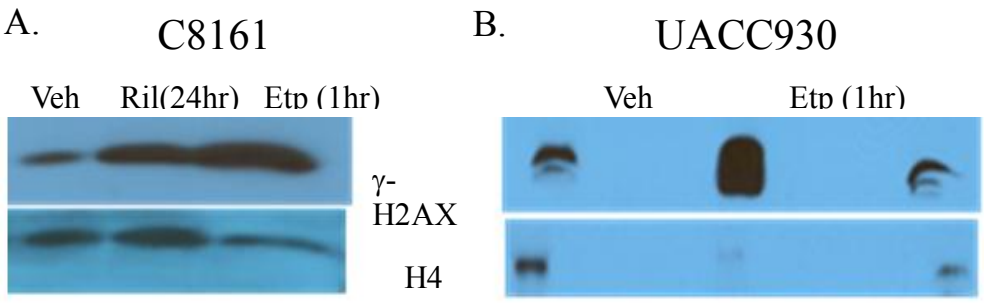

Figure 9. Western blot showing histone 2A phosphorylation

(A.) C8161 (GRM1-positive) and (B.) UACC930 (GRM1-negative) human melanoma cells were not treated (NT), treated with vehicle (Veh, DMSO), Riluzole (10 µM) or etoposide (10 µM) for 24 hrs. Nuclear extracts were prepared as described 4 and subjected to Western immunoblot. Histone 4 (H4) levels were used as loading controls.

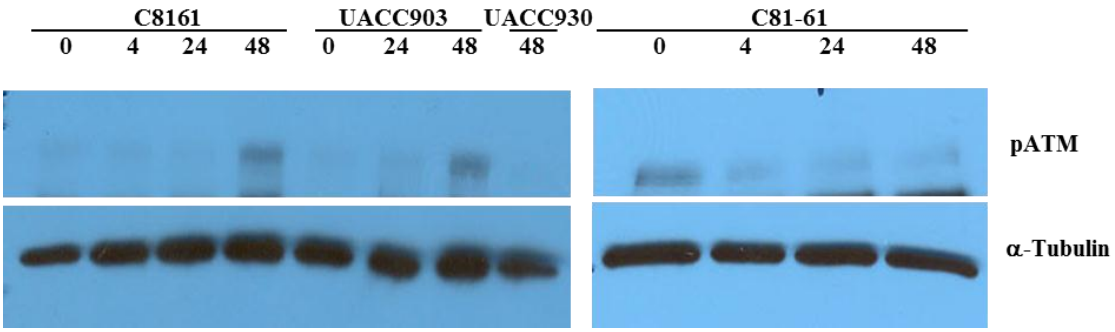

Figure 10. ATM is activated in GRM1 expressing cells treated with riluzole

C8161 (GRM1-positive. wild type B-RAF), UACC903 (GRM1-positive and mutated B-RAF^{V600E}), UACC930 (GRM1-negative and mutated B-RAF^{V600E}), and C81-61 (GRM1 negative and wild type B-RAF) cells were treated with riluzole (10 μM) for various time points. Levels of activated ATM (pATM) were evaluated by Western immunoblots. Levels of α-Tubulin were used as loading controls.

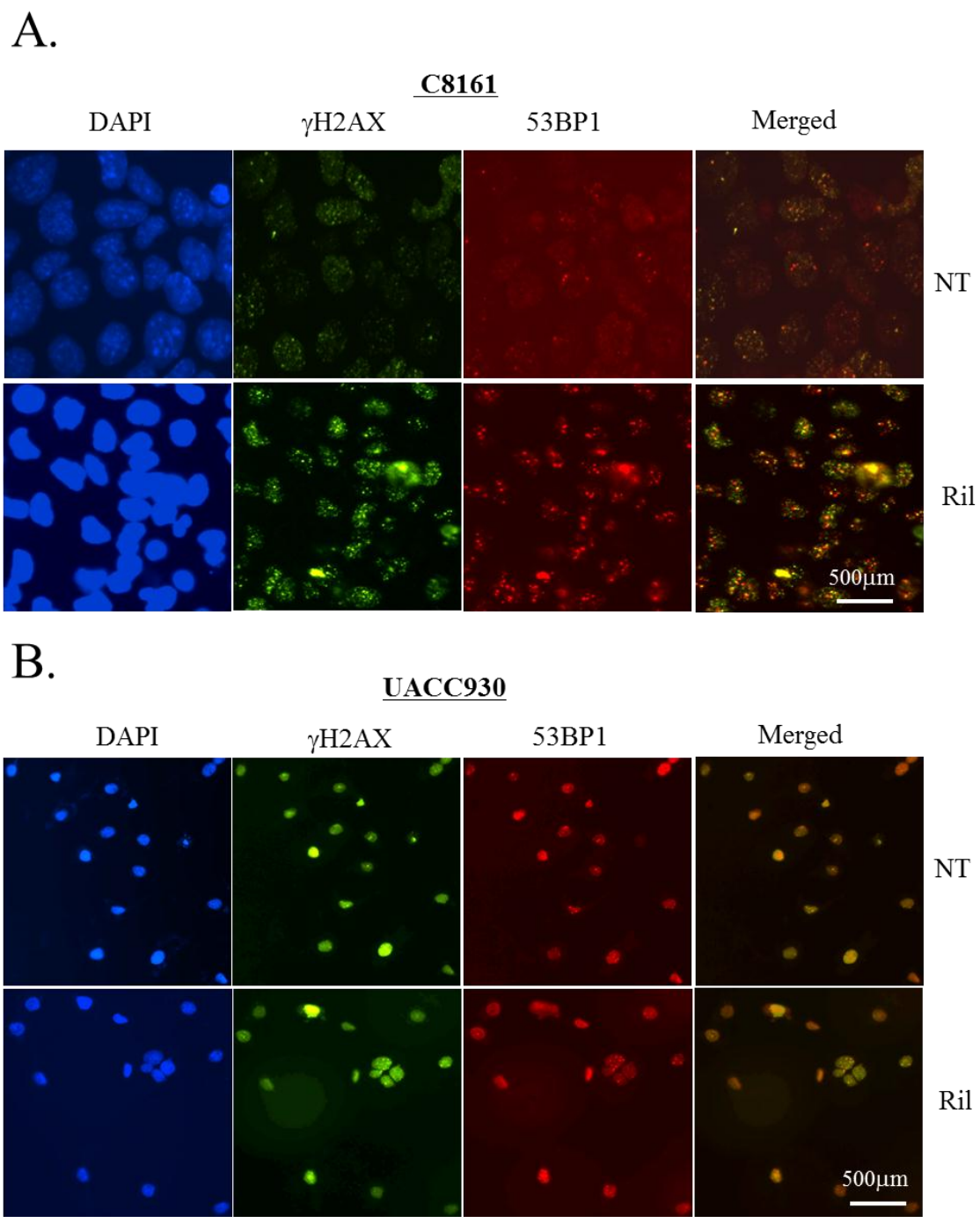
A.
C8161
DAPI
γH2AX
53BP1
Merged
NT
Ril
500μm
B.
UACC930
DAPI
γH2AX
53BP1
Merged
NT
Ril
500μm

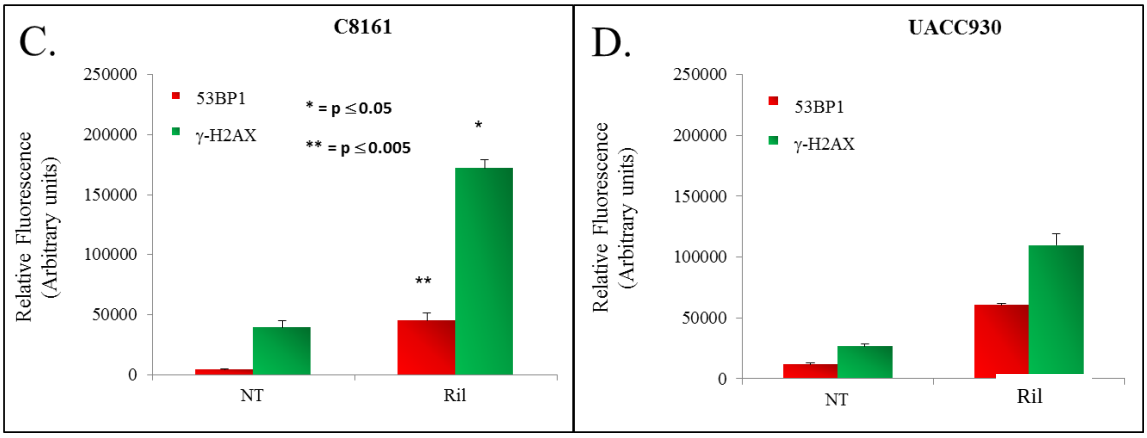

Figure 11. Riluzole induces DNA DSBs in GRM1 expressing human melanoma cells.

(A.) GRM1 expressing human melanoma cells C8161 and (B.) UACC930 human melanoma cells that express a truncated, non-functional version of GRM1 were treated with 10 μM of etoposide for 1 h as a positive control (not shown) or 10 μM riluzole for 3 h. Immunofluorescence staining was performed using anti-bodies against 53BP1 (red) and γ-H2AX (green) to show colocalization to sites of DNA DSBs. DAPI is shown as a nuclear control. Immunofluorescence was quantified and is shown (C and D). Each bar represents mean ± SEM, n=10. * $p \leq 0.05$; ** $p \leq 0.005$.

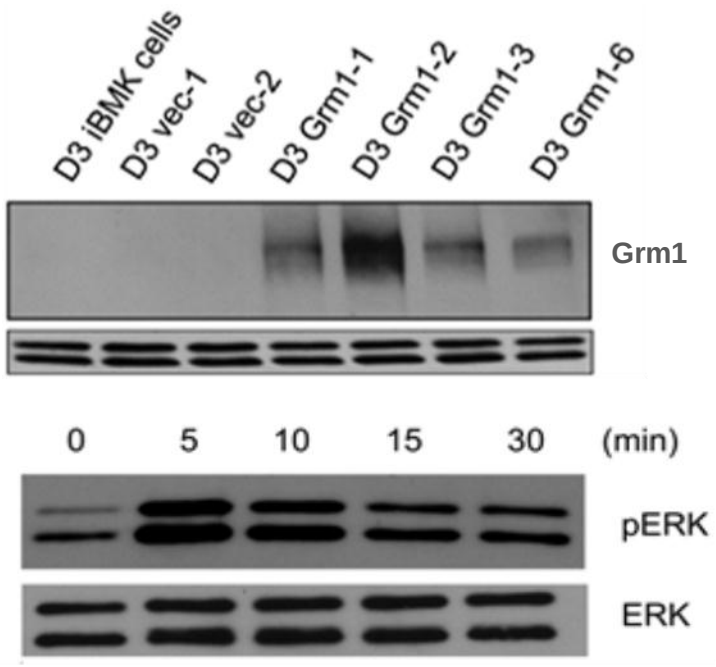

Martino and Wall et. al., Oncogene, 2012

Figure 12. D3-Grm1 clones express functional Grm1

(A.) Expression of exogenous Grm1 receptor in D3 iBMK epithelial cell clones. (B.) MAPK/ERK is activated by Grm1 agonist, L-quisqualate, in D3-Grm1 cells, as assessed by immunoblotting, which demonstrated enhanced levels of phosphorylated ERK (pERK).

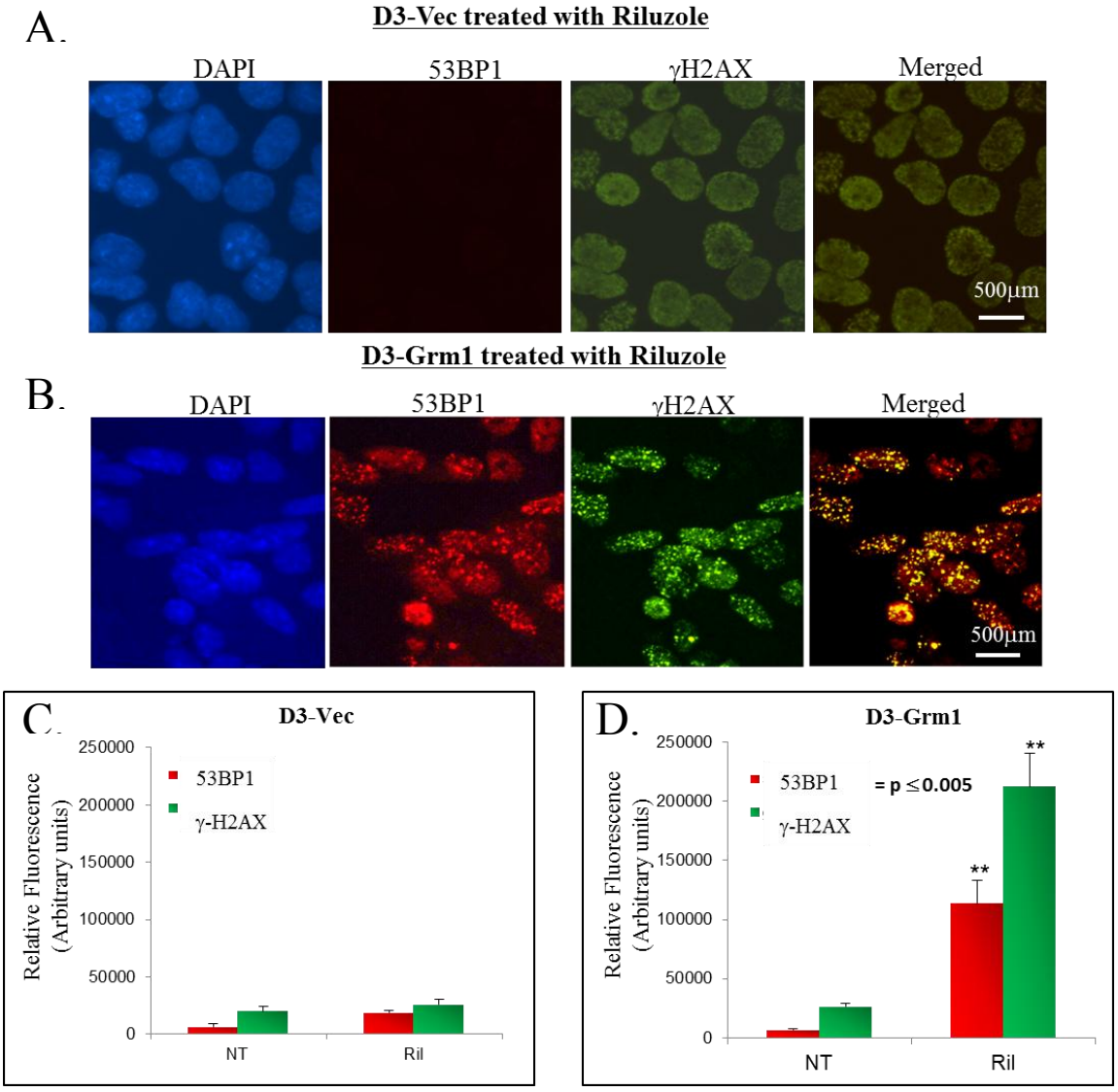

Figure 13. Amount of DSB in riluzole treated human melanoma cells is independent of apoptosis.

Stable clones isolated from apoptosis deficient, immortalized baby mouse kidney epithelial cells containing either (A.) empty vector (D3-Vec) or (B.) exogenous cDNA encoding the murine *Grm*1 cDNA (D3-Grm1) were treated with riluzole for 3 h and immunofluorescence stains performed using DAPI as nuclear control and 53BP1 and γ-H2AX as a measure of DNA DSBs. Quantitation of immunofluorescence staining is shown (C. and D.). Each bar represents mean ± SEM, n=10. * $p \leq 0.05$; ** $p \leq 0.005$.

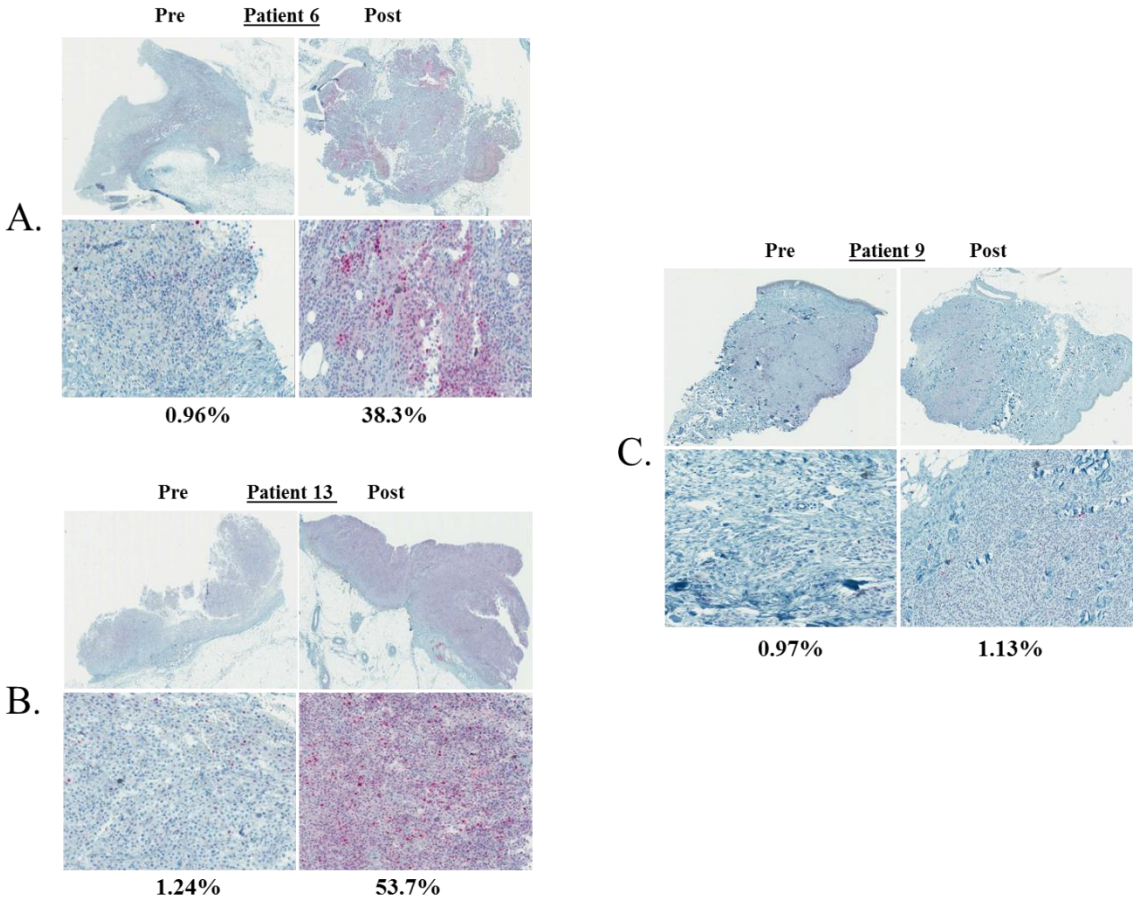

Figure 14. Markers of DNA damage detected in post-treatment human melanoma tumor samples from responding patients in Phase 2 trial of riluzole.

IHC against γ-H2AX in pre-and post-riluzole treated specimens from responders of a recently completed Phase II riluzole trial. Positive staining is indicated by pinkish color in the nucleus (Vector Red, Vector Labs). Panels are either 10X magnifications or 100X magnifications. Patients 6 and 13 (A and B) are two post-treatment responders and show higher positive staining in post-riluzole treatment biopsies compared to pre-treated ones compared to a non-responder, patient 9 (C.) which shows no difference in staining intensities between pre- and post-riluzole treated biopsies.

Section II. The molecular mechanisms of riluzole-induced G_2/M arrest in GRM1 expressing human melanoma cells

Aim 2: Rationale

Riluzole is an FDA approved drug used for the treatment of amyotrophic lateral sclerosis (ALS) and also has off-label uses in other psychiatric and neurologic disorders. Riluzole has been shown to influence glutamatergic signaling by decreasing the amount of available ligand (glutamate) for the receptor [24, 312, 313]. We have shown that riluzole is able to arrest melanoma cells in G_2/M phase of the cell cycle and enhance the effects of ionizing irradiation on human melanoma cell that express GRM1. In both instances, an increase in the apoptotic cell population was detected, which was further confirmed biochemically by elevated levels of apoptotic marker, the cleaved form of caspase 3. In addition, previous studies performed to assess the extent of DNA damage in riluzole treated mice exposed to γ-irradiation revealed enhanced staining in tumors from these xenograft-bearing mice treated with riluzole alone. Taken together, these results prompted us to hypothesize that riluzole elicits its cytotoxic effects on GRM1-expressing cells by way of inducing oxidative stress via the accumulation of "unreleased" intracellular levels of glutamate, which alters the homeostasis of glutamate/cystine exchange resulting in a decrease in the amount of available cystine reduce to cysteine, which is required for the synthesis of glutathione (GSH), leading to enhanced intracellular levels of ROS.

Materials and Methods

K. Cell culture

Immortalized non-tumorigenic human melanocytes, hTERT/CDK^{R24C}/p53^{DD} were provided by Dr. David Fisher (Harvard Medical School, Boston, MA) and maintained in Medium 254 with added human melanocyte growth supplements (Invitrogen, Carlsbad, CA)[295]. C8161 and C81-61 were from Dr. Mary J.C. Hendrix (Children's Memorial Research Center, Chicago, IL). UACC930 and UACC903 were provided by Dr. Jeffery M. Trent (Translational Genomics Research Center, Phoenix, AZ). C8161 and C81-61 were from Dr. Mary J.C. Hendrix (Children's Memorial Research Center, Chicago, IL). Melanoma cell lines were grown in RPMI 1640 plus 10% fetal bovine serum (FBS).

L. DNA transfection

All DNA transfections were performed with DOTAP according to the manufacturer's instructions (Roche, Basel, Switzerland). Coding sequence for the full-length human form of the receptor was subcloned from human GRM1 cDNA (Image Clone) into mammalian expression vector pCI-neo (Promega, Madison, WI). Stable hTERT/CDK^{R24C}/p53^{DD} clones expressing GRM1 were selected using 150 µg/ml of Geneticin in Medium 254 with added human melanocyte growth supplements. Receptor expression was confirmed by Western blotting.

M. Ponasterone inducible system

C8161 cells were transfected with 4 µg of pVgRXR plasmid DNA (A gift from Dr. Danny Rangasamy, The Australia National University, Canberra, Australia) with the Lipofectamine 2000 reagent as per manufacturer's protocol. Stable clones expressing pVgRXR receptor were selected for using 5 µg/ml of Zeocin in RPMI-1640 medium

supplemented with 10% FBS. Receptor expression was confirmed by Western immunoblotting. C8161 pVgRXR cells were transfected with 4 µg of siGRM1 plasmid DNA with the siRNA sequence 5' GATGTACATCATTATTGCC 3'[314], cloned into the pIND vector containing 5 repeats of ecdysone response elements [315], using Lipofectamine 2000 per manufacturer's protocol. Stable C8161 pVgRXR siGRM1 clones were generated by selection with 5 µg/ml Zeocin and 300 µg/ml G418. Induction of siGRM1 was achieved by treating the cells with 1-10 µM of Ponasterone A (PonA) as described [316, 317].

N. Immunofluorescent staining

Cells were grown on glass coverslips to the appropriate density and synchronized by serum starvation for 48 h. Following synchronization cells were treated as indicated. At each time point, cells were fixed with 4% paraformaldehyde in PBS and permeabilized for 10 minutes in 0.5% Triton X-100 in PBS at room temperature. Cells were then washed with PBS and blocked in 5% goat serum/PBS. Primary antibodies (53BP1 anti rabbit IgG and phospho H2A anti mouse IgG) were incubated at room temperature in blocking solution. Cells were washed with PBS for 5 min and incubated with Fluorophore-conjugated secondary antibody (Alexa Fluor 488 goat anti-mouse IgG and Alex Fluor 546 goat anti rabbit IgG, Invitrogen, Carlsbad, CA) for 1 h in blocking solution. Cells were washed with PBS for 5 min and mounted using Vectashield (Vector Laboratories, Burlingame, CA). Images were captured using a Nikon Eclipse microscope coupled with a Coolsnap EZ camera powered by NIS-Elements BR 3.1 software. All quantifications were performed using ImageJ software.

O. Western immunoblots

Whole cell protein lysates were prepared as described previously [318]. Briefly, cells were washed with ice-cold PBS and extraction buffer was added and cells were collected. After incubation on ice for 20 min, supernatants were collected by centrifugation at 25,000 x g at 4°C for 20 min. Protein concentration was determined using DC protein assay kit (Bio-Rad, Hercules, CA). Routinely, 25 µg of whole cell protein lysates were loaded for each lane in Western immunoblots.

P. Detection of reactive oxygen species (ROS)

Cells were seeded at 3 x 10^5 per well in a 6 well plate and treated as indicated. At appropriate time points, cells were loaded with dihydrorhodamine 123 (DHR123) for at least 20 min at 37º C in a humidified 5% CO_2/95% air incubator. The plates containing the cells were washed by several changes of growth medium, trypsinized and cells collected by centrifugation at 300 x g, washed, and resuspended in PBS. Cells were immediately measured by the Flow Cytometry Facility Core at Rutgers University using a Beckman Coulter FC500 Analyzer (Epics XL-MCL model). Rhodamine 123 derived from DHR123 by oxidation was excited with an air-cooled argon ion laser at 488 nm. Fluorescent emission of the marker was detected between 525 and 535 nm. Cell debris and multi-cell aggregates were electronically gated out. For ROS rescue studies, cells were either pretreated with *N*-acetyl cysteine pH 7.4 at a final concentration of 10 mM for 30 min prior to the addition of riluzole or co-incubated with reduced glutathione ethyl ester at a final concentration of 1 mM.

Q. Measurement of intracellular levels of glutathione (GSH)

Intracellular levels of total glutathione were measured using a GSH/GSSG quantification kit (Dojindo Laboratories, Kumamoto, Japan) according to manufacturer's instructions. Briefly, cells were seeded at 5 x 10^5 cells in 100 mm culture dishes. Cells were treated, collected and pelleted by centrifugation at 200 x g for 5 min at the indicated time points. Pellets were washed with ice cold PBS and resuspended in 80 µl of 10 mM HCl solution. Cells were lysed by freezing and thawing twice and 5% sulfasalicylic acid solution was added to a final concentration of 1%. Cells were pelleted by centrifugation at 8000 x g for 10 min and supernatant was collected. Each sample (20 µl) was placed in a 96 well plate in triplicate in combination with 120 µl of buffer solution from the kit and incubated for 1 hour at 37° C after which time 20 µl of substrate, coenzyme, and enzyme working solutions were added. Samples were incubated for 10 min at 37° C and the absorbance read at 405 nm in a Tecan infinite M200 plate reader (Tecan, Durham NC). Concentration of glutathione was calculated using calibration curve and presented as fold difference compared to untreated cells.

R. Measurement of intracellular levels of glutamate

Amplex Red Glutamic Acid/Glutamate Oxidase assay kit (Invitrogen-Molecular Probes) was used to measure intracellular levels of glutamate. Cells were plated at 10^5 cells per 60 mm in media alone or media containing 10 µM of riluzole. After specified time, cells were removed from the plate using trypsin. Cells were counted to attain density and pelleted at 300 x g. Cells were rinsed twice using PBS then resuspended in 200 µL of

PBS. Cell membranes were weakened by three freeze and thaw cycles. Cells were transferred to a precooled dounce homogenizer with 30 strokes using a pestle to rupture mitochondrial membrane. The suspension was then measured for the amount of glutamate according to the manufacturer's protocol.

Results

2.1 Riluzole-induced DNA damage only occurs in human melanoma cells that express functional GRM1

To unequivocally determine whether our previous observations of riluzole-induced DNA damage was dependent on GRM1 expression we took advantage of isogenic cell lines: immortalized, non-tumorigenic human melanocytes, hTERT/CDK^{R24C}/p53^{DD} either transfected with an empty vector or one that contains cDNA encoding human GRM1 in a mammalian expression vector (pCI Neo). Isogenic clones were selected and expression of the receptor was assessed by Western immunoblot and its functionality was confirmed by responsiveness of the cells to stimuli/inhibitors of the receptor (Figure 15). We then assessed levels of riluzole-induced damage by way of co-localization of 53BP1 and γ-H2AX using immunofluorescent staining of these GRM1-expressing clones after riluzole treatment. Immunofluorescent assays were performed using the same controls and treatment groups as described in Section I for the human melanoma cell lines. We found that hTERT/CDK^{R24C}/p53^{DD} cells did not show discrete foci co-localization of 53BP1 and γ-H2AX after exposure to riluzole when compared to untreated control (Figure 16A). In contrast, we found that with the introduction of the exogenous GRM1 receptor there was induction of DSB by riluzole indicative by the co-localization of 53BP1 and γ-H2AX foci in hTERT/CDK^{R24C}/p53^{DD} –GRM1(Figure 16B**).** Fluorescence intensity was quantified and is shown (Figures 16C and 16D). hTERT/CDK^{R24C}/p53^{DD} cells treated with riluzole show no significant difference compared to untreated cells while hTERT/CDK^{R24C}/p53^{DD}-GRM1 isogenic cells show an

increase in the amount of co-localization of both γ-H2AX ($p < 0.05$) and 53 BP1 ($p < 0.005$) when exposed to riluzole

To further confirm that GRM1 expression is required in riluzole-mediated DNA damage we isolated several stable C8161 isogenic clones that express an inducible sh-GRM1 RNA containing the modified mammalian ecdysone-inducible hsp70 expression vector were established (Figure 17A) [319, 320]. In the presence of the inducer, ponasterone A (PonA), an analogue of ecdysone, the expression of GRM1 is reduced (Figure 17B) [1]. C8161 isogenic clones containing the inducible siRNA to GRM1 were either induced with PonA or left uninduced and treated with riluzole for 24 hours or left untreated. Immunofluorescence staining against γH2AX and 53BP1 was performed to assess the formation of foci. In the absence of the inducer riluzole elicited DNA damage when compared no treatment (Figure 18A). In contrast, C8161 cells in which siGRM1 was induced show much reduced amount of co-localized γH2AX and 53BP1 foci which points to a decrease in riluzole sensitivity with a decline in functional GRM1 receptor (Figure 18B). Further quantification of the fluorescence intensity show a significant increase in the amount of signal from both markers compared to no treatment in cells where GRM1 is expressed (Figure 18C) in contrast to cell in which GRM1 was silenced (Figure 18D) These results further confirm the requirement of GRM1 in riluzole mediated DSBs.

2.2 Riluzole promotes accumulation of intracellular glutamate in GRM1 positive human melanoma cells

We have shown that human melanoma cells that express functional GRM1 have elevated levels of extracellular glutamate in their surrounding environment (Figure 5) [11]. Treatment with riluzole inhibits the release of glutamate from the intracellular to extracellular space thus likely enhancing intracellular accumulation of glutamate. To assess this, GRM1 positive C8161 and GRM1 negative UACC930 human melanoma cell lines as well as hTERT/CDK^{R24C}/p53^{DD} and hTERT/CDK^{R24C}/p53^{DD}-GRM1 isogenic cell lines were treated with 10 μM of riluzole for 24, 48, and 72 h after which time cells were collected and assessed for intracellular concentrations of glutamate (Figures 19A and B). We found that GRM1 expressing C8161 cells treated with riluzole had approximately a two-fold increase in intracellular glutamate concentrations at 48 hours after treatment compared to untreated samples (Figure 19B). In contrast, GRM1-negative UACC930 cells showed no alteration in the amount of glutamate within the cells after treatment with riluzole. Normal human melanocytic cell line hTERT/CDK^{R24C}/p53^{DD} showed a decrease of the amount of intracellular glutamate, however, in hTERT/CDK^{R24C}/p53^{DD}-GRM1 cells, there was a dramatic increase in the amount of glutamate concentrations within the cells (Figures 19A and B).

2.3 Riluzole treatment in GRM1-expressing human melanoma cells increases oxidative stress

Results from these experiments strongly suggest riluzole plays a role in inducing DNA DSBs independent of apoptosis, however, how riluzole treatment elicits DNA damage remains an open question. We postulated that riluzole inhibition of glutamate release from within the cell to the extracellular environment leads to a build-up of

intracellular glutamate and this abundance of glutamate could produce adverse effects within the cell, possibly as a result of a compromise in intracellular homeostasis. It is known that the export of glutamate is coupled to the import of cystine, by plasma membrane transporters which regulate bidirectional transfer of specific amino acids across the plasma membrane [321]. Cystine is reduced to cysteine, which is a building block for the antioxidant glutathione (GSH) that plays a predominant role in cellular defenses against oxidative and nitrosative stress as well as reactive electrophiles [322, 323]. Therefore, an excess of intracellular glutamate results in disruption of glutamate/cystine homeostasis thus interfering with the glutamate/cystine-antiporter system resulting in a reduced level of cysteine, a decrease in GSH synthesis and an accumulation of reactive oxygen species (ROS). To begin to test this hypothesis, we measured the levels of intracellular ROS formation in two GRM1-expressing human melanoma cell lines, C8161 and UACC903. Cells were treated with 10 μM of Riluzole for 12, 24, and 48 h using a cell-permeable ROS-specific fluorogenic marker, dihydrorhodamine 123 (DHR123) and analyzed by flow cytometry. Examples of one-parameter fluorescence histograms of C8161 at 24 h post-treatment are shown (Figures 20A and B). Results of both C8161 and UACC903 are summarized in Figure 20C. We found that 24 hours following the treatment with riluzole, there was a 50% increase in the mean DHR123 fluorescence in C8161 cells when compared to untreated C8161 cells. UACC903 cells demonstrated a 14% increase when compared to control. This indicates that treatment with riluzole results in an increase in ROS within these cells.

The antioxidant function of glutathione is well established in physiological and pathological states [324]. GSH can either scavenge radicals by hydrogen donation directly or act as a cofactor for other antioxidant enzymes [325]. Because GSH itself is not effectively transported into cells, compounds such as *N*-acetyl cysteine (NAC) and GSH ethyl ester (GSH-Et) have been developed to increase cysteine transport into the cell (NAC) or to deliver a GSH moiety directly into the cell, bypassing enzymatic control of γ-glutamyl transpeptidase (GGT) and γ- glutamylcysteine synthetase (GCS) [326, 327]. GSH esters are hydrolyzed to GSH intracellularly whereas NAC is hydrolyzed to cysteine and participates in GSH synthesis by formation of γ-glutamylcysteine. It is the availability of cysteine that usually limits endogenous GSH synthesis. To see if we could rescue human melanoma cells from an increase of ROS, C8161 and UACC903 human melanoma cells were either preincubated with a 10 mM NAC solution for 30 min prior to riluzole exposure or dosed with 1 mM of a reduced form of GSH-Et at the time of riluzole treatment. Cells were harvested at 12, 24, and 48 h at which time they were loaded with dihydrorhodamine 123, washed and analyzed by flow cytometry. Pretreatment of C8161 or UACC903 cells with NAC followed by riluzole exposure led to a reduction of 20% or 6% in ROS levels (Figures 20A and C). Co-incubation of riluzole and GSH-Et resulted in a decrease of 32% or 9% of ROS levels (Figures 20B and C). The ability of supplementation of cysteine (NAC) as well as an exogenous form of GSH that is readily absorbed by the cell can rescue the cells from an increase in ROS supports the notion that riluzole elicits its effects on GRM1- expressing human melanoma cells, in part, by decreasing the amount of available endogenous GSH.

These experiments were repeated using the immortalized non-tumorigenic normal human melanocytes and the stable GRM1-expressing clone previously derived from them. We observed that the parental cells, hTERT/CDK^{R24C}/p53^{DD}, demonstrated no significant differences between groups that were left either untreated, treated with vehicle (DMSO) or riluzole (Figure 21A) while the GRM1-expressing isogenic cell line showed a 15-34% increase in ROS levels within 12 hours following riluzole treatment and the highest levels detected at 24 hours (Figure 21B). Calculated fold changes in ROS levels are shown in Figure 21C. These results demonstrate that (i) an increase in ROS is detected starting at 12 hours post treatment and that (ii) riluzole-mediated ROS formation is correlated with GRM1 expression.

2.4 Decrease in GSH in human melanoma cells that express GRM1

Cellular GSH levels reflect a steady state balance between synthesis and loss. A sufficient accumulation in ROS leads to an increase in the rate of GSH consumption within the cell, which results in cellular injury such as damage to DNA, protein, and lipid membranes. We treated human melanoma cell lines with 10 μM of riluzole for the 24 and 48 hour time points (Figure 22) at which time cells were harvested and assessed for intracellular levels of GSH using a commercially available kit. We found that while riluzole shows little effect on levels of GSH in immortalized non-tumorigenic human melanocytic cell line hTERT/CDK^{R24C}/p53^{DD} at 24 and 48 hours, GRM1- expressing human melanoma cell line C8161 shows a time dependent decrease in levels of GSH over 48 h (Figure 22). GRM1 negative UACC930 cells displayed similar trend as seen in normal melanocytes, possibly due to the lack of functional GRM1 in these cells while

hTERT/CDK^{R24C}/p53^{DD}–GRM1 cells displayed similar decreases in intracellular GSH compared to C8161. These results show that riluzole is able to alter intracellular concentrations of the endogenous antioxidant GSH and is dependent of a functional GRM1.

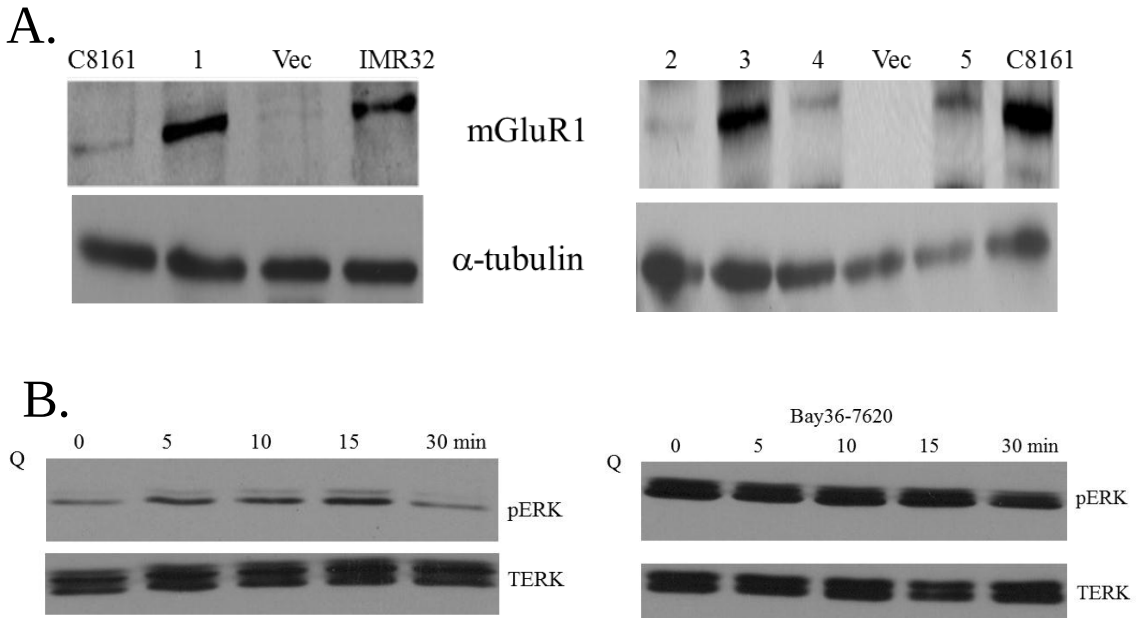

Figure 15. GRM1 expression in hTERT/CDK4^{R24C}/p53^{DD} human melanocytes transformed with human *GRM1*

Western immunoblots of stable GRM1-human melanocytic clones, hTERT/CDK4^{R24C}/p53^{DD} -GRM1. (A.) Lanes 1 and 10 are GRM1 expressing C8161, lanes 2 and 8 are vector controls, lane 3, 5, 6, 7, and 9 are five independent GRM1-human melanocytic clones, lane 4 is IMR32, human neuroblastoma cell line, a positive control for GRM1 expression. (B.) MAPK/ERK is activated by GRM1 agonist, L-quisqualic acid and shows no altered modulation when preincubated with the non-competative antagonist of GRM1, Bay 36-7620.

A.

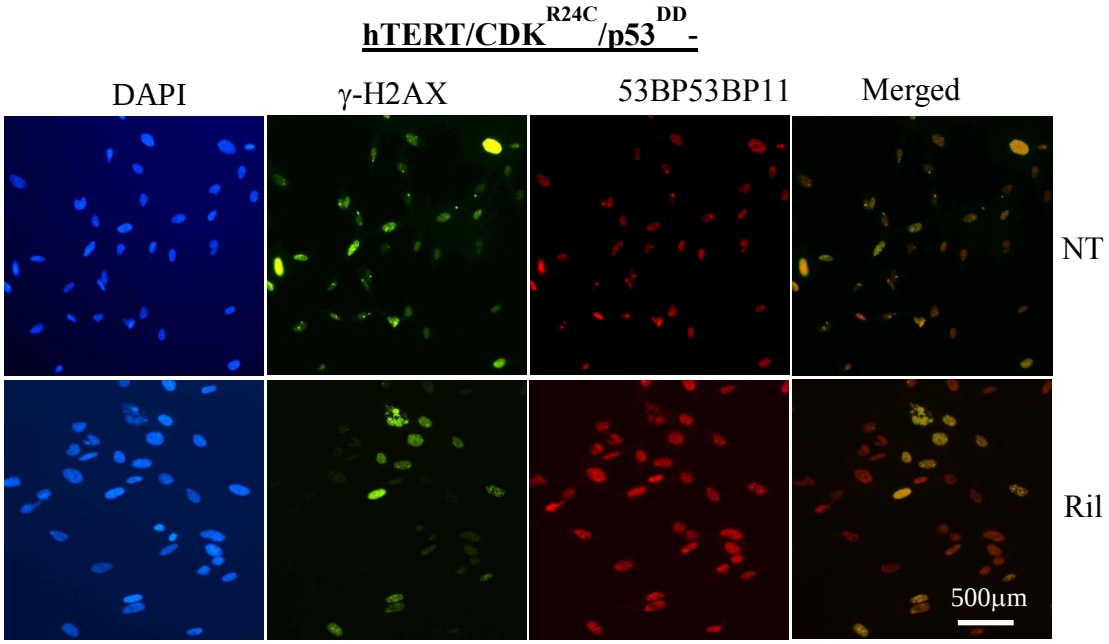
hTERT/CDK^R24C/p53^DD-
DAPI
γ-H2AX
53BP53BP11
Merged
NT
Ril
500μm

B.

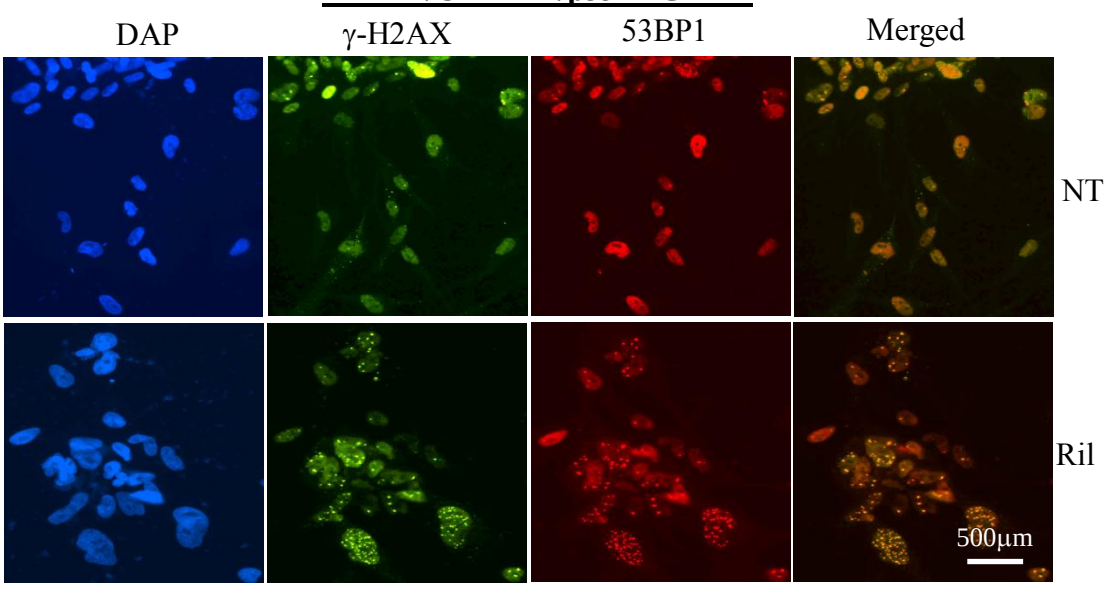
hTERT/CDK^R24C/p53^DD-GRM1
DAP
γ-H2AX
53BP1
Merged
NT
Ril
500μm

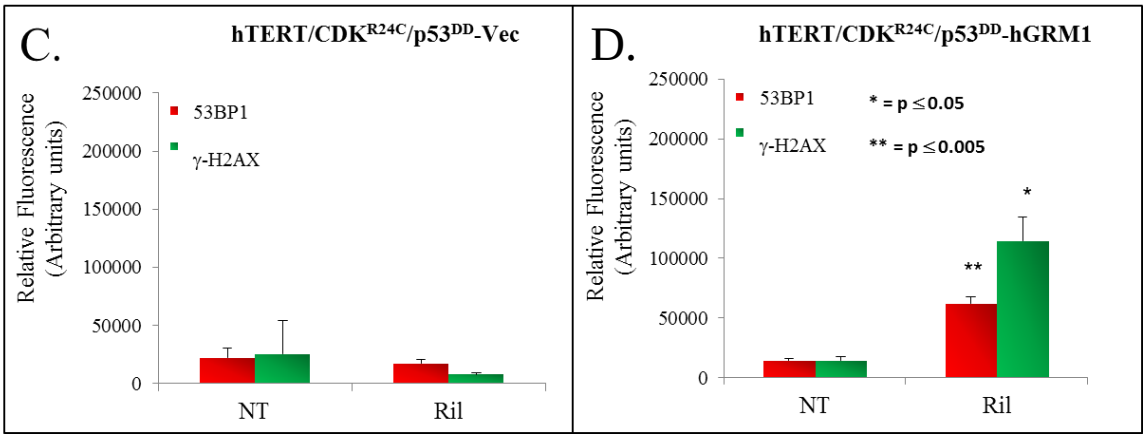

Figure 16. Riluzole induces DNA DSBs in human only in melanocytic cells that express GRM1

(A.) A stable vector-only clone derived from immortalized, non-tumorigenic, normal human melanocytes hTERT/CDK^{R24C}/p53^{DD} or (B.) a stable GRM1-expressing-hTERT/CDK^{R24C}/p53^{DD} isogenic clone were assessed for DNA damage following treatment with 10μM riluzole for 3 h using markers for DSB, 53BP1 and γ-H2AX . Immunofluorescence was quantitated and values are shown (.C and D.). Each bar represents mean ± SEM, n=10. * $p \leq 0.05$; ** $p \leq 0.005$.

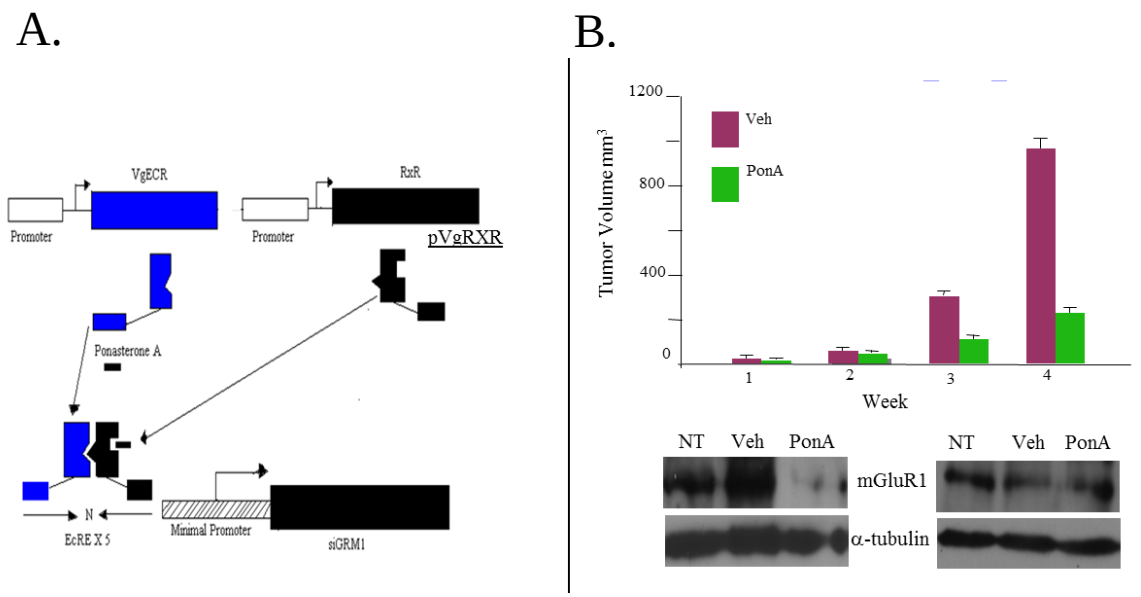

Figure 17. PonA inducible shGRM1 clones .

(A.) Schematic showing ponasterone A inducible siRNA expression system. (B.) (Bottom) pVgRXR shGFP control, no treatment (NT), vehicle (Veh, DMSO) or with the inducer of the ecdysone system, the insect molting steroid 20-OH ecdysone (Ponasterone A, PonA, 5µM). Levels of GRM1 were decreased only shhGRM1 clone but not shGFP clone, α-tubulin was used to show equal loading. (Top) In vivo xenografts with the same shGRM1cells as in panel A. The inducer PonA (10mg/kg) was given I.P. twice a week. Reduced tumor volume was detected in PonA treated mice. C: Western immunoblots of stable GRM1-human melanocytic clones. Lanes 1 and 10 are GRM1 expressing C8161 cells, lanes 2 and 8 are vector control clones, lane 3, 5, 6, 7, and 9 are the five independent stable GRM1-human melanocytic clones, lane 4 is IMR32, human neuroblastoma cell line, a positive control for GRM1 expression.

A.

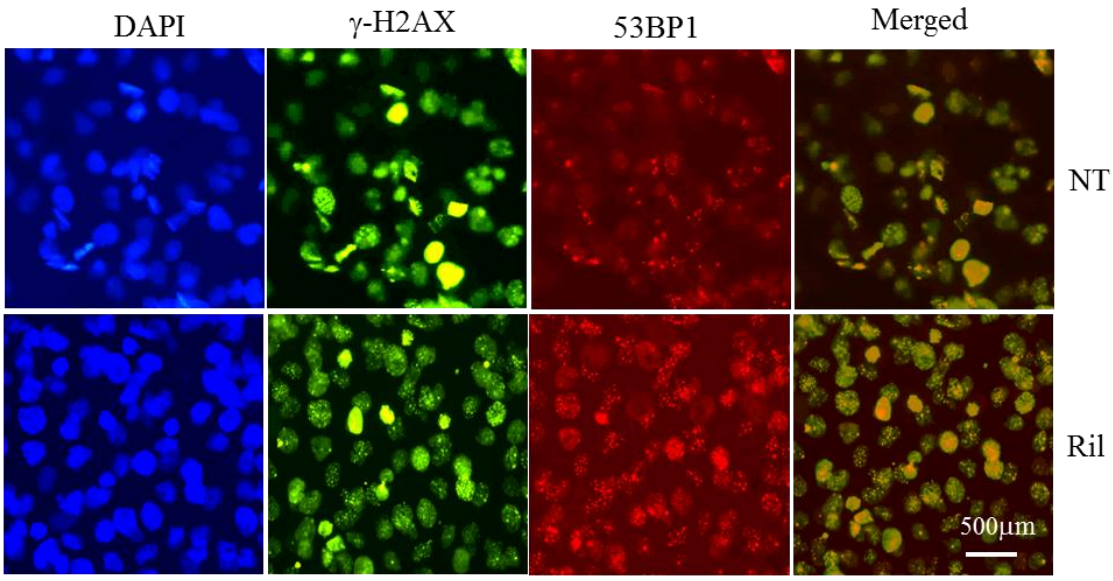
No induction
DAPI
γ-H2AX
53BP1
Merged
NT
Ril
500µm

B.

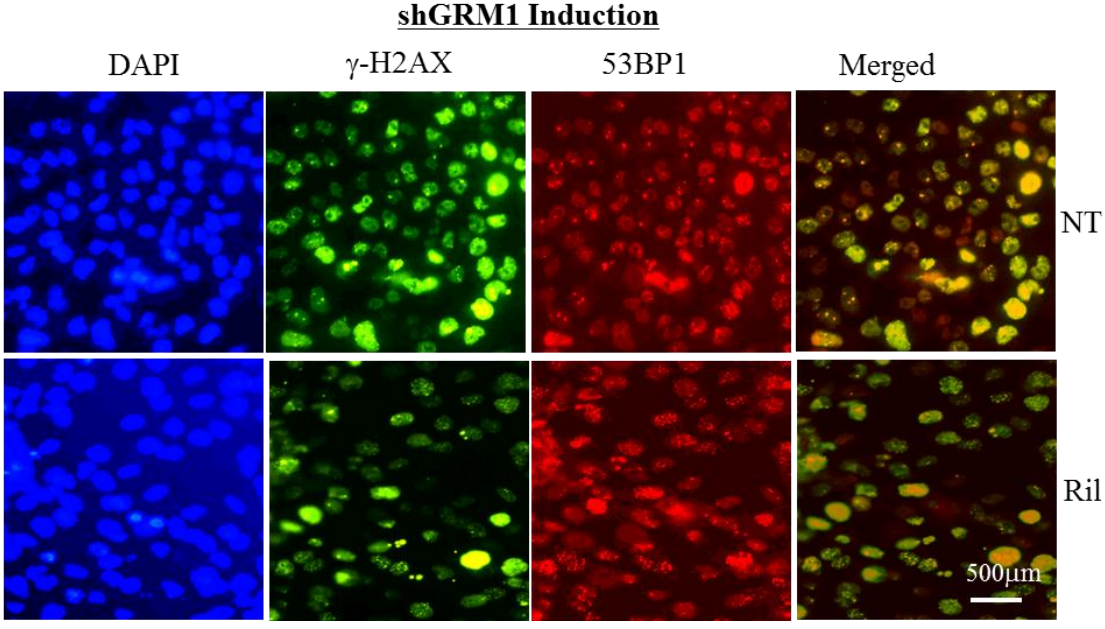
shGRM1 Induction
DAPI
γ-H2AX
53BP1
Merged
NT
Ril
500µm

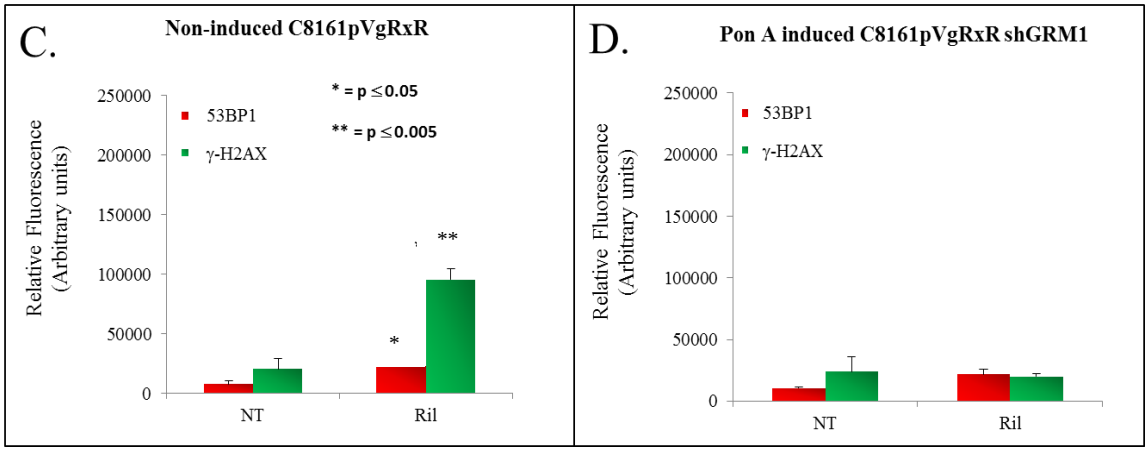

Figure 18. Knock down of GRM1 expression reduces amount of DSB in riluzole treated human melanoma cells independent of apoptosis.

Stable C8161 human melanoma clones harboring an empty vector (A and C) or a PonA-inducible shGRM1 (B and D) were treated with 10 µM etoposide for 30 min as a positive control (not shown) and 10 µM of riluzole for 3 h. Immunofluorescence staining was performed using DAPI as nuclear control and 53BP1 and γ-H2AX were used to show sites of DNA DSB. Quantifications of the immunofluorescence images are shown (C and D). Each bar represents mean ± SEM, n=10. * $p \leq 0.05$; ** $p \leq 0.005$.

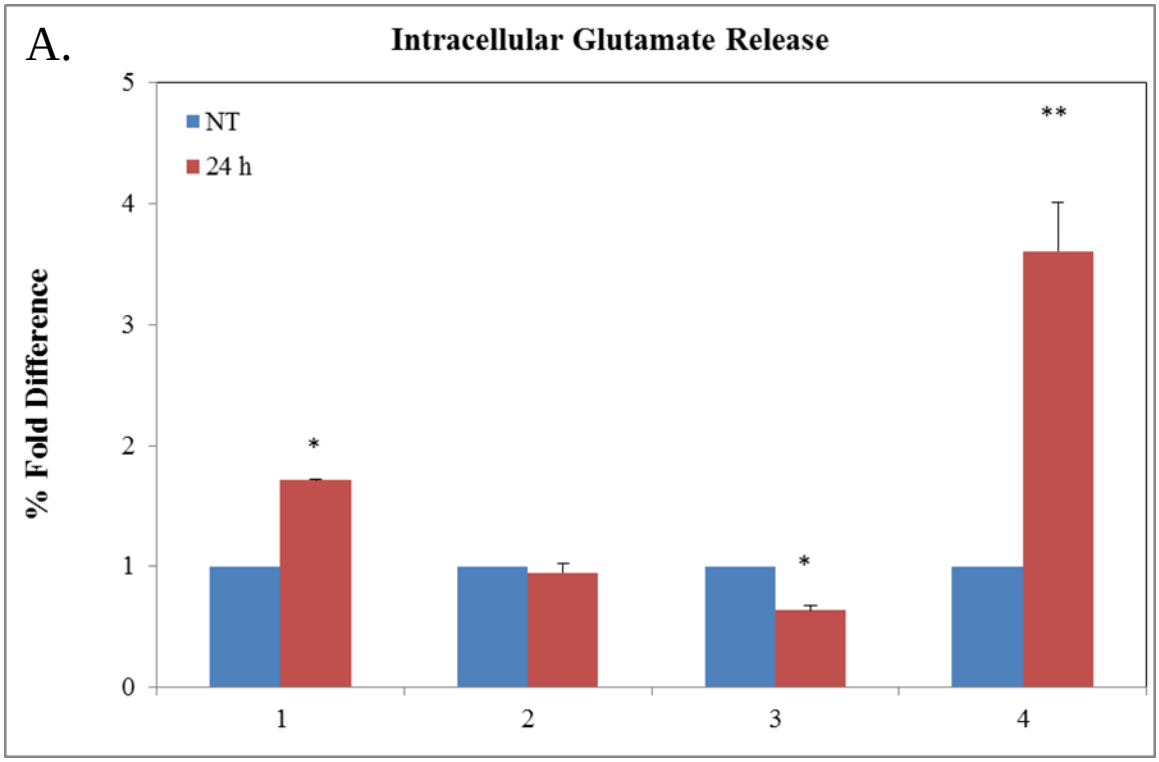
A.
Intracellular Glutamate Release
% Fold Difference
NT
24 h
0
1
2
3
4
5
*
*
**
1
2
3
4

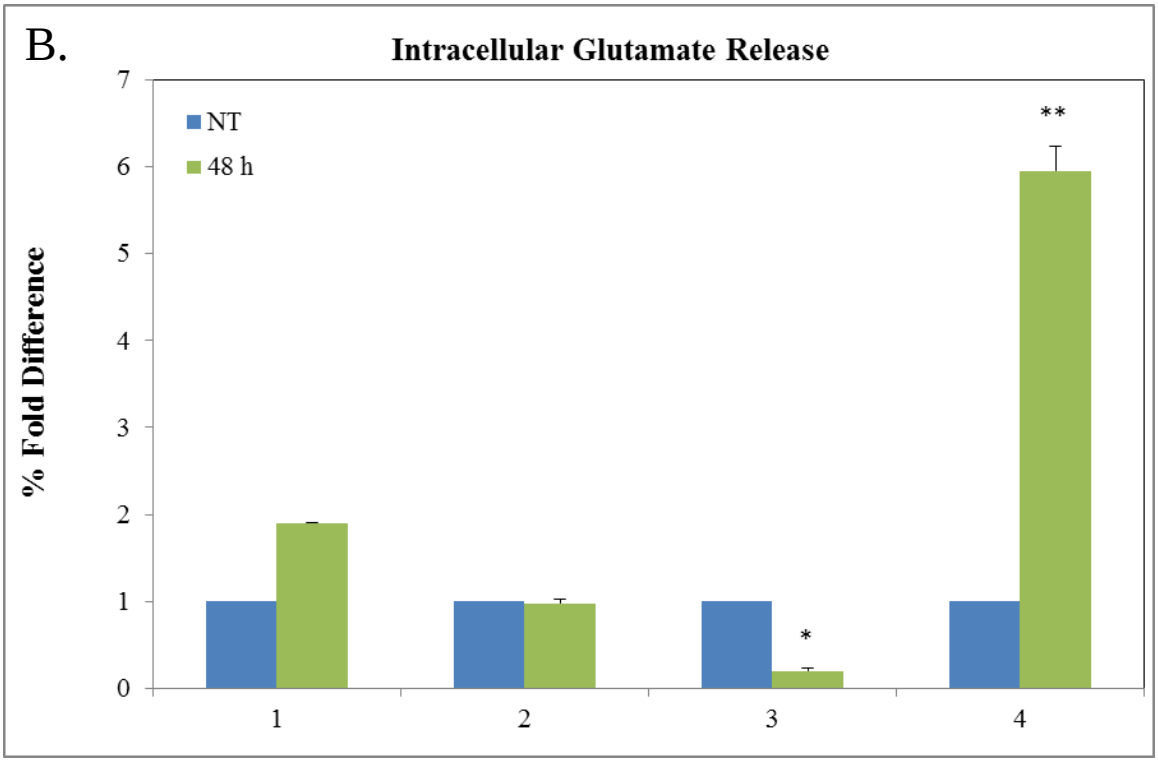
B.
Intracellular Glutamate Release
% Fold Difference
NT
48 h
0
1
2
3
4
5
6
7
*
**
1
2
3
4

Figure 19. **Riluzole treatment of GRM1-positive human melanoma cells induces an increase in intracellular levels of glutamate**

Human melanoma cells C8161 and UACC930 were assessed for intracellular levels of glutamate after treatment with riluzole for 24 and 48 h. Immortalized human melanocytes, hTERT/CDK^{R24C}/p53^{DD}, and GRM1-expressing isogenic clones hTERT/CDK^{R24C}/p53^{DD}-GRM1 were also assessed. Concentrations of glutamate were normalized to the number of viable cells within each treatment group and are shown graphically as percent of non-treated (NT) cells. Statistical analysis was performed between untreated and treated pairs to show significance. Each bar represents mean ± SEM, n=10. * $p \leq 0.05$; ** $p \leq 0.005$

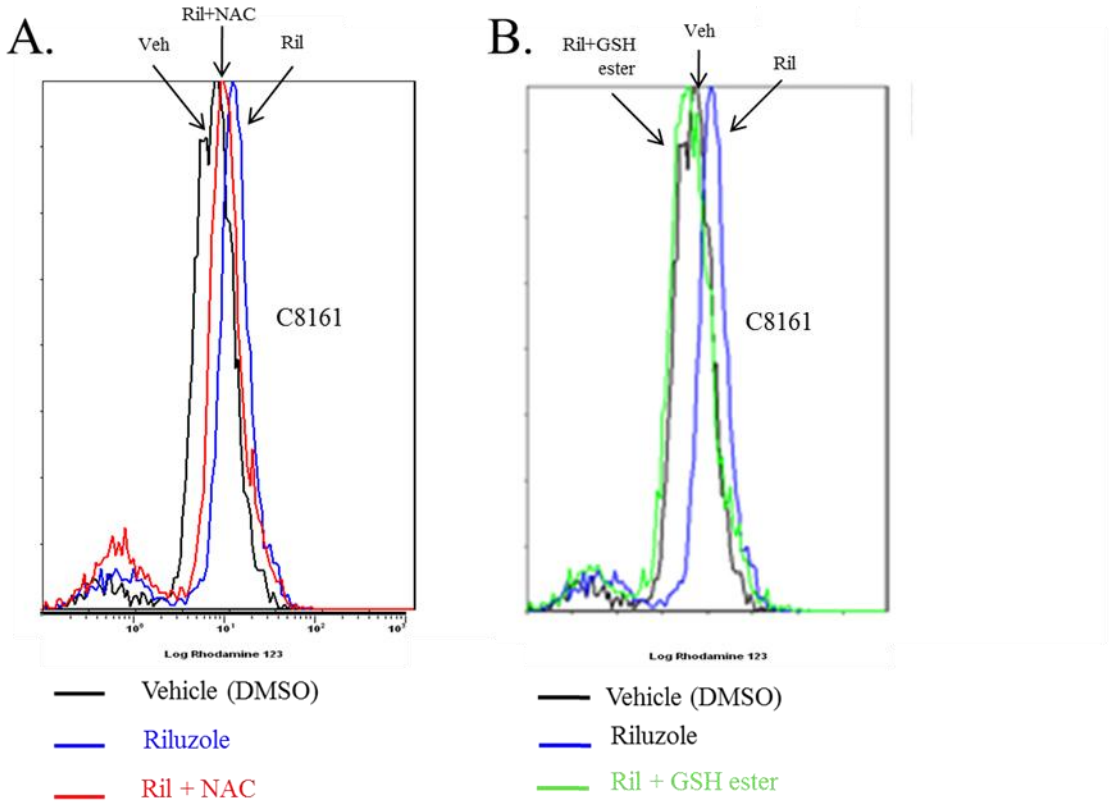

C.

Cell lines	No treatment (NT)	Vehicle (DMSO)	Riluzole 24 h	Riluzole + NAC 24 h	Riluzole + GSH ester 24 h
C8161	1.00	1.00	1.51	1.21	1.02
UACC903	1.00	1.02	1.14	1.08	1.04

Figure 20. Riluzole treatment results in an increase in ROS in human melanoma cells and is rescued by inclusion of NAC or reduced GSH-Et.

GRM1-expressing human melanoma cells C8161 and UACC903 were pre-incubated with either **(A.)** 10 mM NAC for 30 min or co-incubated with **(B.)** 1 mM reduced GSH-Et. Cells were then treated with 10 μM of riluzole for 12, 24, and 48 h and assessed for levels of ROS using DHR123 followed by flow cytometry. The results of both human melanoma cells lines are summarized in **(C.)** as the fold difference normalized to untreated samples.

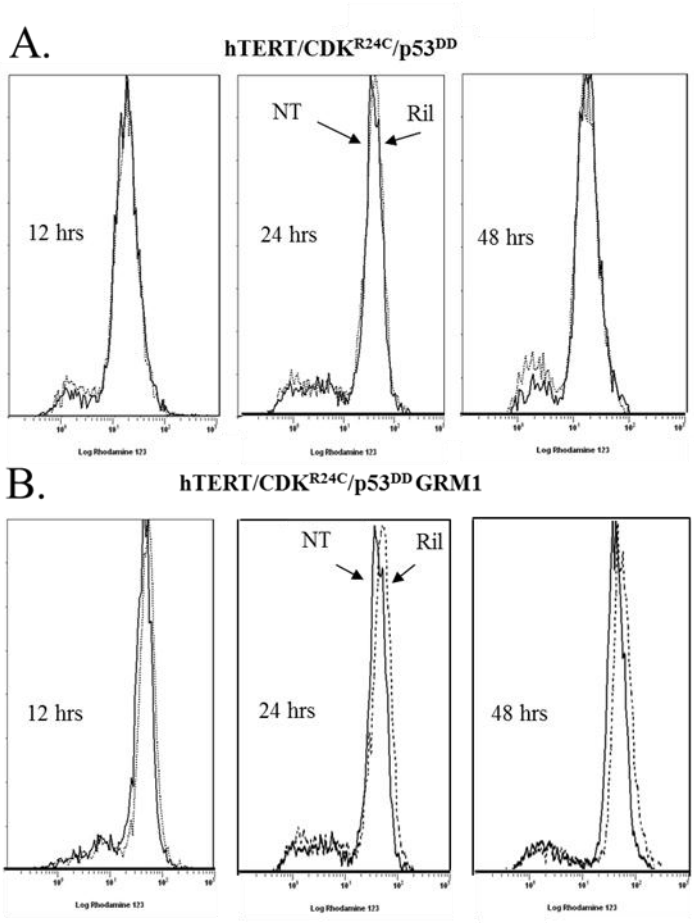

C.

Cell lines	No treatment (NT) 12h	24h	48h	Vehicle (DMSO) 12h	24h	48h	Riluzole 12h	24h	48h
hTERT/CDK^{R24C}/p53^{DD}	1.00 1.00	1.00		1.00	1.03	0.97	0.94	1.08	0.94
hTERT/CDK^{R24C}/p53^{DD} GRM1	1.00 1.00	1.00		1.10	0.95	0.98	1.21	1.34	1.15

Figure 21. GRM1 expression is necessary for riluzole-elicited increases in ROS.

(A.) Immortalized, non-tumorigenic human melanocytes hTERT/CDK^{R24C}/p53^{DD} or (B.) hTERT/CDK^{R24C}/p53^{DD}–GRM1 cells were treated with 10 μM of riluzole for 12, 24, and 48 h. Cells were loaded with DHR123 and fluorescence intensities used as a measure of ROS production. Results are summarized as the fold difference of untreated cells in (C.)

A.

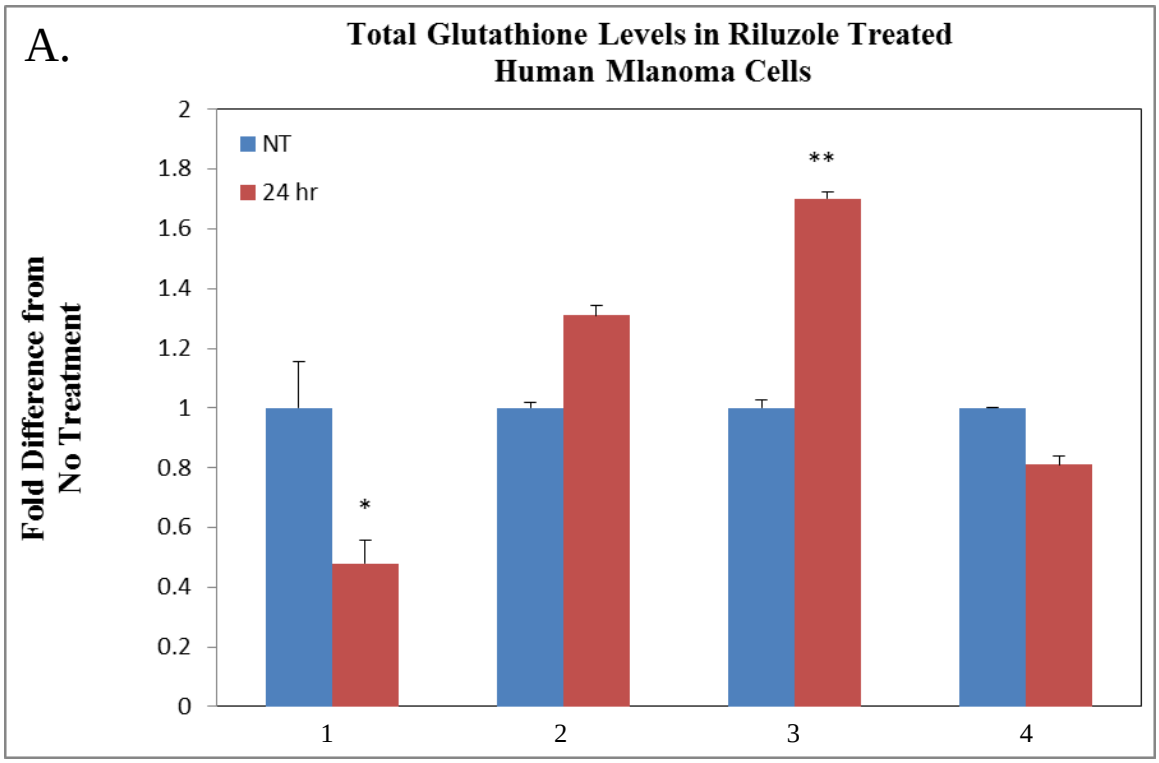
Total Glutathione Levels in Riluzole Treated Human Mlanoma Cells
Fold Difference from No Treatment
NT
24 hr
2
1.8
1.6
1.4
1.2
1
0.8
0.6
0.4
0.2
0
*
**
1
2
3
4

B.

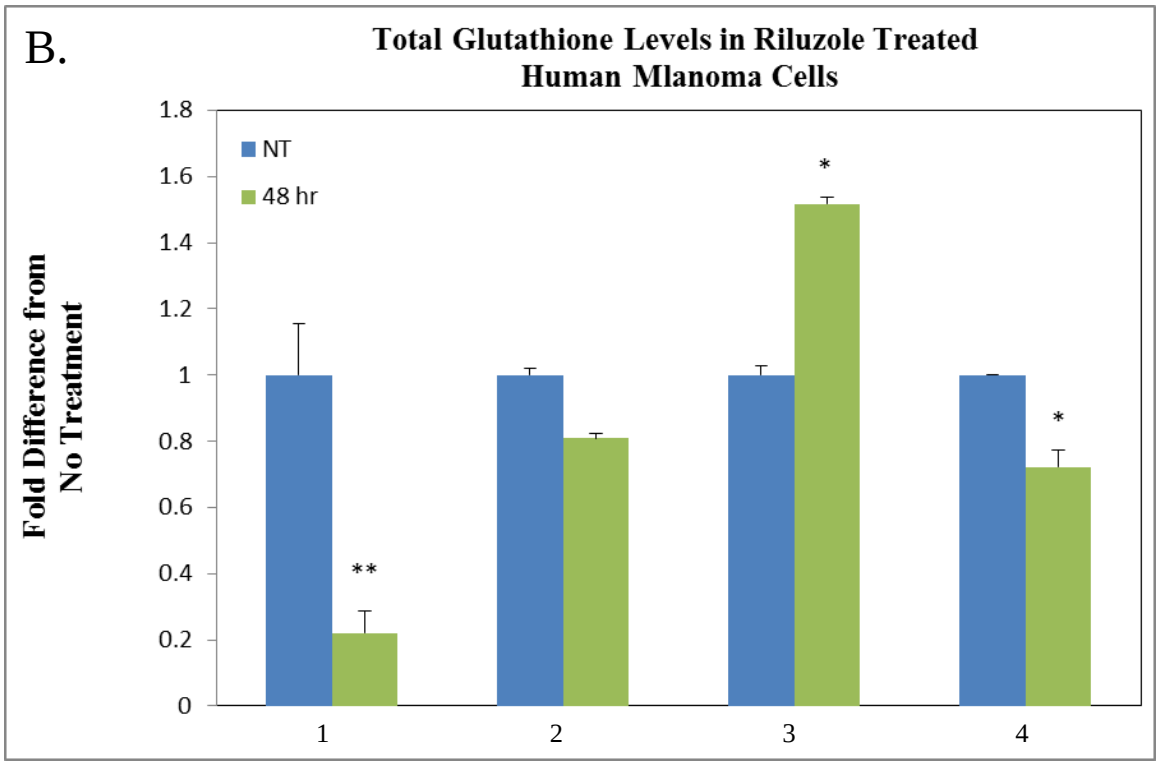
Total Glutathione Levels in Riluzole Treated Human Mlanoma Cells
Fold Difference from No Treatment
NT
48 hr
1.8
1.6
1.4
1.2
1
0.8
0.6
0.4
0.2
0
**
*
*
1
2
3
4

Figure 22. Riluzole treatment of GRM1-positive human melanoma cells induces a reduction in glutathione levels

(A.) Immortalized non-tumorigenic human melanocytes, hTERT/CDK^{R24C}/$p53^{DD}$ and the isogenic cell line hTERT/CDK^{R24C}/$p53^{DD}$-GRM1 as well as human melanoma cell lines UACC930 and C8161 cells were treated with 10 μM riluzole for 24 and 48 h. and total intracellular glutathione levels were assessed and are shown as a percent of untreated cells (NT). SEM, n=10. * $p \leq 0.05$; ** $p \leq 0.005$.

Section III: Riluzole is a Radio-Sensitizing Agent in an *in vivo* Model of Brain Metastasis Derived from GRM1 Expressing Human Melanoma Cells

Aim 3: Rationale

Brain metastases represent a common terminal or pre-terminal event in many patients harboring malignancies including those diagnosed with metastatic melanoma. Current treatment for patients having brain metastases involves combinations of steroids, surgical resection, stereotactic radiosurgery (SRS), and whole brain radiation therapy (WBRT). As opposed to other forms of cancers, melanoma patients with brain metastases that receive these forms of treatment have inferior results, with a one year survival rate of less than 13%. This finding confirms the known relative radioresistance of melanoma cell lines found *in vitro.* Based on results presented in Sections I and II of this thesis, we wished to assess *in vivo* the radiosensitizing activity of riluzole in an orthotopically implanted, intracranial human melanoma xenograft animal model.

Materials and Methods

S. Cell culture and DNA transfections

C8161 human melanoma cell line was provided by Dr. Mary J.C. Hendrix (Children's Memorial Research Center, Chicago, IL). [296]. U87MG glioma cells were purchased from ATCC (Manassas, VA). Melanoma cells were grown in RPMI 1640 plus 10% fetal bovine serum (FBS); U87MG were grown in Dulbecco's modified Eagle Medium (DMEM) supplemented with 5% FBS. DNA transfections were performed with DOTAP according to the manufacturer (Roche, Basel, Switzerland). Coding sequence for the modified firefly luciferase, *luc*+, was subcloned into a mammalian expression vector pCI-neo (Promega, Madison, WI,). Stable *luc*+- transfected clones (C8161-Luc) were selected in growth medium plus 300 μg/ml Geneticin (Invitrogen, Carlsbad, CA).

T. Lucigenin chemiluminescence assay

To be certain that the luciferase in stable C8161-luc clones were functional we assessed luciferase activity in these cells, We transiently transfected in the Renilla luciferase construct using DOTAP (Roche, Basel, Switzerland) according to manufacturer's instructions. At 48 h post-transfection, cell lysates were collected from both control construct-containing cells and stable C8161-luc-containing clones. Firefly and Renilla luciferase activity levels quantified using the Dual-Glo luciferase assay system (Promega, Madison, WI) according to the manufacturer's specifications by a Veritas Microplate Luminometer (Turner Biosystems, Sunnyvale, CA).

U. Xenograft animal model

One million cells were injected subcutaneously into the dorsal flanks of each mouse, when the tumor volumes reach 6-10 mm^3 as measured by vernier caliper the mice were randomized into groups with similar tumor volume distribution and treatment is then initiated. The groups were no treatment (NT), vehicle (Veh, DMSO) and riluzole (10 mg/kg) treatment administrated via oral gavage daily for 37 days. Quantitation of the bioluminescence signal intensities acquired by IVIS small animal imaging system as follows: Luciferin (15 mg/ml) stock solution was used and each animal received intraperitoneal injection of luciferin (6 mg/mouse) at least 20-30 min prior to acquisition of images. The data were expressed as photon flux (photons/s/cm2/steradian, where steradian refers to the photons emitted). The background photon flux was subtracted from the signal intensities measured at the same site. Data were normalized to peak signal intensity of each time course.

V. Orthotopic human melanoma cell injections in immunodeficient nude mice

For the brain metastasis model, luciferase-expressing C8161-luc cells were inoculated intracranially into 6 week old immunodeficient mice using a stereotactic device. C8161-luc cells were harvested, counted, and adjusted to 100,000/5 µl in sterile low melting agarose to a final concentration of 0.33%. Mice were anesthetized using 20 mg/ml avertin (250-300 ul per 10 grams body weight) by way of intraperitoneal injection and maintained throughout the procedure by inhalation of 5% isoflurane mixed with pure oxygen. The mouse head was secured into the stereotactic frame using ear bars on the device. Marcaine (0.5%) with epinephrine was injected subcutaneously at the proposed incision site as a local anesthetic and to prevent bleeding. A 1 cm midline scalp incision was made to expose the skull and a small hole drilled through the skull using a #33G drill

bit at coordinates 0.5 mm anterior and 2 mm lateral to the bregma. A Hamilton syringe with 10 µl capacity was used to deliver the cells to allow a slow, accurate injection rate (0.6 µl/min) as to eliminate pressure at the injection point that could cause reflux of the suspension. The incisions were closed using the skin adhesive, Vetbond (3M Corporation, St. Paul, MN).

W. Visualization of orthotopic mouse model of brain metastasis

The luciferase substrate, D-luciferin potassium salt (Perkin Elmer, Waltham, MA) was prepared at a final concentration of 15 mg/ml in sterile PBS. Luciferin (6 mg/mouse) was delivered via intra peritoneal injection. After 10-20 minutes, animals were visualized using IVIS optical imaging system (Caliper Life Sciences, Waltham, MA) at a medium binning for 1 minute. Upon initial detection of luminescence signal, mice were randomly divided into four groups: group 1 was treated daily by oral gavage with the dimethyl sulfoxide (DMSO, vehicle) only, group 2 was treated with vehicle daily and once weekly for 3 weeks with 4 Gy of irradiation only (IR), group 3 was treated with 10 mg/kg of riluzole by oral gavage daily (Ril), and group 4 was treated with 10 mg/kg of riluzole by oral gavage daily followed by a once weekly exposure of 4 Gy of irradiation for 3 weeks (Ril + IR). The irradiation was performed by the following protocol: mice were placed in an individual container approved by Rutgers LAS for use in the γ-irradiator (Gammator 50, cesium 137 source; Radiation Machine Corp.) with a sleeve of lead coving the body of the animal with exception of the head. The mice were irradiated with 3 weekly fractions of 4 Gy to the groups receiving irradiation. Tumors were measured weekly using the IVIS small animal imaging system for the detection of luminescent signal.

Results

4.1 Isolation of stable luciferase-expressing C8161 cells

Bioluminescence using the reporter enzyme firefly luciferase (Fluc) and the substrate, luciferin, enables noninvasive optical imaging of living animals with extremely high sensitivity. This type of analysis enables studies of gene expression, tumor growth, and cell migration over time in live animals that was previously not possible. We introduced luciferase cDNA into C8161 GRM1-positive human melanoma cells. Several stable clones (C8161-luc) were isolated. Expression was confirmed by luminescence detection in the presence of the substrate (Figure 23). Luminescence detection in C8161-luc cells was significantly high compared to positive control (plasmid with luciferase under SV40 promoter) indicating successful expression of the luciferase containing construct as well as well as selection efficiency.

4.2 Tumor volumes of subcutaneously injected cells measured by IVIS optical imagining system

As a pilot experiment to be certain that the measurement of subcutaneously inoculated tumor cells that were measured using a vernier caliper are similar to the images acquired by IVIS optical imagining system, we injected one million luciferase-expressing cells into the dorsal flanks of athymic nude mice. When the tumors reached a minimal volume between six to ten cubic millimeters, as measured by Vernier caliper, the mice were randomized into groups to attain similar volume distribution per group. The groups were no treatment (NT), vehicle treated (Veh, DMSO), and riluzole (10mg/kg). Riluzole and vehicle treated animals were administered treatment via oral gavage daily for 37 days. In parallel to tumor measurement with a vernier caliper, the bioluminescence

signal of the tumors was measured using the IVIS small animal imaging system. This study allowed us to compare the physical measurements (Vernier caliper) to chemical measurements (bioluminescence) and see if a similar measurement could be established using either method (Figure 24). From the data, we conclude that the tumor measurements attained from both methods are very similar and that there is a definite correlation between the two allowing us to use the IVIS system to monitor tumor progression in an intracranial model of brain metastasis.

4.3 Combination of riluzole and IR reduces human melanoma cell growth in orthotopic model of brain metastasis

The brain is a common site of metastasis for patients with various neoplasias including melanoma, breast cancer, lung cancer, and colorectal cancer. Despite maximally tolerated doses of radiation to the whole brain, patients with multiple brain metastases from solid tumors often show progression in the brain contributing to neurological deterioration, decreased quality of life, and poor survival. We previously showed *in vitro* cultured *GRM1*- positive human melanoma cells were more sensitive to irradiation in the presence of riluzole. To mimic brain metastases observed in melanoma patients, we examined brain metastases in an animal model C8161-luc cells were injected intracranially and monitored for tumor establishment using luminescent imaging. Upon initial detection animals were imaged weekly to determine if riluzole could further sensitize orthotopic tumors to the effects of IR. Our results in the intracranial model show that riluzole and irradiation alone resulted in decreased luminescence compared to

vehicle treated alone (Figure 25). The combination of riluzole and irradiation resulted in smaller tumor cell growth as suggested by luminescent signal detected.

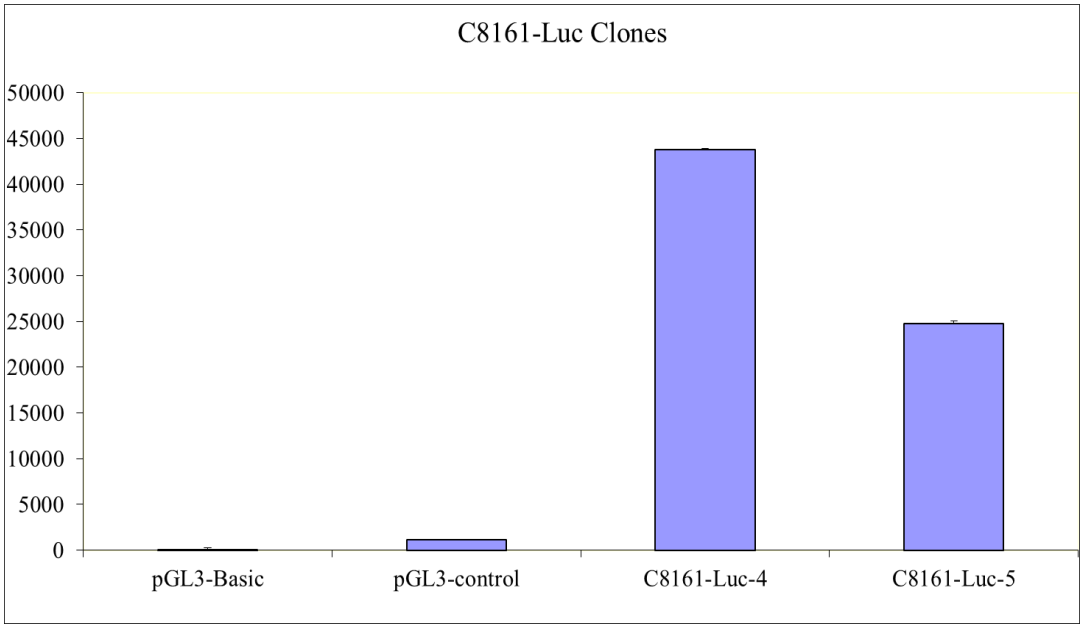

Figure 23. Stable C8161 luciferase containing clones

C8161 containing the construct pCI-Neo-*Luc+* were assessed for luminescence using Veritas Microplate Luminometer. pGL3-Basic vector (Promega) was used as a negative control and pGL3-control vector (Promega) was used at a positive control.

A.

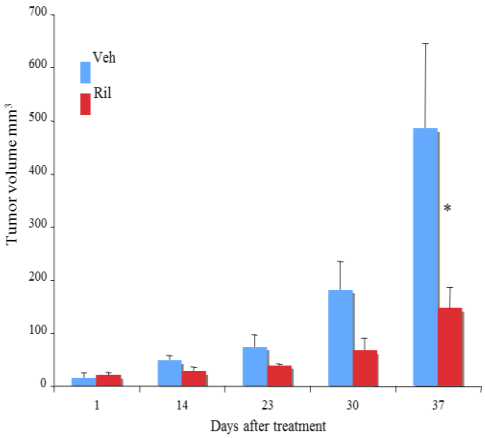

B.

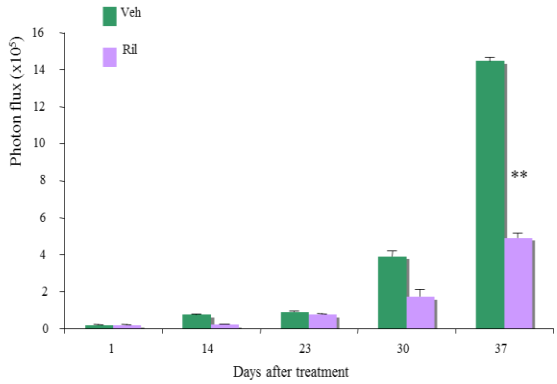

C. Initial Treatment

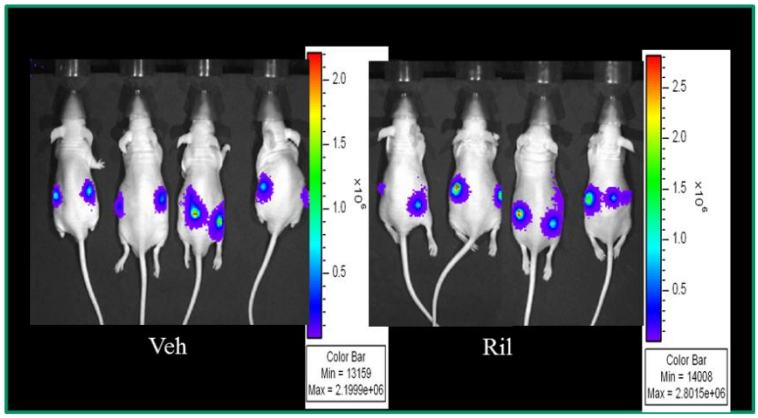

D. Post Treatment

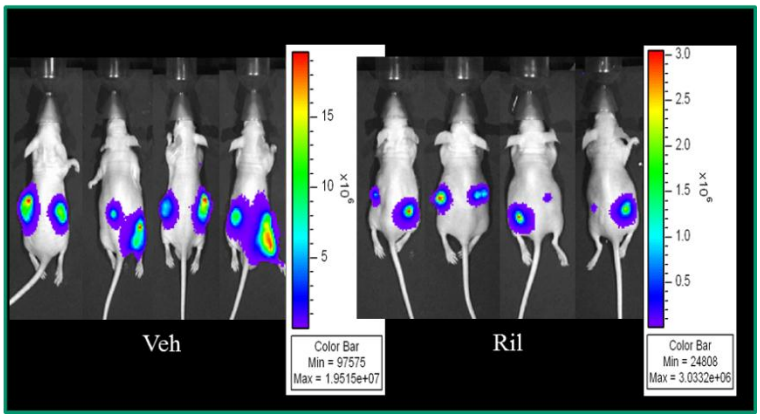

Figure 24. Comparison of actual tumor volume vs. luminescence intensity

(A.) Human cancer cells expressing luciferase were used to establish a correlation between physical and bioluminescent measurement. The data were expressed as photon flux (photons/s/cm2/steradian, where steradian refers to the photons emitted). The background photon flux was subtracted from the signal intensities measured at the same site. Data were normalized to peak signal intensity of each time course and expressed as mean values with standard deviations. **, $p<0.05$, comparison of riluzole treated mice with vehicle treated ones. C. Grayscale photograph of the mice was first acquired followed by the acquisition and overlay of the pseudo-color luminescent image from violet (least intense) to red (most intense), representing the distribution of detected photon counts emerging from active luciferase within the animal. Panel (C.) are images taken on the first day of treatment, vehicle (DMSO) or riluzole (10mg/kg) administered by oral gavage daily. Panel (D.) are images from the last day of treatment.

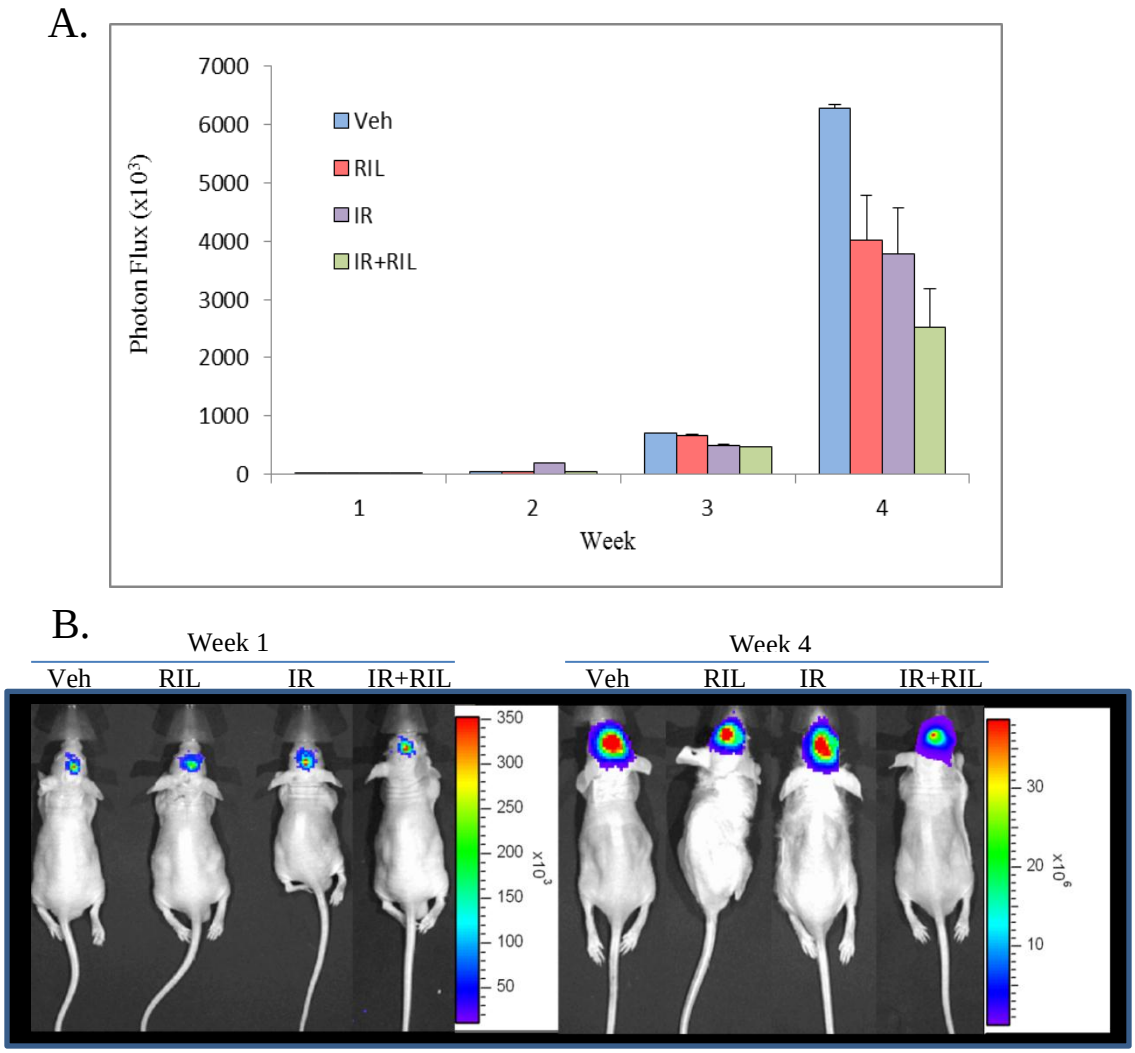

Figure 25. Intracranial orthotopic transplants of human melanoma

(A.) C8161-*luc*+ human melanoma cells were introduced into the brains of nude mice. Once luminescent signal was detected, animals were separated into groups at treated with either DMSO (Veh), riluzole (10 mg/kg), ionizing radiation (4 Gy) or a combination of the two. Animals were terminated after 3 weeks of treatment. (B.) Images of select animals showing initials and terminal images

Section IV. Discussion

G-protein coupled receptors (GPCRs) represent a class of therapeutic targets that have been widely exploited for drug designs and development. Metabotropic glutamate receptors (GRMs) belong to Class C GPCRs and are predominantly involved in maintaining cellular homeostasis in the central nervous system (CNS) [328]. The natural ligand of GRMs, glutamate, interacts with receptor proteins leading to the activation of multiple signaling pathways [1, 273, 283]. More recently, aberrant glutamate signaling has been shown to play a role in the transformation and maintenance of various cancer types, including melanoma. Glutamate secretion from these cells has been found to stimulate regulatory pathways that control tumor growth, proliferation and survival [11, 301]. In addition to synaptic transmissions, accumulating evidence suggesting other functional roles of glutamatergic signaling in human malignancies has presented intriguing possibilities to make GRMs putative, novel targets for human cancer treatments (Table 2). To this end, the aberrant expression of metabotropic glutamate receptor 1 (GRM1) was found as the driving force in inducing melanomagenesis in transgenic mouse models. Since then, other subtypes of GRMs have been implicated in the pathogenesis of various cancer types such as malignant gliomas and medulloblastomas. As such, increased efforts have been generated to elucidate the mechanisms by which GRMs confer oncogenic potentials.

Our laboratory has studied glutamate signaling in melanoma. We have previously described an unknown mechanism of melanoma pathogenesis in which the expression of an otherwise normal receptor protein, metabotropic glutamate receptor 1 (GRM1) in an

unnatural cellular environment (melanocytes) is able to upregulate proliferation and tumor progression both *in vitro* and *in vivo*. We postulate that the oncogenic transformation of cell types by way of GRMs occurs by the establishment of autocrine or paracrine feedback in which the cell releases the ligand which binds and activates the receptor, maintaining its activation, as well as that of downstream effector proteins leading to enhanced proliferation as demonstrated earlier for other GPCRS with oncogenic activity [262, 263] In mouse and human melanoma cell lines, stimulation of GRM1 by glutamate results in activation of phospholipase C (PLC) which in turn cleaves phosphatidylinositol 4,5-bisphosphate (PIP2) to secondary messengers inositol triphosphate (IP3) and diacylglycerol (DAG) [329, 330]. DAG remains bound to the membrane where it activates protein kinase C (PKC) that in turn can activate the MAPK and PI3K/AKT pathways [275, 276, 277, 278, 279]. PKC plays a key role in a multitude of cellular processes including apoptosis, malignant transformation, and metastasis [274]. It is well known that the RAS-RAF-MEK-ERK module of the MAPK signaling cascade controls cell proliferation and inhibits apoptosis. PI3K/AKT pathway activation is important for tumor cell survival, epithelial-mesenchymal transition (EMT), and angiogenesis [280]. Therefore, activation of ectopically expressed GRM1 in melanocytes would activate signaling pathways known to be important in the pathogenesis of melanoma and interruption of this pathway would result in a decrease in cell proliferation and survival. Despite the lack of specific GRM1 antagonists with clinical applications, our group has used Rilutek® (riluzole), an FDA approved drug for the treatment of Amyotropic Lateral Sclerosis (ALS) in clinical trials for the treatment of melanomas [293, 331, 332, 333]. Riluzole is known to inhibit the intracellular release of glutamate to

the surrounding cellular environment, allowing the drug to act as a putative antagonist, not through direct interation with the receptor itself but by decreasing the levels of free ligand available to bind to the receptor resulting in its decreased activation [24, 25].

We have demonstrated that human melanoma cells that express functional GRM1 also have elevated levels of free glutamate in the surrounding environment resulting in autocrine/paracrine activity of the surface receptor [11]. Following exposure to riluzole, GRM1-expressing human melanoma cells accumulate in the G_2/M phase of the cell cycle 24 hours after treatment. Cell cycle checkpoints coordinate cell cycle progression with DNA repair and apoptosis to minimize the probability of replicating damaged DNA [334]. The G_2/M checkpoint prevents cells from entering mitosis when there is DNA damage present [335]. This was followed by a shift of the cell population into the sub G_1 phase of the cell cycle, which is indicitive of apoptic cell death. It is known that cells in the G_2/M phase of the cell cycle are more sensitive to the effects of DNA damaging agents, such as ionizing radiation (IR). This led us to perform studies combining riluzole with IR in an attempt to take advantage of rilzuole-mediated G_2/M arrest in order to enhance the lethal effects of IR in cancer cells . We found that *in vitro,* human melanoma cells that express GRM1, when treated with riluzole are more susceptible to the sublethal doses of ionizing irradiation. Using a xenograft model, we showed that riluzole is able to enhance the lethal effects of ionizing radiation in human melanoma cells that express GRM1, resulting in significant tumor growth inhibition *in vivo* [4]. Tumors from these xenografts were excised and IHC was performed using a marker of DNA DSB, γ-H2AX. As expected, the excised tumors from animals treated with ionizing radiation alone or in

combination with riluzole showed positive for the stain. However, to our surprise, xenograft samples from riluzole treated animals alone showed positive or increased positivity in staining for γH2AX that was comparable to levels found in tumors treated with IR [4]. We hypothesized from these studies that perhaps it was possible that riluzole on its own is able to cause DNA damage in an GRM1-dependent manner causing the cells to arrest in the G_2/M phase of the cell cycle to allow the repair of damaged DNA [336, 337].

Agents that are able to cause DNA damage and mutation have been the mainstay of cancer therapy for decades. Drugs that induce covalent crosslinks between DNA bases (i.e. cysplatin, carboplatin, oxaliplatin and mitomycin C), compounds that attach alkyl groups to bases (such as methyl methanesulponate and temozolomide) and agents that cause single strand breaks (SSBs) or double strand breaks (DSBs) by trapping topoisomerase I or II enzymes on DNA (such as camptothecin and etoposide) have provided the core of cancer treatment for the past half-century [181]. To determine whether riluzole on its own was able to induce genomic insult, we probed human melanoma cells treated with riluzole for intracellular colocalization by way of immunofluorescence for two markers of DNA damage, p53 binding protein 1 (53BP1) and phosphorylated histone variant 2AX (γH2AX). 53BP1 is a nuclear protein belonging to a family of evolutionary conserved DNA damage checkpoint proteins containing BRCA1 (breast cancer susceptibility protein) C-terminal (BRCT) domains and has been shown to localize rapidly to sites of DNA double strand breaks (DSBs) which functions upstream of ataxia-telangiectasia mutated (ATM) in response to DNA damage [305].

53BP localization forms discrete foci along stretches of DNA or chromatin on either side of the DNA DSB. H2AX is one of three types of conserved histone H2A protein species. Following exposure of cells to agents that cause DNA DSB, such as IR, H2AX is rapidly γ-phosphorylated and localized to sites of DNA DSBs forming foci at large regions of chromatin around the break [338]. Upon treatment with riluzole, we found that human melanoma cells that expressed a functional form of GRM1, C8161, showed discrete foci formation of both 53BP1 and γ-H2AX starting at 3 hours with increasing amounts of punctated foci formation up to 24 h although levels of 53BP1 were uniformly lower than that of γH2AX. These results might be reasonable since 53BP1 needs to be recruited to the foci after DNA damage and, in contrast, since H2AX already exists at the site of DNA DSBs [339]. The majority of cells assessed past 24 hours were found to lose adherence, possibly due to death response. We further investigated another human melanoma cell line, UACC930, for appearance of punctated foci co-localized at sites of DNA DSBs. UACC930 cells express a truncated, non-functional version of GRM1, therefore allowing it to act as a negative control for the receptor. As expected, we found that there existed no rise in number of 53BP1 or γ-H2AX foci when compared to untreated UACC930 cells. These results confirm our previous immunohistological data showing that riluzole treatment alone, in a xenograft model of human melanoma, is able to elicit DNA damage repair (DDR) in response to DNA DSBs. These foci were only observed to form in C8161 cells and not UACC930 cells suggesting a requirement of GRM1 expression in riluzole-mediated DNA damage.

During the earliest stages of checkpoint activation, members of the Rad group of checkpoint proteins, which are thought to act as DNA damage sensors, relay information to members of phosphoinositide 3-kinase related kinases (PIKKs) [340]. In mammalian cells, DNA-damage-induced checkpoints that occur at the G_2/M boundary are transduced by two PIKK family members, ATM (ataxia-telangiectstasia mutated) and ATR (ATM and Rad3-related) which phosphorylate numerous target proteins involved in cell cycle arrest, DNA repair, and apoptosis in response to DNA damage [184, 341]. ATM and ATR are thought to share responsibilities as the apical protein kinases in all cell-cycle checkpoints. Upon exposure of double-strand break-inducing agents, kinase domain of ATM becomes catalytically active within 1 hour after cellular exposure to IR or radiomimetic agents [342]. Alternatively, ATR responds to DNA damage by undergoing intranuclear localization, redistributing into DNA damage-induced nuclear foci [340]. This suggests that ATR is does not undergo activation by genotoxic agents or its activation is restricted to ATR molecules that translocate into the nucleus. In this study, GRM1 positive human melanoma cells exposed to relatively low concentrations of riluzole were shown to have increased levels of activated ATM compared to cell lines that did not express functional GRM1, with the maximum levels being detected 48 hours after treatment which correlates with our cell cycle data showing possible G_2/M accumulation at a similar time.

ATM phosphorylates p53 directly on Ser 15 or indirectly through phosphorylation of the regulation checkpoint kinase, Chk2, which then phosphorylates p53 on Ser20 as

well as Ser 216 of Cdc25C [343]. Phosphorylation of p53 on Ser20 contributes to its stabilization by interfering with its binding to MDM2 and activation, which plays a pivotal role in the G_1 checkpoint, participates in the G_2 checkpoint and promotes apoptotic cell death [344]. Phosphorylation of mitosis-promoting Cdc25C creates a binding site for 14-3-3 proteins. In the 14-3-3 bound form, Cdc25C is either catalytically inhibited and/or sequestered in the cytoplasm, prohibiting its activation and inhibiting mitosis [345]. This could explain our results showing that riluzole treatment of GRM1-expressing human melanoma cells ultimately resulted in sub G_1 cell cycle arrest and that these cells had increased levels of the activated form of caspase-3, indicative of apoptosis. Further assessment in levels of activated Chk1 and 2 as well as phosphorylated Cdc25C would determine the role of ATR in the ATM-mediated DNA response observed. Furthermore, ATM dependent checkpoint activation suggests the prominence of homologous recombination (HR) as the major mode of DNA DSB repair. In late G2 phase of the cell cycle, HR is the major mode of DNA dsb repair whereas DNA-PK-dependent nonhomologous end joining (NHEJ) serves as the major mode of DNA dsb repair during G_1 [346]. Studies performed by Takeda and colleagues showed using reverse genetics that ATM and late stage S-G_2 recombinational repair mechanism resided in the same maintenance pathway suggesting that ATM activation has a direct tie to homologous recombination [347].

Isogenic disease models are used to genetically match ‘normal cells’ with the various genetic variations that can be found in a specific population in order to model human disease. To further assess the role of GRM1 in riluzole-mediated DNA DSB

response, exogenous cDNA to GRM1 was introduced into an immortalized human melanocytic cell line, hTERT/CDK^{R24C}/p53^{DD}. Stable isogenic cell lines that expressed GRM1 (hTERT/CDK^{R24C}/p53^{DD}-GRM1) were selected and assessed for receptor functionality via modulation of downstream effector molecules [348]. Upon exposure to riluzole, we observed an increase in the levels of co-localization of 53BP1 and γ-H2AX similar to those seen in C8161 cells which express an endogenous form of the receptor. This was in contrast to the parental cell line were there was no increase in the amounts of either protein, even up to 24 hours post treatment. Since we were able to induce DSB using riluzole after introducing an exogenous form of GRM1 into a melanocytic cell line, it would make logical sense that if the receptor were necessary for riluzole-induced DNA DSB, loss of function of the endogenous form of the receptor in a melanoma cell line that has been shown to require its activation for proliferation and survival should result in a decrease in the amount of DSB produced after exposure to riluzole. To answer this question we decided to conditionally knock down GRM1 in C8161 human melanoma cells using an inducible shRNA to GRM1. We have previously reported on the requirement of GRM1 in these cells for growth and proliferation [11]. We performed parallel *in vitro* studies treating C8161-shGRM1 with riluzole either in the presence or the absence of the inducer of the shRNA, ponasterone A. We found that C8161-shGRM1 cells in which GRM1 was knocked down exhibited a decreased amount of foci co-localization of both 53BP1 and γH2AX when compared to cells that were left untreated. C8161 shGRM1 cells, in which the shGRM1 was left uninduced, when treated to riluzole, had elevated levels of DSBs that were observed for the parental riluzole treated C8161 cells. Collectively, these data revealed the presence of an immediate response of

cells that express GRM1 to the introduction of DNA DSBs when exposed to riluzole. However, since we know that riluzole treatment has been shown to ultimately result in human melanoma cell death we had to demonstrate that it was indeed the DNA DSBs that were leading to cells death.

We had reported previously that human melanoma cells expressing GRM1 were found to accumulate in the G_2/M phase of the cell cycle followed by a shift after 24 hours of the cell population into the sub G_1 phase of the cell cycle, which is indicative of apoptotic cell death [4, 11]. Reproductive cell death may be caused by three-nonexclusive processes: irreversible blockage of cell division, necrosis, and apoptosis. Many DNA damaging agents are known to induce apoptosis, though whether DSBs are the result of apoptotic cell response or the apoptotic cell response leads to DSBs depends on the mode of action of the agent. To address whether the co-localization of γ-H2AX and 53BP1 we are observing are either the cause or consequence in riluzole-mediated cell death in our system, we established several stable isogenic cell lines that expressed the murine form of metabotropic glutamate receptor 1 (Grm1) using an immortalized baby mouse kidney (iBMK) epithelial cell line that was previously made apoptosis-deficient (D3) via the deletion of pro-apoptotic proteins, BAX and BAK (D3-Grm1) [282]. The cell lines were assessed for expression of Grm1 on the protein level by detection of the receptor via Western immunoblot. Further downstream modulation of ERK was used to demonstrate functionality of the receptor. Using this model, we are able to demonstrate that, upon expression of Grm1 in these cells, there was a definite introduction of DNA DSB response as seen by the colocalization of 53BP1 and γ-H2AX foci in the nuclei of

the isogenic D3-Grm1 cell line after exposure to riluzole. This is in contrast to the vector containing line (D3-Vec) in which there was no observed difference between the cells that were treated or left untreated with riluzole. These studies demonstrated that the DNA DSBs that were being elicited by riluzole were not only dependent on expression of GRM1 but also that riluzole-induced DNA DSBs were independent of apoptotic cell response. This suggests that the previous sub G_1 cell cycle arrest that was observed in GRM1 expressing human melanoma was the result of genomic insult induced by riluzole exposure. These results led us to believe that the inhibition of glutamate from within these cells was causing irreparable damage to the genome. However, how this damage was being elicited remained unclear.

It is known that ionizing radiation (IR) generates reactive oxygen species (ROS) such as superoxide anions, hydrogen peroxide, and hydroxyl radicals and oxides of nitrogen of metabolic origin or that occur as a consequence of reactions secondary to metabolism [349]. Extraordinary high levels of ROS as a result of exposures to IR or chemicals that either directly produce or stimulate the metabolic production of ROS would reasonably be expected to alter the overall redox status of cells [350]. Our previous results in this thesis led us to hypothesize that perhaps inhibition of glutamate release via riluzole is leading to an increase in the amount of intracellular ROS. We found that GRM1-expressing human melanoma cells treated with riluzole did indeed show an increase in the generation of ROS when compared to untreated cells. This was further confirmed in our isogenic hTERT/CDK^{R24C}/$p53^{DD}$-GRM1 cell line which showed that introduction of GRM1 resulted in an increase in levels of ROS indicating that

riluzole-induced DSB are perhaps caused, directly or indirectly, by an increase in the amounts of intracellular ROS. It is known that cells possess a wide range of interlinked antioxidant defense mechanisms that protect from ROS. However, the capacity of these systems is not unlimited and it is possible that excessive ROS production would breach these levels resulting in a decrease in the amount of available antioxidants.

The tripeptide glutathione (GSH) is the major endogenous antioxidant produced in cells [351]. It can directly neutralize free radicals and reactive oxygen compounds by hydrogen donation, act as a cofactor for the enzyme GSH-peroxidase that scavenges hydrogen peroxide, and maintain exogenous antioxidants such as vitamin E in their reduced form. It is known that cysteine derivatives act as cysteine delivery systems that increase GSH synthesis, resulting in increased intracellular GSH concentration. The cysteine derivative *N*- acetyl-L-cysteine (NAC) is hydrolyzed within the cell to cysteine and it is the availability of this amino acid that is usually the rate limiting step in GSH synthesis [352]. The administration of NAC has been shown to lead to increase intracellular GSH synthesis resulting in decreased oxidative stress *in vitro* [353]. We proposed that the inhibitory effect of riluzole on the release of intracellular glutamate in GRM1 expressing human melanoma was causing an increase in the levels of ROS possibly by depleting intracellular concentrations of GSH. If this is the case, it should be possible to rescue the cells by providing them with an alternative source of cysteine. To do this, human melanoma cell lines used in our previous experiments that express GRM1 were pretreated with NAC prior to riluzole treatment. When the cells were collected and assessed, we found that the cells that had been pretreated with NAC showed a substantial

decrease in the levels of ROS detected. To confirm this observation, we repeated the assay, this time using an ester of GSH, GSH reduced ethyl ester (GSH-Et) was used to rescue the cells from increased ROS. GSH-Et are transported into the cell where it is converted into GSH [326]. Our results show that human melanoma cells that express endogenous GRM1 have an almost 100% rescue from the ROS induced by riluzole treatment compared with untreated cells. These results led us to further examine our hypothesis that riluzole elicits its DNA DSBs on GRM1 expressing human melanoma cells by causing an increase in ROS resulting in an decrease specifically in the amount of intracellular GSH. This was confirmed by measuring the levels of total GSH in riluzole treated GRM1 expressing human melanoma cells. We found that compared to either cells that did not harbor the receptor (hTERT/CDK^{R24C}/p53^{DD}) or human melanoma cells that expressed a nonfunctional version of the receptor (UACC930), human melanoma cells that express GRM1, when treated with riluzole, showed a time dependent decrease in the amounts of intracellular GSH. These data collectively suggest that, in GRM1-expressing human melanoma cells, the increase of ROS is the result of a decrease in intracellular GSH. This could be the result of the cells inability to release glutamate.

The sodium-independent cystine/glutamate antiporter/exchanger, system x_c^- (xCT), is a rate-limiting step for GSH synthesis in various cell types [354]. xCT functions as the exchange system for cystine/glutamate, with cystine entry into the cells in exchange for the release of glutamate at a ratio of 1:1. Once inside the cell, the cystine is rapidly reduced to two molecules of cysteine, the rate-limiting substrate for the biosynthesis of GSH. It is possible that by inhibiting the release of glutamate from within

the cells disrupts intracellular concentrations of cysteine [355]. This would result in a decrease in the amount of GSH causing an imbalance in redox homeostasis. Although xCT is expressed in various malignant tumors, its role and implication in our system is currently being investigated by our laboratory. We detected various levels of xCT in several human melanoma cell lines and in normal human melanocytes with no apparent correlations with xCT levels, genotypes at BRAF/N-RAS, or stage of the disease being noted (data not shown). To further assess the role of xCT in our system, we have attained xCT-null mouse melanocytes (SUT2 cells) derived from a mouse model of Hermansky-Pudlak syndrome, a rare autosomal recessive disorder which results in oculocutaneous albinism, platelet abnormality, and lysosomal accumulation of ceroid lipfuscin [356]. In culture, SUT2 cells have been shown to have reduced intracellular levels of GSH and are maintained by supplementation of β-mercaptoethanol (BME) in the growth medium to supply cysteine. By introducing either exogenous GRM1 alone or with functional xCT, we can further assess the involvement of xCT in glutamatergic signaling by examining if xCT is required for the maintenance of cellular homeostasis, is a potential target for riluzole in riluzole-mediated inhibition of glutamate release, or if there are other glutamate exchange transporters at play in our system.

Our group has performed a phase 0 to explore mechanistic and pharmcodynamic effects of riluzole in human melanomas in which 12 patients with stage III/IV resectable melanoma received riluzole for 14 days. 4 of the 12 patients (34%) showed significant post-treatment decreases in tumor levels of pAKT and/or pERK. In order to determine if there were detectable differences in the levels of markers of DNA DSB, protein lysates

prepared from biopsies resected from responding and non-responding patients were assessed for 53BPI using Western immunoblots (data not shown). Interestingly, we see that there is an increase in the amount of protein in post treatment biopsy samples compared to that found in the initial biopsy in patients that were deemed responders of the therapy. In non-responding patients there was no increase in the amount of 53BP1 detected. These results suggest that inhibiting glutamate signaling causes an increase in the expression of 53BP1 in a subset of human melanomas. This is surprising, however, since the assembly of 53BP1 foci is not dependent on its increased expression. 53BP1 becomes hyperphosphorylated and translocates to the nucleus, forming nuclear foci at the sites of DNA damage. Therefore, it is not the level of expression of 53BP1 that determines the amount of DNA DSBs but it's concentration at actual sites of the breaks and the number of foci formed that represents genomic insult. Further preliminary immunohistological assessment of pre and post biopsies from two responders of a recently completed phase II trial demonstrate that riluzole treatment does indeed result in a marked increase in the amount of DNA DSBs determined by the marked increase in levels of γH2AX found in post-treatment biopsy samples. These *in vivo* results are very intriguing imply a specificity of riluzole to tumor tissue.

Our group has completed a proof of principle Phase 0 trial with riluzole that provided convincing evidence that glutamatergic signaling is operative in human melanomas [293]. In addition, about 35% of patients in a Phase II trial had stable disease for several months [311]. It is unlikely that riluzole as a single agent will offer long lasting efficacy in genetically diverse human cancers including melanoma. Combinatorial

therapies have been initiated for the past few years with the hope that targeting more than one signaling pathway may provide sustained disease-free conditions [2, 4]. Our analyses of preliminary assessment using pre- and post-treatment samples from responding patients in single agent riluzole Phase II trial showed marked increases in the number of positive γ-H2AX stains only in the responding post-treatment samples. These preliminary results are very intriguing and imply that, as shown in the experimental settings, riluzole appears to also induce DSBs in melanoma lesions that have been found to express GRM1. DNA-damaging chemotherapies have been the mainstay of cancer treatment for the past century. Many cancer drugs employed in the clinic are highly efficient in producing excessive DNA damage that causes cell death directly or following DNA replication [357]. However, the uniqueness of our finding with riluzole is several-fold. Riluzole's ability to induce DSBs depends on a functional receptor that has acquired an oncogenic potential. One of the consequences of cell transformation/tumor formation by this receptor is the establishment of autocrine loops that ensures the receptor is constitutively activated in an aberrant cellular environment where the "normal" cells do not express the receptor. Riluzole disrupts the autocrine loops by inhibiting the release of the ligand, glutamate. Accumulation of glutamate disturbs the intracellular homeostasis of glutamate/cystine, limits GSH synthesis leading to enhanced levels of ROS and DSBs which when irreparable drive the damaged cells into apoptosis. Taken together, riluzole's tumor suppressive activity can be explained not only by its ability to lower extracellular glutamate but also by increasing the level of oxidative stress in melanoma cells that express GRM1. Our findings suggest that combining riluzole with other available

regiments could deliver additional therapeutic responses offering further treatment for a targeted subset of human melanomas.

Although surgery can be curative in stage I, II, or III disease, a large number of patients will develop distant metastases. Active systemic disease is associated with a poor prognosis and a mortality rate of almost 100% [300]. Although brain metastases represents a relatively minor problem in the management of malignant melanoma, it is an indicator for palliative radiation therapy [22]. In contrast to most other cancer cell types, significant evidence exists that at least some melanoma cell lines have increased aptitude for the repair of sub-lethal DNA damage caused by ionizing radiation [22, 358]. As an attempt to address the perceived radio-resistance of melanoma, many groups have adopted radiotherapy schedules that deliver larger daily fractions of radiation (hypo-fractionation) to exploit the sensitivity of cells to larger fraction sizes [16, 17]. However, these large daily fractions cannot be delivered to the whole brain for patients with brain metastases due to the risk of late neurotoxicity [358]. With an incidence of approximately 170,000 to 200,000 cases per year, brain metastases are an exceedingly common event in the progression of many human malignancies with lung, breast and skin (melanoma) being the most common. Melanoma is the fourth most common cause of brain metastases and is the second highest in incidence proportion percentage [359]. The median survival of melanoma patients with brain metastases treated with whole brain radiation therapy (WBRT) ranges between 3-5 months.

Our preliminary results suggest that riluzole enhances the lethal effects of ionizing irradiation in melanoma cells that ectopically express GRM1 and that a potential cause is the arrest of cycling melanoma cells into G_2/M phase, a radiosensitive phase of the cell cycle [360]. Based on these findings and the fact that riluzole is able to cross the blood brain barrier, it is particularly relevant that riluzole could be used as a potential therapy with adjuvant radiation to treat melanoma metastases in the brain. In an attempt to mimic melanoma metastasis to the brain, we performed orthotopic human xenograft studies in mice using human melanoma cells that express GRM1. We were able to show that animals that received treated with concurrent riluzole and IR showed a decrease in intracranial tumor growth compared to either modality alone.

Conclusion

Melanoma is a genetically diverse disease owing to the dysfunction of multiple regulatory pathways. As such, it is important to test the therapeutic potential of agents that reflect the genetic diversity of this disease. In addition to ectopic expression of GRM1, mutations in BRAF have been identified in more than 60% of melanomas, most of these due to the substitution of a single amino acid at residue 600 in the B-RAF kinase domain resulting in constitutive activation of the RAF/MAPK/ERK kinase signaling pathway [140]. Melanoma cells with aberrant glutamate receptor signaling also exhibit hyperactive PI3K/AKT and MEK/MAPK pathways [11, 361, 362]. Additionally, a recent examination of a publicly available gene expression data bank identified a variety of GPCRs that are over-expressed in diverse types of cancer tissues [363]. These findings illustrate the role that glutamate receptors and transporters play in the cellular signaling

somatic cell types. The molecular physiology of GPCRs allows them to be regulated by many agonists and antagonists and are the target, directly and indirectly, of approximately 50% of pharmaceutical agents used to treat various human diseases. GPCRs have been shown to have a role in both normal and aberrant mitogenic signaling in functions that regulate cell migration in tumor metastasis and angiogenesis as well as key molecular events implicated in cancer progression and invasion. Based on these findings, it is perhaps not surprising that interruption of the glutamatergic signaling pathway by targeting GPCRs in cancers could result in more effective the treatment of this devastating disease.

Future Directions

For all the proposed future studies we will use a panel of human melanoma cell lines that are positive or negative in GRM1 expression. Mutations in N-RAS/B-RAF comprise the most frequently altered genotypes in melanoma. Although our preliminary results suggest riluzole-induced DNA damage was independent of N-RAS/B-RAF genotypes, however, we need to test multiple lines to avoid a "single cell line observation". Individual cell lines have limited predictive value, however with numerous cell lines, we will more effectively capture the molecular heterogeneity of the tumor as well as their sensitivities to various putative therapeutic reagents.

In order to be absolutely certain that riluzole induces DNA DSB leading to an increase in ROS formation in GRM1 expressing human melanoma cells, additional experiments detecting DNA damage should be performed. We will use the two most widely studied measures of oxidative DNA damage: the 8-oxo-7,8-dihydro-

2’deoxyguanosine (8-oxo-dG) and the COMET assay. The amount of oxidized DNA bases will be measured in control and riluzole treated cells by complementary methods: a) ELISA using specific antibodies to 8-oxo-dG (Cell Biolabs, Inc.) b) HPLC-EC method for directly assaying 8-oxo-dG in isolated DNA through our Analytical Chemistry Facility Core. GRM1-negative cells will be used as negative controls [364, 365]. The COMET assay is also known as single-cell gel electrophoresis, measures DNA strand breaks and alkali-labile sites within individual cells. We will perform the classical COMET assay as described, under both neutral and alkaline conditions to distinguish between single-stranded and double-stranded DNA breaks [366, 367, 368]. By this approach, the nature of the DNA lesions induced by riluzole will be determined.

In addition to COMET assays we will investigate two DNA repair activities. Non-homologous end joining (NHEJ) is considered the major DNA repair mechanism in mammalian cells; however, we will also examine if homologous recombination repair (HRR) is involved. This will be achieved by the DR-GFP reporter assay as described [369]. Briefly, this assay measures homology-directed repair of an I-SceI endonuclease-induced DNA double strand break via GFP reporter gene. For NHEJ assay we will start by evaluating levels of pivotal NHEJ proteins (Ku70, Ku80 and the DNA-PKcs catalytic subunit) by Western immunoblots92, 93. To examine the capacity of riluzole treated cells to engage in NHEJ repair, we will use qualitative and quantitative functional NHEJ assays as described94. To further assess the participation of NHEJ in repair riluzole-induced DNA damage we will take advantage of RNA interference to one of the essential components in NHEJ and examine the consequences of such manipulation. A

complementary approach will be to introduce one of the NHEJ proteins exogenously and perform cell cycle profile, and to monitor alterations in DNA damage.

The sodium independent cystine/glutamate antiporter/exchange transporter (System Xc-, xCT) is a rate-limiting step for GSH synthesis in various cell types [370]. A mouse model of Hermansky-Pudlak syndrome (a genetic disease characterized by abnormalities in biosynthesis and/or trafficking of lysosomal-related organelles) carries a large deletion in the gene encoding for xCT resulting in an unstable truncated protein [371, 372]. Cultured xCT null fibroblasts or melanocytes have reduced intracellular GSH and cannot survive under normal culture conditions unless β-mercaptoethanol (BME) is included in the growth medium to supply cysteine, the reduced form of cystine for GSH synthesis [372]. In preliminary studies we detected various levels of xCT in several human melanoma cell lines and much-reduced levels of expression in normal human melanocytes by way of Western mmunoblots with no apparent correlations between xCT levels, genotypes at BRAF/N-RAS or stage of the disease was noted. We have obtained xCT-null mouse melanocytes from Dr. Bennett and we will use genetic means to manipulate these xCT-null cells to elucidate its role(s) in glutamatergic pathway. We will introduce exogenous GRM1 alone or with functional xCT into these xCT-null melanocytes and we will use these isogenic cells to a) assess if xCT is required for the export of glutamate to maintain cellular homeostasis and to establish autocrine loops, b) examine if xCT is a target of riluzole in riluzole-mediated inhibition of glutamate release, c) evaluate if elevated levels of exogenously introduced xCT could overcome the suppression of glutamate release in the presence of riluzole, d) examine if there are other glutamate exchange transporters that may compensate for the lack of xCT in GRM1-

xCT-null cells. In parallel, we intend to modulate xCT levels in several human melanoma cell lines using inducible siRNA approaches. The availability of siGRM1-human melanoma clones will provide means to evaluate the consequences in xCT function by such manipulations. These in vitro assays will be validated in vivo.

Excitatory amino acid transporters 1-4 (EAAT1-4) are typically found on neuronal cells to help reduce the excitotoxicity effect of excess glutamate released by cells in the central nervous system [373, 374]. Reduced transcript levels of EAAT2/4 were recently detected in a panel of melanoma cell lines 116. To elucidate possible involvement of one or more of EAATs we will first measure levels of EAAT1-4 and examine if there are any correlations between EAAT and GRM1 expression. Depending on the results from these studies, we will then modulate EAAT/GRM1 levels by introducing exogenous EAAT/GRM1 or inducible siRNA and evaluate possible consequences by such manipulations and examine if one or more of these transporters may be involved glutamate uptake from extracellular environment in melanocytes or they may function as xCT in glutamate export in these cells.

References

1. Wangari-Talbot J, Wall BA, Goydos JS, Chen S. Functional Effects of GRM1 Suppression in Human Melanoma Cells. *Mol Cancer Res* 2012 Jul 13.
2. Lee HJ, Wall BA, Wangari-Talbot J, Shin SS, Rosenberg S, Chan JL, et al. Glutamatergic pathway targeting in melanoma: single-agent and combinatorial therapies. *Clin Cancer Res* 2011 Nov 15;17(22):7080-92.
3. Teh JL, Chen S. Glutamatergic signaling in cellular transformation. *Pigment cell & melanoma research* 2012 May;25(3):331-42.
4. Khan AJ, Wall B, Ahlawat S, Green C, Schiff D, Mehnert JM, et al. Riluzole enhances ionizing radiation-induced cytotoxicity in human melanoma cells that ectopically express metabotropic glutamate receptor 1 in vitro and in vivo. *Clin Cancer Res* 2011 Apr 1;17(7):1807-14.
5. Gottesman MM, Fojo T, Bates SE. Multidrug resistance in cancer: role of ATP-dependent transporters. *Nat Rev Cancer* 2002 Jan;2(1):48-58.
6. Hanahan D, Weinberg RA. The hallmarks of cancer. *Cell* 2000;100(1):57-70.
7. Compagni A, Christofori G. Recent advances in research on multistage tumorigenesis. *Br J Cancer* 2000 Jul;83(1):1-5.
8. Chen S, Zhu H, Wetzel WJ, Philbert MA. Spontaneous melanocytosis in transgenic mice. *J Invest Dermatol* 1996 May;106(5):1145-51.
9. Zhu H, Reuhl K, Zhang X, Botha R, Ryan K, Wei J, et al. Development of heritable melanoma in transgenic mice. *J Invest Dermatol* 1998 Mar;110(3):247-52.
10. Pollock PM, Cohen-Solal K, Sood R, Namkoong J, Martino JJ, Koganti A, et al. Melanoma mouse model implicates metabotropic glutamate signaling in melanocytic neoplasia. *Nat Genet* 2003 May;34(1):108-12.
11. Namkoong J, Shin SS, Lee HJ, Marin YE, Wall BA, Goydos JS, et al. Metabotropic glutamate receptor 1 and glutamate signaling in human melanoma. *Cancer Res* 2007 Mar 1;67(5):2298-305.
12. Skerry TM, Genever PG. Glutamate signalling in non-neuronal tissues. *Trends Pharmacol Sci* 2001 Apr;22(4):174-81.
13. Kleinschmidt A, Bear MF, Singer W. Blockade of "NMDA" receptors disrupts experience-dependent plasticity of kitten striate cortex. *Science* 1987 Oct 16;238(4825):355-8.
14. Behar TN, Scott CA, Greene CL, Wen X, Smith SV, Maric D, et al. Glutamate acting at NMDA receptors stimulates embryonic cortical neuronal migration. *J Neurosci* 1999 Jun 1;19(11):4449-61.
15. Young D, Waitches G, Birchmeier C, Fasano O, Wigler M. Isolation and characterization of a new cellular oncogene encoding a protein with multiple potential transmembrane domains. *Cell* 1986 Jun 6;45(5):711-9.
16. Ballo MT, Ang KK. Radiation therapy for malignant melanoma. *Surg Clin North Am* 2003 Apr;83(2):323-42.
17. Ballo MT, Ang KK. Radiotherapy for cutaneous malignant melanoma: rationale and indications. *Oncology* 2004 Jan;18(1):99-107; discussion -10, 13-4.
18. Ballo MT, Bonnen MD, Garden AS, Myers JN, Gershenwald JE, Zagars GK, et al. Adjuvant irradiation for cervical lymph node metastases from melanoma. *Cancer* 2003 Apr 1;97(7):1789-96.
19. Ballo MT, Garden AS, Myers JN, Lee JE, Diaz EM, Jr., Sturgis EM, et al. Melanoma metastatic to cervical lymph nodes: Can radiotherapy replace formal dissection after local excision of nodal disease? *Head Neck* 2005 Aug;27(8):718-21.
20. Ballo MT, Ross MI, Cormier JN, Myers JN, Lee JE, Gershenwald JE, et al. Combined-modality therapy for patients with regional nodal metastases from melanoma. *Int J Radiat Oncol Biol Phys* 2006 Jan 1;64(1):106-13.
21. Ballo MT, Zagars GK, Gershenwald JE, Lee JE, Mansfield PF, Kim KB, et al. A critical assessment of adjuvant radiotherapy for inguinal lymph node metastases from melanoma. *Ann Surg Oncol* 2004 Dec;11(12):1079-84.
22. Habermalz HJ, Fischer JJ. Radiation therapy of malignant melanoma: experience with high individual treatment doses. *Cancer* 1976 Dec;38(6):2258-62.
23. Leeper DB, Schneiderman MH, Dewey WC. Radiation-induced division delay in synchronized Chinese hamster ovary cells in monolayer culture. *Radiat Res* 1972 May;50(2):401-17.

24. Doble A. The pharmacology and mechanism of action of riluzole. *Neurology* 1996 Dec;47(6 Suppl 4):S233-41.
25. Kretschmer BD, Kratzer U, Schmidt WJ. Riluzole, a glutamate release inhibitor, and motor behavior. *Naunyn Schmiedebergs Arch Pharmacol* 1998 Aug;358(2):181-90.
26. Akamatsu K, Shibata MA, Ito Y, Sohma Y, Azuma H, Otsuki Y. Riluzole induces apoptotic cell death in human prostate cancer cells via endoplasmic reticulum stress. *Anticancer Res* 2009 Jun;29(6):2195-204.
27. Malgouris C, Daniel M, Doble A. Neuroprotective effects of riluzole on N-methyl-D-aspartate- or veratridine-induced neurotoxicity in rat hippocampal slices. *Neurosci Lett* 1994 Aug 15;177(1-2):95-9.
28. Jiang BH, Liu LZ. PI3K/PTEN signaling in angiogenesis and tumorigenesis. *Adv Cancer Res* 2009;102:19-65.
29. Degenhardt K, Chen G, Lindsten T, White E. BAX and BAK mediate p53-independent suppression of tumorigenesis. *Cancer Cell* 2002 Sep;2(3):193-203.
30. Rogers HW, Weinstock MA, Harris AR, Hinckley MR, Feldman SR, Fleischer AB, et al. Incidence estimate of nonmelanoma skin cancer in the United States, 2006. *Arch Dermatol* 2010 Mar;146(3):283-7.
31. Witkin EM. Ultraviolet-induced mutation and DNA repair. *Annual Review of Genetics* 1969;3(1):525-52.
32. Pfeifer GP. Formation and processing of UV photoproducts: effects of DNA sequence and chromatin environment. *Photochem Photobiol* 2008;65(2):270-83.
33. Popp S, Waltering S, Herbst C, Moll I, Boukamp P. UV-B-type mutations and chromosomal imbalances indicate common pathways for the development of Merkel and skin squamous cell carcinomas. *Int J Cancer* 2002 May 20;99(3):352-60.
34. Alam M, Ratner D. Cutaneous squamous-cell carcinoma. *N Engl J Med* 2001 Mar 29;344(13):975-83.
35. Grossman D, Leffell DJ. The molecular basis of nonmelanoma skin cancer: new understanding. *Arch Dermatol* 1997 Oct;133(10):1263-70.
36. Yu HS, Liao WT, Chai CY. Arsenic carcinogenesis in the skin. *J Biomed Sci* 2006 Sep;13(5):657-66.
37. Yuspa SH. The pathogenesis of squamous cell cancer: lessons learned from studies of skin carcinogenesis. *J Dermatol Sci* 1998 May;17(1):1-7.
38. Weyers W, Horster S, Diaz-Cascajo C. Tumor of Follicular Infundibulum Is Basal Cell Carcinoma. *Am J Dermatopath* 2009 Oct;31(7):634-41.
39. Raasch BA, Buettner PG, Garbe C. Basal cell carcinoma: histological classification and body-site distribution. *Br J Dermatol* 2006 Aug;155(2):401-7.
40. Lee DA, Miller SJ. Nonmelanoma skin cancer. *Facial plastic surgery clinics of North America* 2009;17(3):309-24.
41. Neville JA, Welch E, Leffell DJ. Management of nonmelanoma skin cancer in 2007. *Nature Clinical Practice Oncology* 2007;4(8):462-9.
42. Geisse J, Caro I, Lindholm J, Golitz L, Stampone P, Owens M. Imiquimod 5% cream for the treatment of superficial basal cell carcinoma: results from two phase III, randomized, vehicle-controlled studies. *J Am Acad Dermatol* 2004;50(5):722-33.
43. Crowson AN. Basal cell carcinoma: biology, morphology and clinical implications. *Modern pathology* 2006;19:S127-S47.
44. Freedberg IM, A. Z. Eisen, K. Wolff, K. F. Austen, L. A. Goldspit, S. I. Katz, T. B. Fitzpatrick, editor. *Fitzpatrick's Dermaology in General Medicine*. New York: McGraw-Hill Health Profession Division; 1999.
45. Kraemer KH, Lee MM, Andrews AD, Lambert WC. The role of sunlight and DNA repair in melanoma and nonmelanoma skin cancer. The xeroderma pigmentosum paradigm. *Arch Dermatol* 1994 Aug;130(8):1018-21.
46. Kasper M, Regl G, Frischauf AM, Aberger F. GLI transcription factors: mediators of oncogenic Hedgehog signalling. *Eur J Cancer* 2006 Mar;42(4):437-45.
47. Ziegler A, Leffell DJ, Kunala S, Sharma HW, Gailani M, Simon JA, et al. Mutation hotspots due to sunlight in the p53 gene of nonmelanoma skin cancers. *Proc Natl Acad Sci U S A* 1993 May 1;90(9):4216-20.

48. Lee ML, Tomsu K, Von Eschen KB. Duration of survival for disseminated malignant melanoma: results of a meta-analysis. *Melanoma Res* 2000 Feb;10(1):81-92.
49. Ries LAG MD, Krapcho M, Stinchcomb DG, Howlader N, Horner MJ, Mariotto A, Miller BA, Feuer EJ, Altekruse SF, Lewis DR, Clegg L, Eisner MP, Reichman M, Edwards BK (eds). SEER Cancer Statistics Review, 1975-2005. Bethesda, MD: National Cancer Institute; 2008.
50. Ries LA, Wingo PA, Miller DS, Howe HL, Weir HK, Rosenberg HM, et al. The annual report to the nation on the status of cancer, 1973-1997, with a special section on colorectal cancer. *Cancer* 2000 May 15;88(10):2398-424.
51. Jemal A, Siegel R, Ward E, Murray T, Xu J, Smigal C, et al. Cancer statistics, 2006. *CA Cancer J Clin* 2006 Mar-Apr;56(2):106-30.
52. Jemal A, Chu KC, Tarone RE. Recent trends in lung cancer mortality in the United States. *J Natl Cancer Inst* 2001 Feb 21;93(4):277-83.
53. Weinstock MA. Do sunscreens increase or decrease melanoma risk: an epidemiologic evaluation. *J Investig Dermatol Symp Proc* 1999 Sep;4(1):97-100.
54. Siegel R, DeSantis C, Virgo K, Stein K, Mariotto A, Smith T, et al. Cancer treatment and survivorship statistics, 2012. *CA: a cancer journal for clinicians* 2012 Jul-Aug;62(4):220-41.
55. Jemal A, Siegel R, Ward E, Hao Y, Xu J, Murray T, et al. Cancer statistics, 2008. *CA Cancer J Clin* 2008 Mar-Apr;58(2):71-96.
56. Jemal A, Siegel R, Ward E, Hao Y, Xu J, Thun MJ. Cancer statistics, 2009. *CA Cancer J Clin* 2009 Jul-Aug;59(4):225-49.
57. JJ BRaN. Biology of Melanocytes In: Arndt KA LP, Robinson JK, and Wintroub BU, editor. *Cutaneous Medicine and Surgery: Integrated Program in Dermatology*. Philadelphia: W.B. Saunders Co.; 1996. p. 1203-18.
58. Geller AC, Miller DR, Annas GD, Demierre MF, Gilchrest BA, Koh HK. Melanoma incidence and mortality among US whites, 1969-1999. *JAMA* 2002 Oct 9;288(14):1719-20.
59. Balch CM, Gershenwald JE, Soong SJ, Thompson JF, Atkins MB, Byrd DR, et al. Final Version of 2009 AJCC Melanoma Staging and Classification. *Journal of Clinical Oncology* 2009 Dec 20;27(36):6199-206.
60. Elder D. Tumor progression, early diagnosis and prognosis of melanoma. *Acta Oncol* 1999;38(5):535-48.
61. Garbe C, Eigentler TK. Diagnosis and treatment of cutaneous melanoma: state of the art 2006. *Melanoma Res* 2007 Apr;17(2):117-27.
62. Nathan FE, Mastrangelo MJ. Systemic therapy in melanoma. *Seminars in Surgical Oncology* 1998 Jun;14(4):319-27.
63. Steel KP, Barkway C. Another role for melanocytes: their importance for normal stria vascularis development in the mammalian inner ear. *Development* 1989 Nov;107(3):453-63.
64. Masson P. Pigment cells in man. *Ann N Y Acad Sci* 1948;4:15-51.
65. Jimbow K, Quevedo WC, Jr., Fitzpatrick TB, Szabo G. Some aspects of melanin biology: 1950-1975. *J Invest Dermatol* 1976 Jul;67(1):72-89.
66. Kukita A. Changes in tyrosinase activity during melanocyte proliferation in the hair growth cycle. *J Invest Dermatol* 1957 Apr;28(4):273-4.
67. Lallier TE. Cell lineage and cell migration in the neural crest. *Ann N Y Acad Sci* 1991;615:158-71.
68. Yoshida M, Takahashi Y, Inoue S. Histamine Induces Melanogenesis and Morphologic Changes by Protein Kinase A Activation via H2 Receptors in Human Normal Melanocytes. 2000;114(2):334-42.
69. Clark WH, Elder DE, Guerry D, Epstein MN, Greene MH, Van Horn M. A study of tumor progression: the precursor lesions of superficial spreading and nodular melanoma. *Hum Pathol* 1984;15(12):1147-65.
70. Dorsey C, Montgomery H. Blue Nevus and Its Distinction from Mongolian Spot and the Nevus of Ota123. *Journal of Investigative Dermatology* 1954;22(3):225-36.
71. Rhodes AR, Melski JW, Sober AJ, Harrist TJ, Mihm MC, Fitzpatrick TB. Increased intraepidermal melanocyte frequency and size in dysplastic melanocytic nevi and cutaneous melanoma. A comparative quantitative study of dysplastic melanocytic nevi, superficial spreading melanoma, nevocellular nevi, and solar lentigines. *Journal of Investigative Dermatology* 1983;80(5):452-9.
72. Hofmann-Wellenhof R, Blum A, Wolf IH, Piccolo D, Kerl H, Garbe C, et al. Dermoscopic classification of atypical melanocytic nevi (Clark nevi). *Arch Dermatol* 2001;137(12):1575.

73. Schmoeckel C. Classification of melanocytic nevi: do nodular and flat nevi develop differently? *Am J Dermatopathol* 1997;19(1):31.
74. Armstrong BK. The Epidemiology and Prevention of Cancer in Australia. *Aust Nz J Surg* 1988 Mar;58(3):179-87.
75. Duffy K, Grossman D. The dysplastic nevus: From historical perspective to management in the modern era: Part I. Historical, histologic, and clinical aspects. *J Am Acad Dermatol* 2012;67(1):1. e-. e16.
76. Albert LS, Rhodes AR, Sober AJ. Dysplastic melanocytic nevi and cutaneous melanoma: markers of increased melanoma risk for affected persons and blood relatives. *J Am Acad Dermatol* 1990;22(1):69-75.
77. Wenner KA. Atypical Mole (Dysplastic Nevus).
78. Heenan PJ, Clay CD. Epidermotropic metastatic melanoma simulating multiple primary melanomas. *Am J Dermatopathol* 1991 Aug;13(4):396-402.
79. Bengoechea-Beeby MP, Velasco-Oses A, Mourino Fernandez F, Reguilon-Rivero MC, Remon-Garijo L, Casado-Perez C. Epidermotropic metastatic melanoma. Are the current histologic criteria adequate to differentiate primary from metastatic melanoma? *Cancer* 1993 Sep 15;72(6):1909-13.
80. Clark Jr W, Ainsworth A, Bernardino E, Yang CH, Mihm Jr C, Reed R. The developmental biology of primary human malignant melanomas. Semin Oncol; 1975; 1975. p. 83.
81. Silverman AR, Nieland ML. Pathology of selected skin lesions of the head and neck. *Surgical Pathology of the Head and Neck* 2001;2:1565-621.
82. Podczaski E, Cain J. Cutaneous malignant melanoma. *Clinical obstetrics and gynecology* 2002;45(3):830-43.
83. Mancianti ML, Gyorfi T, Shih IM, Valyi-Nagy I, Levengood G, Menssen HD, et al. Growth regulation of cultured human nevus cells. *Journal of Investigative Dermatology* 1993;100:281S-7S.
84. Herlyn M, Thurin J, Balaban G, Bennicelli JL, Herlyn D, Elder DE, et al. Characteristics of cultured human melanocytes isolated from different stages of tumor progression. *Cancer Res* 1985;45(11 Part 2):5670-6.
85. Elder DE, Van Belle P, Elenitsas R, Halpern A, Guerry DP. Neoplastic progression and prognosis in melanoma. Seminars in cutaneous medicine and surgery; 1996: Elsevier; 1996. p. 336-48.
86. Hayward NK. Molecular pathology of cutaneous melanoma. *Molecular pathology of early cancer IOS Press, Amsterdam, Berlin, Oxford, Tokyo, Washington DC* 1999:207-31.
87. Carlson JA, Slominski A, Linette GP, Jr MCM, Ross JS. Biomarkers in melanoma: staging, prognosis and detection of early metastases. *Expert Rev Mol Diagn* 2003;3(3):303-30.
88. Scholzen T, Gerdes J. The Ki-67 protein: from the known and the unknown. *J Cell Physiol* 2000;182(3):311-22.
89. Gimotty PA, Van Belle P, Elder DE, Murry T, Montone KT, Xu X, et al. Biologic and prognostic significance of dermal Ki67 expression, mitoses, and tumorigenicity in thin invasive cutaneous melanoma. *Journal of Clinical Oncology* 2005;23(31):8048-56.
90. Mitsiades CS, Anderson KC. Epigenetic modulation in hematologic malignancies: challenges and progress. *J Natl Compr Canc Netw* 2009 Nov;7 Suppl 8:S1-12; quiz S4-6.
91. FitzGerald MG, Harkin DP, Silva-Arrieta S, MacDonald DJ, Lucchina LC, Unsal H, et al. Prevalence of germ-line mutations in p16, p19ARF, and CDK4 in familial melanoma: analysis of a clinic-based population. *Proceedings of the National Academy of Sciences* 1996;93(16):8541-5.
92. Nicolson GL. Gene expression, cellular diversification and tumor progression to the metastatic phenotype. *Bioessays* 2005;13(7):337-42.
93. Fearon ER, Dang CV. Cancer genetics: Tumor suppressor meets oncogene. *Current Biology* 1999 Jan 28;9(2):R62-R5.
94. Levine AJ. The tumor suppressor genes. *Annu Rev Biochem* 1993;62(1):623-51.
95. Hanahan D, Weinberg RA. Hallmarks of cancer: the next generation. *Cell* 2011;144(5):646-74.
96. Weinberg RA. Oncogenes and tumor suppressor genes. *CA: a cancer journal for clinicians* 2008;44(3):160-70.
97. Fearon ER. Tumor suppressor genes. *The genetic basis of human cancer* 1998;7(3):145.
98. van Golen KL, Wu ZF, Qiao XT, Bao LW, Merajver SD. RhoC GTPase, a novel transforming oncogene for human mammary epithelial cells that partially recapitulates the inflammatory breast cancer phenotype. *Cancer Res* 2000;60(20):5832-8.

99. Cheng JQ, Godwin AK, Bellacosa A, Taguchi T, Franke TF, Hamilton TC, et al. AKT2, a putative oncogene encoding a member of a subfamily of protein-serine/threonine kinases, is amplified in human ovarian carcinomas. *Proceedings of the National Academy of Sciences* 1992;89(19):9267-71.
100. Aaronson SA. Growth factors and cancer. *Science (New York, NY)* 1991;254(5035):1146.
101. Darnell JE. Transcription factors as targets for cancer therapy. *Nature Reviews Cancer* 2002;2(10):740-9.
102. Hubbard SR. Structural analysis of receptor tyrosine kinases. *Progress in biophysics and molecular biology* 1999;71(3):343-58.
103. Ma PC, Maulik G, Christensen J, Salgia R. c-Met: structure, functions and potential for therapeutic inhibition. *Cancer and Metastasis Reviews* 2003;22(4):309-25.
104. Besmer P, Murphy JE, George PC, Qiu F, Bergold PJ, Lederman L, et al. A new acute transforming feline retrovirus and relationship of its oncogene v-kit with the protein kinase gene family. 1986.
105. Rönnstrand L. Signal transduction via the stem cell factor receptor/c-Kit. *Cellular and molecular life sciences* 2004;61(19):2535-48.
106. Lennartsson J, Jelacic T, Linnekin D, Shivakrupa R. Normal and oncogenic forms of the receptor tyrosine kinase kit. *Stem Cells* 2005;23(1):16-43.
107. Fleischman RA. From white spots to stem cells: the role of the Kit receptor in mammalian development. *Trends in Genetics* 1993;9(8):285-90.
108. Huang S, Luca M, Gutman M, McConkey D, Langley KE, Lyman SD, et al. Enforced c-KIT expression renders highly metastatic human melanoma cells susceptible to stem cell factor-induced apoptosis and inhibits their tumorigenic and metastatic potential. *Oncogene* 1996;13(11):2339.
109. Lassam N, Bickford S. Loss of c-kit expression in cultured melanoma cells. *Oncogene* 1992;7(1):51.
110. Lutzky J, Bauer J, Bastian BC. Dose-dependent, complete response to imatinib of a metastatic mucosal melanoma with a K642E KIT mutation. *Pigment cell & melanoma research* 2008;21(4):492-3.
111. Hodi FS, Friedlander P, Corless CL, Heinrich MC, Mac Rae S, Kruse A, et al. Major response to imatinib mesylate in KIT-mutated melanoma. *Journal of Clinical Oncology* 2008;26(12):2046-51.
112. Carvajal RD, Antonescu CR, Wolchok JD, Chapman PB, Roman RA, Teitcher J, et al. KIT as a therapeutic target in metastatic melanoma. *JAMA: the journal of the American Medical Association* 2011;305(22):2327.
113. Bottaro DP, Rubin JS, Faletto DL, Chan AM, Kmiecik TE, Vande Woude GF, et al. Identification of the hepatocyte growth factor receptor as the c-met proto-oncogene product. *Science* 1991 Feb 15;251(4995):802-4.
114. Galland F, Stefanova M, Lafage M, Birnbaum D. Localization of the 5' end of the MCF2 oncogene to human chromosome 15q15----q23. *Cytogenet Cell Genet* 1992;60(2):114-6.
115. Christensen JG, Burrows J, Salgia R. c-Met as a target for human cancer and characterization of inhibitors for therapeutic intervention. *Cancer Lett* 2005;225(1):1-26.
116. Jeffers M, Rong S, Vande Woude GF. Enhanced tumorigenicity and invasion-metastasis by hepatocyte growth factor/scatter factor-met signalling in human cells concomitant with induction of the urokinase proteolysis network. *Mol Cell Biol* 1996 Mar;16(3):1115-25.
117. Di Renzo MF, Narsimhan RP, Olivero M, Bretti S, Giordano S, Medico E, et al. Expression of the Met/HGF receptor in normal and neoplastic human tissues. *Oncogene* 1991 Nov;6(11):1997-2003.
118. Matsumoto K, Nakamura T. Emerging multipotent aspects of hepatocyte growth factor. *J Biochem* 1996;119(4):591-600.
119. Bergam PL, Bhoumik A, Ronai Z. Altered Signal Transduction in Melanoma. *From Melanocytes to Melanoma* 2006:119-47.
120. Maulik G, Shrikhande A, Kijima T, Ma PC, Morrison PT, Salgia R. Role of the hepatocyte growth factor receptor, c-Met, in oncogenesis and potential for therapeutic inhibition. *Cytokine & growth factor reviews* 2002;13(1):41.
121. Engelman JA, Luo J, Cantley LC. The evolution of phosphatidylinositol 3-kinases as regulators of growth and metabolism. *Nat Rev Genet* 2006 Aug;7(8):606-19.
122. Jiang BH, Liu LZ. PI3K/PTEN signaling in tumorigenesis and angiogenesis. *Biochim Biophys Acta* 2008 Jan;1784(1):150-8.
123. Du K, Montminy M. CREB is a regulatory target for the protein kinase Akt/PKB. *J Biol Chem* 1998 Dec 4;273(49):32377-9.

124. Zhou H, Li XM, Meinkoth J, Pittman RN. Akt regulates cell survival and apoptosis at a postmitochondrial level. *J Cell Biol* 2000 Oct 30;151(3):483-94.
125. Romashkova JA, Makarov SS. NF-kappaB is a target of AKT in anti-apoptotic PDGF signalling. *Nature* 1999 Sep 2;401(6748):86-90.
126. Kane LP, Shapiro VS, Stokoe D, Weiss A. Induction of NF-kappaB by the Akt/PKB kinase. *Curr Biol* 1999 Jun 3;9(11):601-4.
127. Mayo LD, Donner DB. A phosphatidylinositol 3-kinase/Akt pathway promotes translocation of Mdm2 from the cytoplasm to the nucleus. *Proc Natl Acad Sci U S A* 2001 Sep 25;98(20):11598-603.
128. Zhou BP, Liao Y, Xia W, Zou Y, Spohn B, Hung MC. HER-2/neu induces p53 ubiquitination via Akt-mediated MDM2 phosphorylation. *Nat Cell Biol* 2001 Nov;3(11):973-82.
129. Staal SP. Molecular cloning of the akt oncogene and its human homologues AKT1 and AKT2: amplification of AKT1 in a primary human gastric adenocarcinoma. *Proc Natl Acad Sci U S A* 1987 Jul;84(14):5034-7.
130. Bellacosa A, de Feo D, Godwin AK, Bell DW, Cheng JQ, Altomare DA, et al. Molecular alterations of the AKT2 oncogene in ovarian and breast carcinomas. *Int J Cancer* 1995 Aug 22;64(4):280-5.
131. Cheng JQ, Ruggeri B, Klein WM, Sonoda G, Altomare DA, Watson DK, et al. Amplification of AKT2 in human pancreatic cells and inhibition of AKT2 expression and tumorigenicity by antisense RNA. *Proc Natl Acad Sci U S A* 1996 Apr 16;93(8):3636-41.
132. Vivanco I, Sawyers CL. The phosphatidylinositol 3-kinase–AKT pathway in human cancer. *Nature Reviews Cancer* 2002;2(7):489-501.
133. Schwartz PS, Manion MK, Emerson CB, Fry JS, Schulz CM, Sweet IR, et al. 2-Methoxy antimycin reveals a unique mechanism for Bcl-x(L) inhibition. *Mol Cancer Ther* 2007 Jul;6(7):2073-80.
134. Datta SR, Dudek H, Tao X, Masters S, Fu H, Gotoh Y, et al. Akt phosphorylation of BAD couples survival signals to the cell-intrinsic death machinery. *Cell* 1997;91(2):231-42.
135. Cardone MH, Roy N, Stennicke HR, Salvesen GS, Franke TF, Stanbridge E, et al. Regulation of cell death protease caspase-9 by phosphorylation. *Science* 1998;282(5392):1318-21.
136. Zhong H, Chiles K, Feldser D, Laughner E, Hanrahan C, Georgescu MM, et al. Modulation of hypoxia-inducible factor 1α expression by the epidermal growth factor/phosphatidylinositol 3-kinase/PTEN/Akt/FRAP pathway in human prostate cancer cells: implications for tumor angiogenesis and therapeutics. *Cancer Res* 2000;60(6):1541-5.
137. Zundel W, Schindler C, Haas-Kogan D, Koong A, Kaper F, Chen E, et al. Loss of PTEN facilitates HIF-1-mediated gene expression. *Genes Dev* 2000;14(4):391-6.
138. Okumura N, Yoshida H, Kitagishi Y, Murakami M, Nishimura Y, Matsuda S. PI3K/AKT/PTEN Signaling as a Molecular Target in Leukemia Angiogenesis. *Adv Hematol* 2012;2012:843085.
139. Maehama T, Dixon JE. The tumor suppressor, PTEN/MMAC1, dephosphorylates the lipid second messenger, phosphatidylinositol 3,4,5-trisphosphate. *J Biol Chem* 1998 May 29;273(22):13375-8.
140. Davies H, Bignell GR, Cox C, Stephens P, Edkins S, Clegg S, et al. Mutations of the BRAF gene in human cancer. *Nature* 2002 Jun 27;417(6892):949-54.
141. Herlyn M, Satyamoorthy K. Activated ras. Yet another player in melanoma? *Am J Pathol* 1996 Sep;149(3):739-44.
142. Karnoub AE, Weinberg RA. Ras oncogenes: split personalities. *Nature Reviews Molecular Cell Biology* 2008;9(7):517-31.
143. Thompson N, Lyons J. Recent progress in targeting the Raf/MEK/ERK pathway with inhibitors in cancer drug discovery. *Current opinion in pharmacology* 2005;5(4):350-6.
144. McCormick F. Signal transduction. How receptors turn Ras on. *Nature* 1993 May 6;363(6424):15-6.
145. Chardin P, Camonis JH, Gale NW, van Aelst L, Schlessinger J, Wigler MH, et al. Human Sos1: a guanine nucleotide exchange factor for Ras that binds to GRB2. *Science* 1993 May 28;260(5112):1338-43.
146. Moodie SA, Wolfman A. The 3Rs of life: Ras, Raf and growth regulation. *Trends Genet* 1994 Feb;10(2):44-8.
147. Ji Z, Flaherty KT, Tsao H. Targeting the RAS pathway in melanoma. *Trends Mol Med* 2012 Jan;18(1):27-35.
148. Haluska FG, Tsao H, Wu H, Haluska FS, Lazar A, Goel V. Genetic alterations in signaling pathways in melanoma. *Clin Cancer Res* 2006 Apr 1;12(7 Pt 2):2301s-7s.

149. Eskandarpour M, Hashemi J, Kanter L, Ringborg U, Platz A, Hansson J. Frequency of UV-inducible NRAS mutations in melanomas of patients with germline CDKN2A mutations. *J Natl Cancer Inst* 2003 Jun 4;95(11):790-8.
150. Wojnowski L, Zimmer AM, Beck TW, Hahn H, Bernal R, Rapp UR, et al. Endothelial apoptosis in Braf-deficient mice. *Nat Genet* 1997 Jul;16(3):293-7.
151. Reuter CW, Catling AD, Jelinek T, Weber MJ. Biochemical analysis of MEK activation in NIH3T3 fibroblasts. Identification of B-Raf and other activators. *J Biol Chem* 1995 Mar 31;270(13):7644-55.
152. Maurer G, Tarkowski B, Baccarini M. Raf kinases in cancer-roles and therapeutic opportunities. *Oncogene* 2011 Aug 11;30(32):3477-88.
153. Inamdar GS, Madhunapantula SRV, Robertson GP. Targeting the MAPK pathway in melanoma: why some approaches succeed and other fail. *Biochem Pharmacol* 2010;80(5):624.
154. Kolch W. Meaningful relationships: the regulation of the Ras/Raf/MEK/ERK pathway by protein interactions. *Biochem J* 2000 Oct 15;351 Pt 2:289-305.
155. Santarpia L, Lippman SM, El-Naggar AK. Targeting the MAPK-RAS-RAF signaling pathway in cancer therapy. *Expert Opin Ther Targets* 2012 Jan;16(1):103-19.
156. Poulikakos PI, Rosen N. Mutant BRAF melanomas--dependence and resistance. *Cancer Cell* 2011 Jan 18;19(1):11-5.
157. Dong J, Phelps RG, Qiao R, Yao S, Benard O, Ronai Z, et al. BRAF oncogenic mutations correlate with progression rather than initiation of human melanoma. *Cancer Res* 2003 Jul 15;63(14):3883-5.
158. Pollock PM, Cohen-Solal K, Sood R, Namkoong J, Martino JJ, Koganti A, et al. Melanoma mouse model implicates metabotropic glutamate signaling in melanocytic neoplasia. *Nat Genet* 2003 May;34(1):108-12.
159. Bale SJ, Dracopoli NC, Tucker MA, Clark WH, Jr., Fraser MC, Stanger BZ, et al. Mapping the gene for hereditary cutaneous malignant melanoma-dysplastic nevus to chromosome 1p. *N Engl J Med* 1989 May 25;320(21):1367-72.
160. Cannon-Albright LA, Goldgar DE, Meyer LJ, Lewis CM, Anderson DE, Fountain JW, et al. Assignment of a locus for familial melanoma, MLM, to chromosome 9p13-p22. *Science* 1992 Nov 13;258(5085):1148-52.
161. Koh J, Enders GH, Dynlacht BD, Harlow E. Tumour-derived p16 alleles encoding proteins defective in cell-cycle inhibition. *Nature* 1995 Jun 8;375(6531):506-10.
162. Serrano M, Hannon GJ, Beach D. A new regulatory motif in cell-cycle control causing specific inhibition of cyclin D/CDK4. *Nature* 1993 Dec 16;366(6456):704-7.
163. Lukas J, Parry D, Aagaard L, Mann DJ, Bartkova J, Strauss M, et al. Retinoblastoma-protein-dependent cell-cycle inhibition by the tumour suppressor p16. *Nature* 1995 Jun 8;375(6531):503-6.
164. Kurki S, Peltonen K, Latonen L, Kiviharju TM, Ojala PM, Meek D, et al. Nucleolar protein NPM interacts with HDM2 and protects tumor suppressor protein p53 from HDM2-mediated degradation. *Cancer Cell* 2004;5(5):465-75.
165. Balch CM, Buzaid AC, Soong SJ, Atkins MB, Cascinelli N, Coit DG, et al. New TNM melanoma staging system: linking biology and natural history to clinical outcomes. Seminars in surgical oncology; 2003: Wiley Online Library; 2003. p. 43-52.
166. Gershenwald JE, Soong S, Balch CM. 2010 TNM Staging System for Cutaneous Melanoma… and Beyond. *Ann Surg Oncol* 2010;17(6):1475-7.
167. Balch CM, Buzaid AC, Soong SJ, Atkins MB, Cascinelli N, Coit DG, et al. Final version of the American Joint Committee on Cancer staging system for cutaneous melanoma. *Journal of Clinical Oncology* 2001;19(16):3635-48.
168. Edge SB, Compton CC. The American Joint Committee on Cancer: the 7th edition of the AJCC cancer staging manual and the future of TNM. *Ann Surg Oncol* 2010;17(6):1471-4.
169. Greene FL, Page DL, Fleming ID, Fritz A, Balch CM, Haller DG, et al. *AJCC cancer staging manual*: Springer New York; 2002.
170. Balch CM, Gershenwald JE, Soong S, Thompson JF, Atkins MB, Byrd DR, et al. Final version of 2009 AJCC melanoma staging and classification. *Journal of Clinical Oncology* 2009;27(36):6199-206.
171. Hustinx R, PAULUS DP, Pierre R, YEUNG DHW, MACAPINLAC DHA, Larson SM. *Clinical PET in oncology*: Mallinckrodt Medical; 1996.

172. Swetter SM, Carroll LA, Johnson DL, Segall GM. Positron emission tomography is superior to computed tomography for metastatic detection in melanoma patients. *Ann Surg Oncol* 2002;9(7):646-53.
173. Tarhini AA, Agarwala SS. Cutaneous melanoma: available therapy for metastatic disease. *Dermatologic Therapy* 2006 Jan-Feb;19(1):19-25.
174. Luce JK, Thurman WG, Isaacs BL, Talley RW. Clinical trials with the antitumor agent 5-(3,3-dimethyl-1-triazeno)imidazole-4-carboxamide(NSC-45388). *Cancer Chemother Rep* 1970 Apr;54(2):119-24.
175. Einhorn LH, McBride CM, Luce JK, Caoili E, Gottlieb JA. Intra-arterial infusion therapy with 5-(3,3-dimethyl-1-triazeno) imidazole-4-carboxamide (NSC 45388) for malignant melanoma. *Cancer* 1973 Oct;32(4):749-55.
176. Marchesia F, Turriziani M, Tortorelli G, Avvisati G, Torino F, De Vecchis L. Triazene compounds: Mechanism of action and related DNA repair systems. *Pharmacological Research* 2007 Oct;56(4):275-87.
177. Middleton. Randomized phase III study of temozolomide versus dacarbazine in the treatment of patients with advanced metastatic malignant melanoma (vol 18, pg 158, 2000). *Journal of Clinical Oncology* 2000 Jun;18(11):2351-2.
178. Alvino E, Castiglia D, Caporali S, Pepponi R, Caporaso P, Lacal PM, et al. A single cycle of treatment with temozolomide, alone or combined with O-6-benzylguanine, induces strong chemoresistance in melanoma cell clones in vitro: Role of O-6-methylguanine-DNA methyltransferase and the mismatch repair system. *International Journal of Oncology* 2006 Oct;29(4):785-97.
179. Baskar R, Lee KA, Yeo R, Yeoh KW. Cancer and radiation therapy: current advances and future directions. *Int J Med Sci* 2012;9(3):193-9.
180. Nunez MI, McMillan T, Valenzuela MT, deAlmodovar JMR, Pedraza V. Relationship between DNA damage, rejoining and cell killing by radiation in mammalian cells. *Radiotherapy and Oncology* 1996 May;39(2):155-65.
181. Lord CJ, Ashworth A. The DNA damage response and cancer therapy. *Nature* 2012 Jan 19;481(7381):287-94.
182. Ross GM. Induction of cell death by radiotherapy. *Endocr Relat Cancer* 1999 Mar;6(1):41-4.
183. Kastan MB, Bartek J. Cell-cycle checkpoints and cancer. *Nature* 2004 Nov 18;432(7015):316-23.
184. Abraham RT. Cell cycle checkpoint signaling through the ATM and ATR kinases. *Genes Dev* 2001 Sep 1;15(17):2177-96.
185. Barranco SC, Romsdahl MM, Humphrey RM. The radiation response of human malignant melanoma cells grown in vitro. *Cancer Res* 1971 Jun;31(6):830-3.
186. Ristic-Fira AM, Todorovic DV, Koricanac LB, Petrovic IM, Valastro LM, Cirrone PGA, et al. Response of a human melanoma cell line to low and high ionizing radiation. *Signal Transduction Pathways, Pt C* 2007;1095:165-74.
187. Olivier KR, Schild SE, Morris CG, Brown PD, Markovic SN. A higher radiotherapy dose is associated with more durable palliation and longer survival in patients with metastatic melanoma. *Cancer* 2007 Oct 15;110(8):1791-5.
188. Mendenhall WM, Amdur RJ, Grobmyer SR, George TJ, Werning JW, Hochwald SN, et al. Adjuvant radiotherapy for cutaneous melanoma. *Cancer* 2008 Mar 15;112(6):1189-96.
189. Katz HR. The results of different fractionation schemes in the palliative irradiation of metastatic melanoma. *Int J Radiat Oncol Biol Phys* 1981 Jul;7(7):907-11.
190. Seegenschmiedt MH, Keilholz L, Altendorf-Hofmann A, Urban A, Schell H, Hohenberger W, et al. Palliative radiotherapy for recurrent and metastatic malignant melanoma: Prognostic factors for tumor response and long-term outcome: A 20-year experience. *International Journal of Radiation Oncology Biology Physics* 1999 Jun 1;44(3):607-18.
191. Ilkovitch D, Lopez DM. Immune modulation by melanoma-derived factors. *Experimental Dermatology* 2008 Dec;17(12):977-85.
192. Atkins MB, Lotze MT, Dutcher JP, Fisher RI, Weiss G, Margolin K, et al. High-dose recombinant interleukin 2 therapy for patients with metastatic melanoma: analysis of 270 patients treated between 1985 and 1993. *J Clin Oncol* 1999 Jul;17(7):2105-16.
193. Atkins MB, Kunkel L, Sznol M, Rosenberg SA. High-dose recombinant interleukin-2 therapy in patients with metastatic melanoma: long-term survival update. *Cancer J Sci Am* 2000 Feb;6 Suppl 1:S11-4.

194. Rosenberg SA, Yang JC, Topalian SL, Schwartzentruber DJ, Weber JS, Parkinson DR, et al. Treatment of 283 consecutive patients with metastatic melanoma or renal cell cancer using high-dose bolus interleukin 2. *Jama* 1994 Mar 23-30;271(12):907-13.
195. Chambers CA, Kuhns MS, Egen JG, Allison JP. CTLA-4-mediated inhibition in regulation of T cell responses: mechanisms and manipulation in tumor immunotherapy. *Annu Rev Immunol* 2001;19:565-94.
196. Egen JG, Allison JP. Cytotoxic T lymphocyte antigen-4 accumulation in the immunological synapse is regulated by TCR signal strength. *Immunity* 2002 Jan;16(1):23-35.
197. Saenger YM, Li YY, Chiou KC, Chan B, Rizzuto G, Terzulli SL, et al. Improved Tumor Immunity Using Anti-Tyrosinase Related Protein-1 Monoclonal Antibody Combined with DNA Vaccines in Murine Melanoma. *Cancer Research* 2008 Dec 1;68(23):9884-91.
198. Di Giacomo AM, Danielli R, Guidoboni M, Calabro L, Carlucci D, Miracco C, et al. Therapeutic efficacy of ipilimumab, an anti-CTLA-4 monoclonal antibody, in patients with metastatic melanoma unresponsive to prior systemic treatments: clinical and immunological evidence from three patient cases. *Cancer Immunology Immunotherapy* 2009 Aug;58(8):1297-306.
199. Newsholme P, Procopio J, Lima MMR, Pithon-Curi TC, Curi R. Glutamine and glutamate—their central role in cell metabolism and function. *Cell biochemistry and function* 2002;21(1):1-9.
200. Bergström J, Fürst P, Noree L, Vinnars E. Intracellular free amino acid concentration in human muscle tissue. *J Appl Physiol* 1974;36(6):693-7.
201. Meister A. Metabolism of glutamine. *Physiol Rev* 1956;36(1):103-27.
202. Spanaki C, Plaitakis A. The role of glutamate dehydrogenase in Mammalian ammonia metabolism. *Neurotox Res* 2011:1-11.
203. Dimski DS. Ammonia metabolism and the urea cycle: function and clinical implications. *Journal of Veterinary Internal Medicine* 2008;8(2):73-8.
204. Lunt SY, Vander Heiden MG. Aerobic glycolysis: meeting the metabolic requirements of cell proliferation. *Annual review of cell and developmental biology* 2011;27:441-64.
205. Vander Heiden MG, Cantley LC, Thompson CB. Understanding the Warburg effect: the metabolic requirements of cell proliferation. *Science Signalling* 2009;324(5930):1029.
206. Warburg O. On the origin of cancer cells. *Science* 1956 Feb 24;123(3191):309-14.
207. Warburg O. On respiratory impairment in cancer cells. *Science* 1956 Aug 10;124(3215):269-70.
208. Warburg O, Wind F, Negelein E. The Metabolism of Tumors in the Body. *J Gen Physiol* 1927 Mar 7;8(6):519-30.
209. DeBerardinis RJ, Mancuso A, Daikhin E, Nissim I, Yudkoff M, Wehrli S, et al. Beyond aerobic glycolysis: transformed cells can engage in glutamine metabolism that exceeds the requirement for protein and nucleotide synthesis. *Proceedings of the National Academy of Sciences* 2007;104(49):19345-50.
210. DeBerardinis RJ, Lum JJ, Hatzivassiliou G, Thompson CB. The biology of cancer: metabolic reprogramming fuels cell growth and proliferation. *Cell Metab* 2008;7(1):11-20.
211. Feron O. Pyruvate into lactate and back: from the Warburg effect to symbiotic energy fuel exchange in cancer cells. *Radiotherapy and Oncology* 2009;92(3):329-33.
212. Moreadith RW, Lehninger AL. The pathways of glutamate and glutamine oxidation by tumor cell mitochondria. Role of mitochondrial NAD(P)+-dependent malic enzyme. *J Biol Chem* 1984 May 25;259(10):6215-21.
213. Deberardinis RJ, Sayed N, Ditsworth D, Thompson CB. Brick by brick: metabolism and tumor cell growth. *Curr Opin Genet Dev* 2008 Feb;18(1):54-61.
214. GAGLIO D. Role of nutrient availability on proliferation and cell cycle excution of immortalized and kras transformed mouse fibroblastic: Università degli Studi di Milano-Bicocca; 2009.
215. Marie S, Shinjo S. Metabolism and brain cancer. *Clinics* 2011;66(S1):33-43.
216. Cairns RA, Harris IS, Mak TW. Regulation of cancer cell metabolism. *Nature Reviews Cancer* 2011;11(2):85-95.
217. Krebs H, Bellamy D. The interconversion of glutamic acid and aspartic acid in respiring tissues. *Biochemical Journal* 1960;75(3):523.
218. McKeehan WL. Glycolysis, glutaminolysis and cell proliferation. *Cell Biol Int Rep* 1982;6(7):635.
219. Moreadith R, Lehninger A. The pathways of glutamate and glutamine oxidation by tumor cell mitochondria. Role of mitochondrial NAD (P)+-dependent malic enzyme. *Journal of Biological Chemistry* 1984;259(10):6215-21.

220. DeBerardinis RJ, Mancuso A, Daikhin E, Nissim I, Yudkoff M, Wehrli S, et al. Beyond aerobic glycolysis: transformed cells can engage in glutamine metabolism that exceeds the requirement for protein and nucleotide synthesis. *Proc Natl Acad Sci U S A* 2007 Dec 4;104(49):19345-50.
221. Estrela JM, Ortega A, Obrador E. Glutathione in cancer biology and therapy. *Crit Rev Clin Lab Sci* 2006;43(2):143-81.
222. Höckel M, Vaupel P. Tumor hypoxia: definitions and current clinical, biologic, and molecular aspects. *J Natl Cancer Inst* 2001;93(4):266-76.
223. Navin N, Krasnitz A, Rodgers L, Cook K, Meth J, Kendall J, et al. Inferring tumor progression from genomic heterogeneity. *Genome Res* 2010;20(1):68-80.
224. Semenza GL. Tumor metabolism: cancer cells give and take lactate. *J Clin Invest* 2008;118(12):3835.
225. Feron O. Pyruvate into lactate and back: from the Warburg effect to symbiotic energy fuel exchange in cancer cells. *Radiotherapy and oncology : journal of the European Society for Therapeutic Radiology and Oncology* 2009 Sep;92(3):329-33.
226. Semenza GL. Tumor metabolism: cancer cells give and take lactate. *J Clin Invest* 2008 Dec;118(12):3835-7.
227. Gilman AG. G proteins: transducers of receptor-generated signals. *Annu Rev Biochem* 1987;56(1):615-49.
228. Mellado M, Vila-Coro A, Martinez C, Rodriguez-Frade J. Receptor dimerization: a key step in chemokine signaling. *Cellular and molecular biology (Noisy-le-Grand, France)* 2001;47(4):575.
229. Strader CD, Fong TM, Graziano M, Tota M. The family of G-protein-coupled receptors. *The FASEB journal* 1995;9(9):745-54.
230. Bourne HR, Meng EC. Structure: rhodopsin sees the light. *Science Signalling* 2000;289(5480):733.
231. Fredriksson R, Lagerstrom MC, Lundin LG, Schioth HB. The G-protein-coupled receptors in the human genome form five main families. Phylogenetic analysis, paralogon groups, and fingerprints. *Mol Pharmacol* 2003 Jun;63(6):1256-72.
232. Bjarnadottir TK, Fredriksson R, Schioth HB. The gene repertoire and the common evolutionary history of glutamate, pheromone (V2R), taste(1) and other related G protein-coupled receptors. *Gene* 2005 Dec 5;362:70-84.
233. Urwyler S. Allosteric modulation of family C G-protein-coupled receptors: from molecular insights to therapeutic perspectives. *Pharmacological Reviews* 2011;63(1):59-126.
234. O'Hara PJ, Sheppard PO, Thogersen H, Venezia D, Haldeman BA, McGrane V, et al. The ligand-binding domain in metabotropic glutamate receptors is related to bacterial periplasmic binding proteins. *Neuron* 1993 Jul;11(1):41-52.
235. Kaupmann K, Huggel K, Heid J, Flor PJ, Bischoff S, Mickel SJ, et al. Expression cloning of GABA(B) receptors uncovers similarity to metabotropic glutamate receptors. *Nature* 1997 Mar 20;386(6622):239-46.
236. Bortolotto ZA, Clarke VRJ, Delany CM, Parry MC, Smolders I, Vignes M, et al. Kainate receptors are involved in synaptic plasticity. *Nature* 1999;402(6759):297-300.
237. Gouaux E. Structure and function of AMPA receptors. *J Physiol* 2004;554(2):249-53.
238. Mattson MP. Apoptosis in neurodegenerative disorders. *Nature Reviews Molecular Cell Biology* 2000;1(2):120-9.
239. Fan MM, Raymond LA. N-methyl-D-aspartate (NMDA) receptor function and excitotoxicity in Huntington's disease. *Prog Neurobiol* 2007 Apr;81(5-6):272-93.
240. Dracheva S, Byne W, Chin B, Haroutunian V. Ionotropic glutamate receptors mRNA expression in the human thalamus: absence of change in schizophrenia. *Brain Res* 2008;1214:23.
241. Won SJ, Kim DY, Gwag BJ. Cellular and molecular pathways of ischemic neuronal death. *Journal of biochemistry and molecular biology* 2002;35(1):67-86.
242. Mayer ML, Armstrong N. Structure and Function of Glutamate Receptor Ion Channels 1. *Annu Rev Physiol* 2004;66:161-81.
243. Wess J. G-protein-coupled receptors: molecular mechanisms involved in receptor activation and selectivity of G-protein recognition. *The FASEB journal* 1997;11(5):346-54.
244. Hamm HE. The many faces of G protein signaling. *J Biol Chem* 1998 Jan 9;273(2):669-72.
245. Bunemann M, Frank M, Lohse MJ. Gi protein activation in intact cells involves subunit rearrangement rather than dissociation. *Proc Natl Acad Sci U S A* 2003 Dec 23;100(26):16077-82.

246. Lappano R, Maggiolini M. G protein-coupled receptors: novel targets for drug discovery in cancer. *Nat Rev Drug Discov* 2011 Jan;10(1):47-60.
247. Lee HJ, Wall B, Chen S. G-protein-coupled receptors and melanoma. *Pigment Cell Melanoma Res* 2008 Aug;21(4):415-28.
248. Lefkowitz RJ. G protein-coupled receptors. *Journal of Biological Chemistry* 1998;273(30):18677-80.
249. Kim CH, Lee J, Lee JY, Roche KW. Metabotropic glutamate receptors: phosphorylation and receptor signaling. *J Neurosci Res* 2007;86(1):1-10.
250. Rozengurt E, Guha S, Sinnett-Smith J. Gastrointestinal peptide signalling in health and disease. *Eur J Surg Suppl* 2002;587:23-38.
251. Teerawattananon Y, Tangcharoensathien V, Tantivess S, Mills A. Health sector regulation in Thailand: recent progress and the future agenda. *Health Policy* 2003 Mar;63(3):323-38.
252. Marinissen MJ, Gutkind JS. G-protein-coupled receptors and signaling networks: emerging paradigms. *Trends Pharmacol Sci* 2001;22(7):368-76.
253. Dorsam RT, Gutkind JS. G-protein-coupled receptors and cancer. *Nat Rev Cancer* 2007 Feb;7(2):79-94.
254. Rzeski W, Turski L, Ikonomidou C. Glutamate antagonists limit tumor growth. *Proc Natl Acad Sci U S A* 2001 May 22;98(11):6372-7.
255. Evan GI, Vousden KH. Proliferation, cell cycle and apoptosis in cancer. *Nature* 2001;411(6835):342-8.
256. Cheng N, Chytil A, Shyr Y, Joly A, Moses HL. Transforming growth factor-beta signaling-deficient fibroblasts enhance hepatocyte growth factor signaling in mammary carcinoma cells to promote scattering and invasion. *Mol Cancer Res* 2008 Oct;6(10):1521-33.
257. Bhowmick NA, Neilson EG, Moses HL. Stromal fibroblasts in cancer initiation and progression. *Nature* 2004 Nov 18;432(7015):332-7.
258. Li F, Wang Y, Zeller KI, Potter JJ, Wonsey DR, O'Donnell KA, et al. Myc stimulates nuclearly encoded mitochondrial genes and mitochondrial biogenesis. *Mol Cell Biol* 2005 Jul;25(14):6225-34.
259. Lundstrom K. Latest development in drug discovery on G protein-coupled receptors. *Curr Protein Pept Sci* 2006 Oct;7(5):465-70.
260. Knox WE, Horowitz ML, Friedell GH. The proportionality of glutaminase content to growth rate and morphology of rat neoplasms. *Cancer Res* 1969 Mar;29(3):669-80.
261. Van Raamsdonk CD, Bezrookove V, Green G, Bauer J, Gaugler L, O'Brien JM, et al. Frequent somatic mutations of GNAQ in uveal melanoma and blue naevi. *Nature* 2009 Jan 29;457(7229):599-602.
262. Burger M, Burger JA, Hoch RC, Oades Z, Takamori H, Schraufstatter IU. Point mutation causing constitutive signaling of CXCR2 leads to transforming activity similar to Kaposi's sarcoma herpesvirus-G protein-coupled receptor. *J Immunol* 1999 Aug 15;163(4):2017-22.
263. Takayama H, LaRochelle WJ, Sharp R, Otsuka T, Kriebel P, Anver M, et al. Diverse tumorigenesis associated with aberrant development in mice overexpressing hepatocyte growth factor/scatter factor. *Proc Natl Acad Sci* 1997;94:701-6.
264. Pin JP, Duvoisin R. The metabotropic glutamate receptors: structure and functions. *Neuropharmacology* 1995 Jan;34(1):1-26.
265. Hermans E, Challiss RA. Structural, signalling and regulatory properties of the group I metabotropic glutamate receptors: prototypic family C G-protein-coupled receptors. *Biochem J* 2001;359(Pt 3):465-84.
266. Ozawa S, Kamiya H, Tsuzuki K. Glutamate receptors in the mammalian central nervous system. *Prog Neurobiol* 1998 Apr;54(5):581-618.
267. Haas HS, Pfragner R, Siegl V, Ingolic E, Heintz E, Schraml E, et al. The non-competitive metabotropic glutamate receptor-1 antagonist CPCCOEt inhibits the in vitro growth of human melanoma. *Oncol Rep* 2007 Jun;17(6):1399-404.
268. Naarala J, Nykvist P, Tuomala M, Savolainen K. Excitatory amino acid-induced slow biphasic responses of free intracellular calcium in human neuroblastoma cells. *FEBS Lett* 1993 Sep 13;330(2):222-6.
269. Iacovelli L, Fulceri F, De Blasi A, Nicoletti F, Ruggieri S, Fornai F. The neurotoxicity of amphetamines: bridging drugs of abuse and neurodegenerative disorders. *Exp Neurol* 2006 Sep;201(1):24-31.
270. Shin SS, Martino JJ, Chen S. Metabotropic glutamate receptors (mGlus) and cellular transformation. *Neuropharmacology* 2008 Sep;55(4):396-402.

271. Takano T, Lin JH, Arcuino G, Gao Q, Yang J, Nedergaard M. Glutamate release promotes growth of malignant gliomas. *Nat Med* 2001 Sep;7(9):1010-5.
272. Ohtani Y, Harada T, Funasaka Y, Nakao K, Takahara C, Abdel-Daim M, et al. Metabotropic glutamate receptor subtype-1 is essential for in vivo growth of melanoma. *Oncogene* 2008 Sep 8;27:7162-70.
273. Shin SS, Namkoong J, Wall BA, Gleason R, Lee HJ, Chen S. Oncogenic activities of metabotropic glutamate receptor 1 (Grm1) in melanocyte transformation. *Pigment cell & melanoma research* 2008 Jun;21(3):368-78.
274. Marin YE, Namkoong J, Cohen-Solal K, Shin SS, Martino JJ, Oka M, et al. Stimulation of oncogenic metabotropic glutamate receptor 1 in melanoma cells activates ERK1/2 via PKCepsilon. *Cell Signal* 2006 Aug;18(8):1279-86.
275. Marin YE, Chen S. Involvement of metabotropic glutamate receptor 1, a G protein coupled receptor, in melanoma development. *J Mol Med* 2004 Nov;82(11):735-49.
276. Busca R, Abbe P, Mantoux F, Aberdam E, Peyssonnaux C, Eychene A, et al. Ras mediates the cAMP-dependent activation of extracellular signal-regulated kinases (ERKs) in melanocytes. *Embo J* 2000 Jun 15;19(12):2900-10.
277. Ferraguti F, Baldani-Guerra B, Corsi M, Nakanishi S, Corti C. Activation of the extracellular signal-regulated kinase 2 by metabotropic glutamate receptors. *Eur J Neurosci* 1999 Jun;11(6):2073-82.
278. Thandi S, Blank JL, Challiss RA. Group-I metabotropic glutamate receptors, mGlu1a and mGlu5a, couple to extracellular signal-regulated kinase (ERK) activation via distinct, but overlapping, signalling pathways. *J Neurochem* 2002 Dec;83(5):1139-53.
279. Choe ES, Wang JQ. Regulation of transcription factor phosphorylation by metabotropic glutamate receptor-associated signaling pathways in rat striatal neurons. *Neuroscience* 2002;114(3):557-65.
280. Stepulak A, Luksch H, Gebhardt C, Uckermann O, Marzahn J, Sifringer M, et al. Expression of glutamate receptor subunits in human cancers. *Histochem Cell Biol* 2009 Oct;132(4):435-45.
281. Onken MD, Worley LA, Long MD, Duan S, Council ML, Bowcock AM, et al. Oncogenic mutations in GNAQ occur early in uveal melanoma. *Invest Ophthalmol Vis Sci* 2008 Dec;49(12):5230-4.
282. Degenhardt K, White E. A mouse model system to genetically dissect the molecular mechanisms regulating tumorigenesis. *Clin Cancer Res* 2006 Sep 15;12(18):5298-304.
283. Martino JJ, Wall BA, Mastrantoni E, Wilimczyk BJ, La Cava SN, Degenhardt K, et al. Metabotropic glutamate receptor 1 (Grm1) is an oncogene in epithelial cells. *Oncogene* 2012 Oct 22.
284. Speyer CL, Smith JS, Banda M, DeVries JA, Mekani T, Gorski DH. Metabotropic glutamate receptor-1: a potential therapeutic target for the treatment of breast cancer. *Breast Cancer Res Treat* 2012 Apr;132(2):565-73.
285. Chang HJ, Yoo BC, Lim SB, Jeong SY, Kim WH, Park JG. Metabotropic glutamate receptor 4 expression in colorectal carcinoma and its prognostic significance. *Clin Cancer Res* 2005 May 1;11(9):3288-95.
286. Choi KY, Chang K, Pickel JM, Badger JD, 2nd, Roche KW. Expression of the metabotropic glutamate receptor 5 (mGluR5) induces melanoma in transgenic mice. *Proc Natl Acad Sci U S A* 2011 Sep 13;108(37):15219-24.
287. Saez E, Nelson MC, Eshelman B, Banayo E, Koder A, Cho GJ, et al. Identification of ligands and coligands for the ecdysone-regulated gene switch. *Proc Natl Acad Sci U S A* 2000 Dec 19;97(26):14512-7.
288. Wiznerowicz M, Szulc J, Trono D. Tuning silence: conditional systems for RNA interference. *Nat Methods* 2006 Sep;3(9):682-8.
289. Marin YE, Namkoong J, Shin SS, Raines J, Degenhardt K, White E, et al. Grm5 expression is not required for the oncogenic role of Grm1 in melanocytes. *Neuropharmacology* 2005;49 Suppl 1:70-9.
290. Van den Bosch L. [The causes and mechanism of selective motor neuron death in amyotrophic lateral sclerosis]. *Verh K Acad Geneeskd Belg* 2006;68(4):249-69.
291. Van Den Bosch L, Van Damme P, Bogaert E, Robberecht W. The role of excitotoxicity in the pathogenesis of amyotrophic lateral sclerosis. *Biochim Biophys Acta* 2006 Nov-Dec;1762(11-12):1068-82.
292. Friedman LM, Furberg CD, DeMets DL. *Fundamentals of clinical trials*: Springer; 2010.
293. Yip D, Le MN, Chan JL, Lee JH, Mehnert JA, Yudd A, et al. A phase 0 trial of riluzole in patients with resectable stage III and IV melanoma. *Clin Cancer Res* 2009 Jun 1;15(11):3896-902.
294. Marin YE, Namkoong J, Cohen-Solal K, Shin SS, Martino JJ, Oka M, et al. Stimulation of oncogenic metabotropic glutamate receptor 1 in melanoma cells activates ERK1/2 via PKCepsilon. *Cell Signaling* 2006;18:1279-86.

295. Garraway LA, Widlund HR, Rubin MA, Getz G, Berger AJ, Ramaswamy S, et al. Integrative genomic analyses identify MITF as a lineage survival oncogene amplified in malignant melanoma. *Nature* 2005 Jul 7;436(7047):117-22.
296. Degenhardt K, Sundararajan R, Lindsten T, Thompson C, White E. Bax and Bak independently promote cytochrome C release from mitochondria. *J Biol Chem* 2002 Apr 19;277(16):14127-34.
297. Degenhardt K, Sundararajan R, Lindsten T, Thompson C, White E. Bax and Bak independently promote cytochrome C release from mitochondria. *J Biol Chem* 2002a Apr 19;277(16):14127-34.
298. Zhu H, Ryan K, Chen S. Cloning of novel splice variants of mouse mGluR1. *Brain Res Mol Brain Res* 1999;73(1-2):93-103.
299. Cohen-Solal KA, Crespo-Carbone SM, Namkoong J, Mackason KR, Roberts KG, Reuhl KR, et al. Progressive appearance of pigmentation in amelanotic melanoma lesions. *Pigment Cell Res* 2002;15(4):282-9.
300. Wang SJ, Wang KY, Wang WC. Mechanisms underlying the riluzole inhibition of glutamate release from rat cerebral cortex nerve terminals (synaptosomes). *Neuroscience* 2004;125(1):191-201.
301. Shin SS, Wall BA, Goydos JS, Chen S. AKT2 is a downstream target of metabotropic glutamate receptor 1 (Grm1). *Pigment cell & melanoma research* 2010 Feb;23(1):103-11.
302. Fernet M, Mégnin-Chanet F, Hall J, Favaudon V. Control of the G2/M checkpoints after exposure to low doses of ionising radiation: implications for hyper-radiosensitivity. *DNA Repair (Amst)* 2010;9(1):48.
303. Shechter D, Dormann HL, Allis CD, Hake SB. Extraction, purification and analysis of histones. *Nat Protoc* 2007;2(6):1445-57.
304. Burden DA, Kingma PS, Froelich-Ammon SJ, Bjornsti MA, Patchan MW, Thompson RB, et al. Topoisomerase II.etoposide interactions direct the formation of drug-induced enzyme-DNA cleavage complexes. *J Biol Chem* 1996 Nov 15;271(46):29238-44.
305. Mochan TA, Venere M, DiTullio RA, Jr., Halazonetis TD. 53BP1, an activator of ATM in response to DNA damage. *DNA Repair (Amst)* 2004 Aug-Sep;3(8-9):945-52.
306. Fernandez-Capetillo O, Allis CD, Nussenzweig A. Phosphorylation of histone H2B at DNA double-strand breaks. *J Exp Med* 2004 Jun 21;199(12):1671-7.
307. Schultz LB, Chehab NH, Malikzay A, DiTullio RA, Jr., Stavridi ES, Halazonetis TD. The DNA damage checkpoint and human cancer. *Cold Spring Harb Symp Quant Biol* 2000;65:489-98.
308. Ward IM, Minn K, van Deursen J, Chen J. p53 Binding protein 53BP1 is required for DNA damage responses and tumor suppression in mice. *Mol Cell Biol* 2003 Apr;23(7):2556-63.
309. Xie A, Scully R. Hijacking the DNA damage response to enhance viral replication: gamma-herpesvirus 68 orf36 phosphorylates histone H2AX. *Mol Cell* 2007 Jul 20;27(2):178-9.
310. de Feraudy S, Revet I, Bezrookove V, Feeney L, Cleaver JE. A minority of foci or pan-nuclear apoptotic staining of gammaH2AX in the S phase after UV damage contain DNA double-strand breaks. *Proc Natl Acad Sci U S A* 2010 Apr 13;107(15):6870-5.
311. Mehnert JM, Wen, Y., Lee, J.H., Dudek, Pruski-Clark, L. L., Shih, W., Chen, S., Goydos, J. S. A phase II Trial of Riluzole, an Antagonist of Metabotropic Glutamate Receptor (GRM1) Signaling, in Advanced Melanoma. . *J Clin Oncol 29 2011* 2011;29:suppl;abstr 8557.
312. McGeer EG, McGeer PL. Pharmacologic approaches to the treatment of amyotrophic lateral sclerosis. *BioDrugs* 2005;19(1):31-7.
313. Miller R. Riluzole for ALS: what is the evidence? *Amyotroph Lateral Scler Other Motor Neuron Disord* 2003 Sep;4(3):135.
314. Shin SS, Namkoong J, Wall BA, Gleason R, Lee HJ, Chen S. Oncogenic activities of metabotropic glutamate receptor 1 (Grm1) in melanocyte transformation. *Pigment Cell Melanoma Res* 2008;21(3):368-78.
315. Rangasamy D, Tremethick DJ, Greaves IK. Gene knockdown by ecdysone-based inducible RNAi in stable mammalian cell lines. *Nat Protoc* 2008;3(1):79-88.
316. No D, Yao TP, Evans RM. Ecdysone-inducible gene expression in mammalian cells and transgenic mice. *Proc Natl Acad Sci U S A* 1996;93(8):3346-51.
317. Dang DT, Chen X, Feng J, Torbenson M, Dang LH, Yang VW. Overexpression of Kruppel-like factor 4 in the human colon cancer cell line RKO leads to reduced tumorigenecity. *Oncogene* 2003 May 29;22(22):3424-30.

318. Cohen-Solal KA, Crespo-Carbone SM, Namkoong J, Mackason KR, Roberts KG, Reuhl KR, et al. Progressive appearance of pigmentation in amelanotic melanoma lesions. *Pigment Cell Res* 2002 Aug;15(4):282-9.
319. Littlewood TD, Hancock DC, Danielian PS, Parker MG, Evan GI. A modified oestrogen receptor ligand-binding domain as an improved switch for the regulation of heterologous proteins. *Nucleic Acids Res* 1995 May 25;23(10):1686-90.
320. Rangasamy D, Tremethick DJ, Greaves IK. Gene knockdown by ecdysone-based inducible RNAi in stable mammalian cell lines. *Nature protocols* 2008;3(1):79-88.
321. Lo M, Wang YZ, Gout PW. The x(c)- cystine/glutamate antiporter: a potential target for therapy of cancer and other diseases. *J Cell Physiol* 2008 Jun;215(3):593-602.
322. Meister A, Anderson ME. Glutathione. *Annu Rev Biochem* 1983;52:711-60.
323. Griffith OW. Biologic and pharmacologic regulation of mammalian glutathione synthesis. *Free Radic Biol Med* 1999 Nov;27(9-10):922-35.
324. Leeuwenburgh C, Ji LL. Glutathione and glutathione ethyl ester supplementation of mice alter glutathione homeostasis during exercise. *J Nutr* 1998 Dec;128(12):2420-6.
325. Steenvoorden DP, Hasselbaink DM, Beijersbergen van Henegouwen GM. Protection against UV-induced reactive intermediates in human cells and mouse skin by glutathione precursors: a comparison of N-acetylcysteine and glutathione ethylester. *Photochem Photobiol* 1998 Jun;67(6):651-6.
326. Anderson ME, Powrie F, Puri RN, Meister A. Glutathione monoethyl ester: preparation, uptake by tissues, and conversion to glutathione. *Arch Biochem Biophys* 1985 Jun;239(2):538-48.
327. Martensson J, Meister A. Mitochondrial damage in muscle occurs after marked depletion of glutathione and is prevented by giving glutathione monoester. *Proc Natl Acad Sci U S A* 1989 Jan;86(2):471-5.
328. Milligan G, Smith NJ. Allosteric modulation of heterodimeric G-protein-coupled receptors. *Trends Pharmacol Sci* 2007;28(12):615-20.
329. Aramori I, Nakanishi S. Signal transduction and pharmacological characteristics of a metabotropic glutamate receptor, mGluR1, in transfected CHO cells. *Neuron* 1992;8:757-65.
330. Francesconi A, Duvoisin R. Role of the second and third intracellular loops of metabotropic glutamate receptors in mediatic dual signal transduction activation. *J biol Chem* 1998;273:5615-24.
331. Bensimon G, Ludolph A, Agid Y, Vidailhet M, Payan C, Leigh PN. Riluzole treatment, survival and diagnostic criteria in Parkinson plus disorders: the NNIPPS study. *Brain* 2009 Jan;132(Pt 1):156-71.
332. Lacomblez L, Doppler V, Beucler I, Costes G, Salachas F, Raisonnier A, et al. APOE: a potential marker of disease progression in ALS. *Neurology* 2002 Apr 9;58(7):1112-4.
333. Mehnert JM, McCarthy MM, Jilaveanu L, Flaherty KT, Aziz S, Camp RL, et al. Quantitative expression of VEGF, VEGF-R1, VEGF-R2, and VEGF-R3 in melanoma tissue microarrays. *Hum Pathol* 2010 Mar;41(3):375-84.
334. Zhou BB, Elledge SJ. The DNA damage response: putting checkpoints in perspective. *Nature* 2000 Nov 23;408(6811):433-9.
335. Murray AW. Creative blocks: cell-cycle checkpoints and feedback controls. *Nature* 1992 Oct 15;359(6396):599-604.
336. Schwartz GK. Development of cell cycle active drugs for the treatment of gastrointestinal cancers: a new approach to cancer therapy. *J Clin Oncol* 2005 Jul 10;23(20):4499-508.
337. Stark GR, Taylor WR. Control of the G2/M transition. *Mol Biotechnol* 2006 Mar;32(3):227-48.
338. Rogakou EP, Boon C, Redon C, Bonner WM. Megabase chromatin domains involved in DNA double-strand breaks in vivo. *J Cell Biol* 1999 Sep 6;146(5):905-16.
339. Kodym R, Horth E. Determination of radiation-induced DNA strand breaks in individual cells by non-radioactive labelling of 3' OH ends. *Int J Radiat Biol* 1995 Aug;68(2):133-9.
340. Tibbetts R, Abraham RT. PI3K-related kinases: Roles in cell-cycle regulation and DNA damage responses. *CANCER DRUG DISCOVERY AND DEVELOPMENT* 2000;5:267-302.
341. Shiloh Y. ATM and related protein kinases: safeguarding genome integrity. *Nat Rev Cancer* 2003 Mar;3(3):155-68.
342. Banin S, Moyal L, Shieh S, Taya Y, Anderson CW, Chessa L, et al. Enhanced phosphorylation of p53 by ATM in response to DNA damage. *Science* 1998 Sep 11;281(5383):1674-7.
343. Abraham RT. Cell cycle checkpoint signaling through the ATM and ATR kinases. *Genes Dev* 2001;15(17):2177-96.
344. Taylor WR, Stark GR. Regulation of the G2/M transition by p53. *Oncogene* 2001;20(15):1803-15.

345. Brown AL, Lee CH, Schwarz JK, Mitiku N, Piwnica-Worms H, Chung JH. A human Cds1-related kinase that functions downstream of ATM protein in the cellular response to DNA damage. *Proceedings of the National Academy of Sciences* 1999;96(7):3745-50.
346. Takata M, Sasaki MS, Sonoda E, Morrison C, Hashimoto M, Utsumi H, et al. Homologous recombination and non-homologous end-joining pathways of DNA double-strand break repair have overlapping roles in the maintenance of chromosomal integrity in vertebrate cells. *Embo J* 1998;17(18):5497-508.
347. Morrison C, Sonoda E, Takao N, Shinohara A, Yamamoto K, Takeda S. The controlling role of ATM in homologous recombinational repair of DNA damage. *Embo J* 2000;19(3):463-71.
348. Namkoong J, Shin SS, Lee HJ, Marin YE, Wall BA, Goydos JS, et al. Metabotropic glutamate receptor 1 and glutamate signaling in human melanoma. *Cancer Res* 2007 Mar 1;67(5):2298-305.
349. Lehnert B, Iyer R. Exposure to low-level chemicals and ionizing radiation: reactive oxygen species and cellular pathways. *Hum Exp Toxicol* 2002;21(2):65-9.
350. Lehnert BE, Iyer R. Exposure to low-level chemicals and ionizing radiation: reactive oxygen species and cellular pathways. *Hum Exp Toxicol* 2002 Feb;21(2):65-9.
351. Halliwell B. Free radicals and antioxidants: a personal view. *Nutr Rev* 1994;52(8):253-65.
352. De Vries N, De Flora S. N-acetyl-l-cysteine. *J Cell Biochem* 2004;53(S17F):270-7.
353. Steenvoorden DP, Beijersbergen van Henegouwen GM. Cysteine derivatives protect against UV-induced reactive intermediates in human keratinocytes: the role of glutathione synthesis. *Photochem Photobiol* 1997 Nov;66(5):665-71.
354. Miura K, Ishii T, Sugita Y, Bannai S. Cystine uptake and glutathione level in endothelial cells exposed to oxidative stress. *Am J Physiol* 1992 Jan;262(1 Pt 1):C50-8.
355. Sato H, Tamba M, Ishii T, Bannai S. Cloning and expression of a plasma membrane cystine/glutamate exchange transporter composed of two distinct proteins. *J Biol Chem* 1999 Apr 23;274(17):11455-8.
356. Oh J, Ho L, Ala-Mello S, Amato D, Armstrong L, Bellucci S, et al. Mutation analysis of patients with Hermansky-Pudlak syndrome: a frameshift hot spot in the HPS gene and apparent locus heterogeneity. *Am J Hum Genet* 1998 Mar;62(3):593-8.
357. Powell SN, Bindra RS. Targeting the DNA damage response for cancer therapy. *DNA Repair (Amst)* 2009 Sep 2;8(9):1153-65.
358. McKay MJ, Kefford RF. The spectrum of in vitro radiosensitivity in four human melanoma cell lines is not accounted for by differential induction or rejoining of DNA double strand breaks. *Int J Radiat Oncol Biol Phys* 1995;31(2):345.
359. Barnholtz-Sloan JS, Sloan AE, Davis FG, Vigneau FD, Lai P, Sawaya RE. Incidence proportions of brain metastases in patients diagnosed (1973 to 2001) in the Metropolitan Detroit Cancer Surveillance System. *Journal of Clinical Oncology* 2004;22(14):2865-72.
360. Broadbent AM, Hruby G, Tin MM, Jackson M, Firth I. Survival following whole brain radiation treatment for cerebral metastases: an audit of 474 patients. *Radiother Oncol* 2004 Jun;71(3):259-65.
361. Prickett TD, Wei X, Cardenas-Navia I, Teer JK, Lin JC, Walia V, et al. Exon capture analysis of G protein-coupled receptors identifies activating mutations in GRM3 in melanoma. *Nat Genet* 2011 Nov;43(11):1119-26.
362. Ohtani Y, Harada T, Funasaka Y, Nakao K, Takahara C, Abdel-Daim M, et al. Metabotropic glutamate receptor subtype-1 is essential for in vivo growth of melanoma. *Oncogene* 2008 Dec 4;27(57):7162-70.
363. Li S, Huang S, Peng SB. Overexpression of G protein-coupled receptors in cancer cells: involvement in tumor progression. *Int J Oncol* 2005 Nov;27(5):1329-39.
364. Jenner A, England T, Aruoma OI, Halliwell B. Measurement of oxidative DNA damage by gas chromatography-mass spectrometry: ethanethiol prevents artifactual generation of oxidized DNA bases. *Biochemical Journal* 1998;331(Pt 2):365.
365. Ravanat JL, Turesky RJ, Gremaud E, Trudel LJ, Stadler RH. Determination of 8-oxoguanine in DNA by gas chromatography-mass spectrometry and HPLC-electrochemical detection: overestimation of the background level of the oxidized base by the gas chromatography-mass spectrometry assay. *Chem Res Toxicol* 1995;8(8):1039-45.
366. Singh NP, McCoy MT, Tice RR, Schneider EL. A simple technique for quantitation of low levels of DNA damage in individual cells. *Exp Cell Res* 1988;175(1):184-91.

367. Fairbairn DW, O'Neill KL. Necrotic DNA degradation mimics apoptotic nucleosomal fragmentation comet tail length. *In Vitro Cellular & Developmental Biology-Animal* 1995;31(3):171-3.
368. Fairbairn DW, Olive PL, O'Neill KL. The comet assay: a comprehensive review. *Mutation Research/Reviews in Genetic Toxicology* 1995;339(1):37-59.
369. Pierce AJ, Johnson RD, Thompson LH, Jasin M. XRCC3 promotes homology-directed repair of DNA damage in mammalian cells. *Genes Dev* 1999;13(20):2633-8.
370. Miura K, Ishii T, Sugita Y, Bannai S. Cystine uptake and glutathione level in endothelial cells exposed to oxidative stress. *American Journal of Physiology-Cell Physiology* 1992;262(1):C50-C8.
371. Li W, Rusiniak ME, Chintala S, Gautam R, Novak EK, Swank RT. Murine Hermansky–Pudlak syndrome genes: regulators of lysosome-related organelles. *Bioessays* 2004;26(6):616-28.
372. Chintala S, Li W, Lamoreux ML, Ito S, Wakamatsu K, Sviderskaya EV, et al. Slc7a11 gene controls production of pheomelanin pigment and proliferation of cultured cells. *Proc Natl Acad Sci U S A* 2005;102(31):10964-9.
373. de Groot JF, Piao Y, Lu L, Fuller GN, Yung WKA. Knockdown of GluR1 expression by RNA interference inhibits glioma proliferation. *J Neurooncol* 2008;88(2):121-33.
374. Lin CLG, Bristol LA, Jin L, Dykes-Hoberg M, Crawford T, Clawson L, et al. Aberrant RNA processing in a neurodegenerative disease: the cause for absent EAAT2, a glutamate transporter, in amyotrophic lateral sclerosis. *Neuron* 1998;20(3):589-602.